REGGE THEORY FOR MULTIPARTICLE AMPLITUDES

R.C. BROWER

Natural Sciences II, University of California, Santa Cruz, Calif. 95060, USA

C.E. DeTAR

*Laboratory for Nuclear Science and Department of Physics,
Massachusetts Institute of Technology, Cambridge, Mass. 02139, USA*

and

J.H. WEIS

*CERN, Geneva, Switzerland
and Physics Department, University of Washington, Seattle, Wash. 98195, USA*

REGGE THEORY FOR MULTIPARTICLE AMPLITUDES

R.C. BROWER

Natural Sciences II, University of California, Santa Cruz, Calif. 95060, USA

C.E. DeTAR*

Laboratory for Nuclear Science and Department of Physics, Massachusetts Institute of Technology, Cambridge, Mass. 02139, USA

J.H. WEIS**

CERN, Geneva, and Physics Department, University of Washington, Seattle, Wash. 98195, USA

Abstract:

   The asymptotic behavior of multiparticle scattering amplitudes is discussed and reviewed with an emphasis on the analytic structure of the amplitudes as a function of the channel invariants. Single and multiple asymptotic limits of the Regge and helicity type are defined and a recipe is given for obtaining the asymptotic behavior of amplitudes in these limits controlled by exchanges of factorizable Regge poles and constrained by analyticity requirements. Applications to inclusive cross sections and the decoupling theorems for a pomeron Regge pole are reviewed as illustrative consequences of unitarity for multi-Regge theory. The present understanding of the relationship of cuts in angular momentum to unitarity is also described and suggestions given for further research. An effort has been made to keep the discussion pedagogical, while at the same time providing an entree to the literature.

Contents:

1. Introduction

1.1. Regge poles in hadron dynamics

Regge in 1959 [116,117] observed that eigensolutions of the Schrödinger equation of different angular momentum could be grouped into families, each family being connected by a single pole in the complex angular momentum plane that moved through the integers in angular momentum as the total energy was increased. These Regge poles, as they came to be called, are connected with the asymptotic behavior of the scattering amplitude as the cosine of the t-channel scattering angle $\cos \theta$ in the four-particle amplitude (fig. 1.1) becomes infinite (section 1.2). Because $\cos\theta$ is linearly related to the invariant $s = (p_a + p_b)^2$, the amplitude for the crossed reaction ab $\rightarrow$ $\bar{a}'\bar{b}'$ has the high energy behavior

$$A_4 \underset{s \to \infty}{\sim} \gamma(t) s^{\alpha(t)} . \tag{1.1}$$

It is natural to try to generalize the idea of Regge behavior to multi-Regge asymptotic behavior of multiparticle amplitudes [94,130,115,63,34,148,13,150]. These extensions were guesses motivated from Regge behavior of four-particle amplitudes and did not attempt to reflect a detailed understanding of the phase and singularity structure of the multiparticle amplitudes.

Let us review the difficulties briefly. Consider the process ac $\rightarrow$ $\bar{a}'\bar{b}'\bar{c}'$ of fig. 2.1. Suppose we were interested in studying a double-Regge asymptotic limit

$$s_1, s_2, s_{12} \to \infty; \qquad\qquad t_1, t_2 \text{ fixed.} \tag{1.2}$$

The expected result is

$$A_5 \sim s_1^{\alpha_1(t_1)} s_2^{\alpha_2(t_2)} \gamma(t_1, t_2, s_{12}/s_1 s_2) . \tag{1.3}$$

The difficulties in formulating a rigorous derivation of such a result center around the notion of the helicity of the reggeons α_1 and α_2. The kinematic analysis of section 2 below shows that it is indeed possible to identify an angle, namely the Toller angle ω_{12}, whose Fourier components are the helicities of both α_1 and α_2 (both, because helicity is not changed by the scalar particle b'). In the limit (1.2) the angle is given by
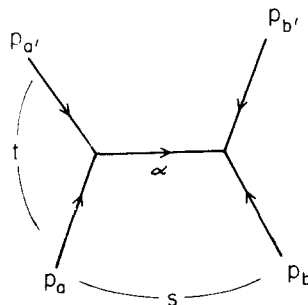

Fig. 1.1. Four-particle amplitude.

$$s_{12}/s_1 s_2 = \{2\sqrt{t_1 t_2} \cos \omega_{12} - t_1 - t_2 + m_{b'}^2\}/\lambda(t_1, t_2, m_{b'}^2) , \tag{1.4}$$

$$\lambda(a, b, c) = a^2 + b^2 + c^2 - 2ab - 2bc - 2ac . \tag{1.5}$$

It is necessary to fix the helicities of the reggeons in the limit (1.2), i.e. to fix $s_{12}/s_1 s_2$, and so the residue γ in (1.3) becomes a function of this ratio.

The amplitude A_5 can have a rather complicated dependence on the ratio $s_{12}/s_1 s_2$, if we consider that it has poles and branch points in all three invariants. This leads in general to an infinite spectrum in helicities for the reggeons, so that

$$\gamma = \sum_{\lambda = -\infty}^{\infty} \gamma_\lambda \exp(i\lambda\omega_{12}) , \tag{1.6}$$

where the series must diverge at values of ω_{12} corresponding through (1.4) to singularities in $s_{12}/s_1 s_2$.

Apart from the technical problems of finding a rigorous derivation of (1.3), there is the practical problem of how one should go about introducing signature into (1.3) in view of the fact that γ must have a phase associated with singularities in $s_{12}/s_1 s_2$. In order to deal with all of these problems, one must first understand what asymptotic singularities in A_5 as a function of s_1, s_2 and s_{12} might be permitted on general grounds and how these singularities enter into γ. A convenient vehicle for studying this question is the generalization of helicity to complex values. It is necessary to consider poles in complex helicity in analogy to poles in complex angular momentum. The existence of complex helicity poles is intimately related to the asymptotic singularity structure of multiparticle amplitudes. An understanding of the consequences of Regge behavior for multiparticle amplitudes cannot be complete without taking them into account. This is a feature unique to multiparticle amplitudes and never appears at the four-particle level.

Progress has been made in recent years towards developing a detailed understanding of multi-Regge behavior, and it is the purpose of this report to describe what we know now. The story is far from complete and is a rich area for further research.

Our present discussion is devoted mainly to the asymptotic behavior produced by Regge poles, since relatively little is known about the role of cuts in the asymptotic behavior of multiparticle amplitudes. We explore the problems in making Regge asymptotic behavior compatible with some fundamental assumptions about the asymptotic singularity structure of amplitudes and show that a theory of multi-Regge behavior can be formulated consistent with a restricted set of asymptotic singularities, namely those arising from normal threshold branch points. Simple Regge poles cannot tell the whole story. We know from unitarity that if there are poles in the J plane then there must be cuts. Our attitude toward J-plane cuts is that they should be understood as being generated from combinations of poles through unitarity. This principle has been suggested previously for cuts and poles in the energy plane (see ref. [37]) under the title "maximal analyticity of the first degree". In keeping with this principle, it is apparent that one must first understand the properties of pole-dominated amplitudes before attempting to understand the properties of Regge cuts.

Apart from the deeper questions relating to the foundations of Regge theory there are other reasons for studying the asymptotic structure of multiparticle amplitudes. We list a few applications:

(i) Phenomenology of inclusive cross sections. Here we need to know how to take the discontinuity of multiparticle amplitudes in a particular channel. What does multi-Regge behavior say about inclusive reactions? Do the Regge-pole contributions factor in the discontinuity, if they do so in the amplitude? How much do we learn about the full amplitude by measuring the discontinuity?

(ii) Phenomenology of exclusive multiparticle production. What is the asymptotic phase of a multiparticle production amplitude? What can be said about the dependence on the Toller angle? What does the presence of a helicity pole have to do with the asymptotic behavior of multiparticle amplitudes?

(iii) Reggeon scattering amplitudes. Can reggeon amplitudes be defined which have properties similar to particle amplitudes (i.e. unitarity, analyticity), so that we can write dispersion relations, finite energy sum rules, etc., for them?

(iv) Theorems about decoupling of the pomeron. If the pomeron is a simple pole in angular momentum, what can one say about its couplings?

For the reader interested in the basic theoretical ideas, we suggest he reads sections 1.2–1.4, 2.1.–2.2, and 3.1–3.5. This allows the reader to complete the analysis of the simplest multi-Regge vertex, namely, the two-reggeon, one-particle vertex. The article as a whole can be viewed as follows. We study the basic three-point reggeon vertices (fig. 1.2) for one reggeon (trivial case, section 1.2), for two reggeons (section 3) and three reggeons (section 4). We discuss the analytic structure in the helicity angle (sections 3.5, 4.2). Then we show that factorized products of these basic vertices occur in general multi-Regge limits (section 5). These ideas are then applied to the inclusive process, where we encounter four- and five-point vertices (section 6). Having discussed the behavior of amplitudes dominated by Regge poles, we turn briefly to unitarization problems. As an illustration, from direct (s) channel unitarity we find bounds on diffractive production (section 7) and from crossed (t) channel unitarity, the two-reggeons cuts (section 8). Clearly these applications represent only the first small steps in an iterative approach to the generation of all J-plane singularities.

We have included an appendix which illustrates the general discussion in the main body of the text by giving the explicit forms in the dual resonance model, since it is the simplest model exhibiting all the Regge pole properties discussed here. The reader may find it useful to refer to the appendix for comparison from time to time.

1.2. Regge poles – Review

In order to motivate our approach to multi-Regge behavior, we begin by reviewing Regge theory for the four-particle amplitude. (For extensive reviews, see Collins and Squires [45] and Collins [44].)

A Regge pole is a pole in the complex angular momentum plane of a partial wave amplitude. Its presence has implications for the asymptotic behavior of a scattering amplitude as the cosine of a scattering angle (and therefore certain channel invariants) become infinite.
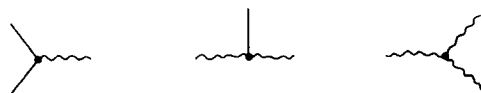
Fig. 1.2. Three-point vertices.

For a scalar 2-to-2 amplitude (fig. 1.1) in the physical region for aa' → $\bar{b}\bar{b}'$, the partial wave amplitudes are defined in the t-channel center-of-momentum frame by the usual Legendre series

$$A(z, t) = \sum_{J=0}^{\infty} (2J+1) P_J(z) \tilde{a}(J, t) , \tag{1.7}$$

where $t = (p_a + p_{a'})^2$ is the square of the total energy and $z = \cos \theta$ is the cosine of the scattering angle in that frame*.

Using the method of Froissart and Gribov, the partial wave amplitudes $\tilde{a}(J, t)$ may be continued into the complex J plane. It is necessary to define separate continuations for even and odd J, and this is done by introducing the signatured amplitudes $A^\tau(z, t)$, $\tau = \pm 1$, which have only right-hand cuts in z and are related to $A(z, t)$ as follows:

$$A(z, t) = [A^+(z, t) + A^+(-z, t)] + [A^-(z, t) - A^-(-z, t)] . \tag{1.8}$$

The asymptotic behavior due to a J-plane pole or cut is obtained from the Sommerfeld–Watson representation of (1.7):

$$A^\tau(z, t) = -\frac{1}{2i} \int_{-\frac{1}{2} - i\infty}^{-\frac{1}{2} + i\infty} \frac{dJ}{\sin \pi J} (2J+1) P_J(-z) \tilde{a}^\tau(J, t) . \tag{1.9}$$

The contour stands to the right of poles in the signatured partial wave amplitude $\tilde{a}^\tau(J, t)$ but to the left of $J = 0$. We recall that in order to be able to push the contour to the left of $\mathrm{Re}\, J = -\frac{1}{2}$ we need to use Mandelstam's trick, which effectively replaces

$$P_J(-z)/\sin \pi J \qquad \text{by} \qquad -Q_{-J-1}(-z)/\cos \pi J . \tag{1.10}$$

Furthermore, since we are chiefly interested in the leading asymptotic behavior, we replace

$$Q_{-J-1}(-z) \sim \frac{\sqrt{\pi} \Gamma(-J)}{\Gamma(-J+\frac{1}{2})} (-2z)^J . \tag{1.11}$$

If we express only the manifest singularity in J in $\Gamma(-J)$ in (1.11) and absorb inessential factors in a redefinition of $\tilde{a}^\tau(J, t)$ we are led to

$$A^\tau(z, t) = \frac{1}{2\pi i} \int dJ \, \Gamma(-J)(-z)^J \tilde{a}^\tau(J, t) , \tag{1.12}$$

where the contour separates poles in $\Gamma(-J)$ from dynamical singularities in $\tilde{a}^\tau(J, t)$. A rightmost factorizable pole at $J = \alpha(t)$ in $\tilde{a}^\tau(J, t)$ leads to an asymptotic behavior of the signatured amplitude

$$A^\tau(z, t) \underset{z \to \infty}{\sim} \tilde{\beta}^{aa'}(t) \tilde{\beta}^{bb'}(t) (-z)^{\alpha(t)} \Gamma(-\alpha(t)) . \tag{1.13}$$

This familiar result expresses not just the fact that the amplitude has power behavior in z. It also

---

* We use the convention that all momentum labels refer to incoming particles. Thus for any antiparticles $p_{\bar{b}} = -p_b$, etc.

carries information about the presence in $A^\tau(z, t)$ of a discontinuity in z. For non-integral $\alpha(t)$ the asymptotic expression appears to have a branch point at $z = \infty$. This is a reflection of the accumulation at infinity of right-hand branch points in z in the signatured amplitude. Since they originate from branch points in the crossed channel invariants $s = (p_a + p_b)^2$ and $u = (p_a + p_{b'})^2$, which are linearly related to z, e.g.,

$$s = A(t)z + B(t) ,$$

$$A(t) = 2 \frac{\lambda^{\frac{1}{2}} [t, m_a^2, m_{a'}^2]}{2\sqrt{t}} \frac{\lambda^{\frac{1}{2}} [t, m_b^2, m_{b'}^2]}{2\sqrt{t}} ,$$

$$B(t) = m_{a'}^2 + m_{b'}^2 + 2 \left(\frac{t + m_{a'}^2 - m_a^2}{2\sqrt{t}} \right) \left(\frac{t + m_{b'}^2 - m_b^2}{2\sqrt{t}} \right) ,$$

$$\lambda(a, b, c) = a^2 + b^2 + c^2 - 2ab - 2bc - 2ac , \qquad (1.14)$$

it is natural to rewrite (1.13) in terms of channel invariants alone:

$$A^\tau(s, t) \underset{s \to \infty}{\sim} \beta^{aa'}(t) \beta^{bb'}(t) (-s)^{\alpha(t)} \Gamma[-\alpha(t)] , \qquad (1.15)$$

where

$$\tilde{\beta}(t) = \beta(t)[A(t)]^{\alpha(t)/2} . \qquad (1.16)$$

For special values of t, the coefficient $A(t)$ in eq. (1.14) is singular. These singularities do not correspond to actual singularities in t and s in $A^\tau(s, t)$ and so are called kinematical singularities. Therefore, they must also appear in $\tilde{\beta}(t)$ in eq. (1.13) but not in $\beta(t)$ in (1.15). Thus eq. (1.15) is a more natural way to express what the presence of a Regge pole implies for the asymptotic behavior of the amplitude. In fact it is also well-suited for analytic continuation in t to the physical region for the s-channel process ab $\to \bar{a}'\bar{b}'$.

We may also re-express the "leading behavior" of the Sommerfeld—Watson transform (1.9) in terms of channel invariants:

$$A^\tau(s, t) = \frac{1}{2\pi i} \int dJ \, \Gamma(-J) (-s)^J a^\tau(J, t) , \qquad (1.17)$$

where

$$a^\tau(J, t) = [A(t)]^{-J} \tilde{a}^\tau(J, t) . \qquad (1.18)$$

This expression contains all the essential features of the Sommerfeld—Watson transform: the partial wave series is obtained as a polynomial in s by closing the contour to the right; for integral $\alpha(t)$ the Regge pole residue is a polynomial of order $J = \alpha(t)$.

Although (1.17) was derived only for the leading s behavior, it is possible to interpret it as an exact expression. It is a Mellin transform representation of the amplitude. Such representations in terms of the invariants were first discussed by Khuri [93]. There is a one-to-one correspondence between the leading member of a family (integrally spaced) of poles in the Mellin variable J at

$J = \alpha(t)$, $\alpha(t) - 1$, ... and a pole in the true angular momentum at $J = \alpha(t)$. Since we are chiefly concerned with the analytic structure manifested by cuts in the asymptotic behavior in s, a structure which is unaffected by additional inverse powers of s, we shall refer loosely to the Mellin variable J in (1.17) as "angular momentum".

For a pole of definite signature we have, from (1.8)

$$A(s, t) \underset{s \to \infty}{\sim} \beta^{aa'}(t)\, \beta^{bb'}(t)\, \Gamma(-\alpha(t))[(-s)^{\alpha(t)} + \tau s^{\alpha(t)}] , \tag{1.19}$$

where left- and right-hand cuts in s are shown explicitly. As long as the singularities in s accumulate on the positive and negative axis at infinity, it is conventional to expect that eq. (1.19) gives a valid representation of the asymptotic behavior of the amplitude for the cut complex s plane $\pi > \arg s > 0$, $2\pi > \arg s > \pi$. Real analyticity requires $\beta(t)$ to be real. The point is that the phase of eq. (1.19) and the range of validity in s depend on prior knowledge of the locations of the singularities at very large s. This knowledge is provided by unitarity and is built into the Froissart–Gribov amplitudes in part through their asymptotic properties for $\operatorname{Re} J \to \infty$. Suppose, instead, there had been a series of branch points which accumulated along the ray $\arg s = \sigma$, but that the power behavior was otherwise the same. These branch points could be represented by an expression just like eq. (1.15), except that the expression would be valid for $2\pi - \sigma > \arg s > \sigma$ and the phase of $\beta(t)$ would need to be adjusted according to the available information in that case. These observations will prove useful in discussing the asymptotic behavior of multiparticle amplitudes.

1.3. Method of attack

The methods which we have outlined for the four-point amplitude in section 1.2 above are the ones we shall adopt in the study of multiparticle amplitudes. The outline of the procedure is as follows:

(i) O(3) *partial wave analysis*. Identify scattering angles, angular momenta, and helicities. Define the asymptotic limit in terms of the scattering angles and express the asymptotic behavior of the amplitude in terms of the angles, as in $(\cos\theta)^{\alpha}$, etc. We motivate this step from our understanding of the four-particle amplitude (1.13).

(ii) *Analytic expression in terms of channel invariants*. Relate the angles to the channel invariants. Re-define the limit and re-express the asymptotic behavior in terms of channel invariants (1.15). These are the variables in which the analytic structure of the amplitude is most simply expressed. At this stage we inject our assumptions about the allowed singularity structure.

(iii) *Mellin representation*. As a matter of convenience we then rewrite the asymptotic behavior in terms of a Mellin transform in the J planes and complex helicity planes (1.17). This provides a succinct representation of the amplitude and facilitates the discussion of helicity singularities.

Apart from the relatively uncontroversial generalization of the four-particle Regge behavior at step (i), the only point where a dynamical assumption is necessary is in step (ii). This is, in fact, the heart of our analysis and is so crucially important to our conclusions that it deserves amplification, which we provide in the following subsection.

1.4. Assumptions

We summarize our assumptions about the asymptotic analytic structure for the Regge-pole contribution:

(A) Uniformity. Multiple asymptotic limits can be reached in any order.

(B) Only normal threshold branch points in any channel invariant affect the asymptotic behavior due to Regge poles.

(C) Complex J-plane poles are moving so that they produce an asymptotic behavior, e.g. $(-s)^\alpha$, giving a discontinuity in s.

Only assumption (B) requires special comment. It is the very strong assumption that the only singularities in asymptotic invariants affecting the asymptotic behavior are normal threshold branch points*. The essentially useful feature of normal threshold singularities as contrasted with higher order Landau singularities is their independence [107]. For in taking multi-Regge asymptotic limits we will be faced with the necessity of interpreting expressions of the form $(-s_A)^{\alpha_A}(-s_B)^{\alpha_B}$ where s_A and s_B refer to two channel invariants of a multiparticle amplitude. If the evident cuts in s_A and s_B in such an expression were independent, we would be safe in interpreting such an expression as representing a product of two functions each cut on the positive real axis. If they were not independent, the cuts in s_B might move in a complicated way as s_A varied. Such an expression would not then be suitable for a straightforward interpolation between various boundary values above and below cuts in s_A and s_B.
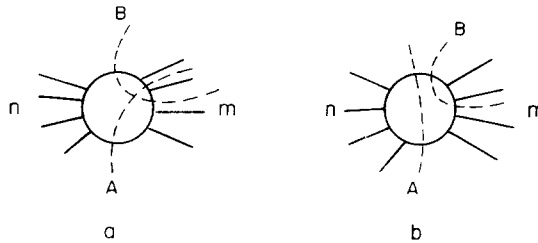
Fig. 1.3. Diagram for n-to-m scattering amplitude showing (a) overlapping channels, (b) non-overlapping channels.

Another useful consequence of the independence of normal threshold singularities is that many combinations of cuts can be ruled out, thereby vastly simplifying the asymptotic structure. To see this, consider an arbitrary n-to-m scattering amplitude as shown in fig. 1.3. It is useful to introduce the notion of overlapping channels. In the figure, the dotted line labeled A (B) separates the momenta of channel A (B). When these lines intersect as in fig. 1.3a we say the channels "overlap". If not, as in fig. 1.3b, they do not. A property of normal threshold singularities is that their discontinuity is free of normal threshold singularities in overlapping channels. Such overlapping double discontinuities appear only when higher order Landau singularities are considered. However, normal threshold singularities do occur simultaneously in non-overlapping channels. Therefore, we can rule out asymptotic terms of the form $(-s_A)^{\alpha_A}(-s_B)^{\alpha_B}$, when s_A and s_B refer to overlapping invariants.

As a corollary to (B) we therefore have:

---

* The single-Regge limit of the four-particle amplitude $s^{\alpha(t)}\beta(t)$ has a simultaneous discontinuity in s and t reflecting a higher order Landau singularity. We are not excluding them. We are concerned with singularities appearing jointly in two or more asymptotic invariants.

(D) No overlapping channel discontinuities: Discontinuities as revealed in (C) do not occur simultaneously in two overlapping channel invariants.

To restrict ourselves to normal thresholds, although we are safe in doing so, may be overly pessimistic. What we know in S-matrix theory about locations of singularities in channel invariants comes from unitarity. Our present understanding of the asymptotic structure of amplitudes in the presence of higher order Landau singularities is far from complete. What we want to emphasize is not so much a particular assumption about the asymptotic singularity structure, as *the importance of making some statement or assumption and the relationship between the assumed structure and the Regge asymptotic behavior.* We believe that further research will indicate in what way our assumptions have been stated too strongly and in what way they would need to be modified so as to make our conclusions more broadly applicable. We remark that all explicit models for multi-Regge amplitudes studied thus far (e.g. ladder model, dual resonance model) satisfy our assumptions. For a possible limitation on these assumptions, see DeGrand and DeTar [153].

As an example of the possibility that our assumptions may be relaxed in some cases, we refer to the Steinmann relations. These follow from axiomatic field theory and there is good reason to suspect that they will eventually be found to be valid in axiomatic S-matrix theory as well [127,9, 126,29,30]. The Steinmann relation [127] states that (D) is valid for any multiparticle amplitude regardless of whether the cuts are due to normal threshold branch points or higher order Landau singularities, provided only that the discontinuities are taken in the physical region of some scattering process*. We occasionally require (D) outside physical regions as well, but on the other hand, only in certain asymptotic regions. Perhaps the Steinmann relations can be extended to these regions as well. This is certainly a subject deserving further study.

1.5. Other approaches

1.5.1. Sommerfeld—Watson approach

We conclude this section with some discussion of the relationship between the approach to multi-Regge behavior taken here and that taken by others. The direct and conventional approach to multi-Regge behavior is to generalize the treatment of the four-particle amplitude:

(i) Specify the analytic structure of the amplitude.

(ii) Define the Froissart—Gribov continuation of the O(3) partial wave amplitudes. Assumption (i) affects the continuation.

(iii) Write the generalized Sommerfeld—Watson transform.

(iv) Assume poles in complex angular momentum. Obtain the Regge asymptotic behavior.

Although this method is almost the reverse of ours, since the assumptions are identical, we of course expect identical conclusions. Specifically, the Regge behavior must be conform to the assumptions (i), although the manner in which the information from (i) is translated into the Froissart—Gribov continuation may be quite subtle. It is for this and pedagogical reasons that we have adopted a more heuristic approach in which the connection between the assumed analytic structure and Regge behavior is more transparent. Indeed the technical difficulties in carrying out this conventional approach are quite awesome, and it may be that our heuristic approach can serve as a useful guide.

---

* To apply the Steinmann relations as we apply (D) one must assume that $(-s_A)^{\alpha_A}(-s_B)^{\alpha_B}$ represents independent cuts in s_A and s_B. Higher order Landau singularities do not always have this property (see refs. [111,112]).

We feel that a rigorous development of the conventional approach would be quite valuable. Actually a good deal of progress has been made in this direction recently by Goddard and White [67] and White [144,147] and we shall refer to these results from time to time for more rigorous support of our analysis. It is interesting to note that technical difficulties have forced a restriction of a detailed treatment to normal threshold singularities, so the conclusions from both approaches should be comparable.

1.5.2. Group theoretic approach

The O(2,1) [and O(3,1)] approach to multi-Regge behavior [13,136,89,90], which is a generalization of Sertorio and Toller's treatment [123,132] of the four-particle amplitude, has also been quite fashionable. It has the advantage of directly treating the amplitude in the physical scattering region of interest. However, the expansion of the amplitude in terms of O(2,1) representations by itself does not give any information. It is only by identifying the O(2,1) representation label with the crossed channel angular momentum, using the equivalence to the O(3) Sommerfeld–Watson-analysis [20,133,108,67] that one knows what representations are expected to be present. Thus in the end one must return to the conventional approach. In any case, again at some stage, information on the singularity structure of the amplitude must be introduced. We shall not discuss the O(2,1) partial wave analysis here, but we shall occasionally use the O(2,1) method to treat physical region kinematics, since it is particularly convenient and elegant.

The proper little group for a momentum transfers changes discontinuously as t varies [O(2,1) for $t < 0$, O(3,1) or E(2) for $t = 0$, and O(3) for $t > 0$]. However, the full amplitude is smooth at $t = 0$ so this complication can be avoided if we express the amplitude in terms of the invariants instead of the group variables as in step (ii).

2. Regge limits for multiparticle amplitudes

In this section we begin applying the method outlined in section 1.3 to multiparticle amplitudes. Here we present the notation and kinematical analysis, defining angles and asymptotic limits. In subsequent sections we investigate the analytic structure.

2.1. Definition of scattering angles

Before defining the scattering angles for a multiparticle amplitude, it is necessary to decide in which channels and in which c.m. frames the partial wave projection is desired. To illustrate the procedure, let us consider the amplitude for the process aa' → b'c̄c' shown in fig. 2.1. (All particles have spin and parity $J^P = 0^+$.) The particle labels are taken by convention to refer to incoming particles, and the momenta are $p_a, p_{a'}, p_{b'} = -p_{\bar{b}'}, p_c = -p_{\bar{c}}, p_{c'} = -p_{\bar{c}'}$, respectively where the bars denote antiparticles. The channel invariants $t_1 = Q_1^2 = (p_a + p_{a'})^2$ and $t_2 = Q_2^2 = (p_c + p_{c'})^2$. We have also indicated for future reference the parameters α_1 and α_2 of the leading Regge trajectories in the (aa') and (cc') channels respectively, and the invariants $s_1 \equiv s_{a'b'} = (p_{a'} + p_{b'})^2$, $s_2 \equiv s_{b'c'} = (p_{b'} + p_{c'})^2$; $s_{12} \equiv s_{ac} = (p_a + p_c)^2$. Our convention for labeling the channel invariants is that the letters a, b, c, ... always refer to the particles in the channel. This provides a unique notation for each channel. Among all the channel invariants overlapping one or more momentum
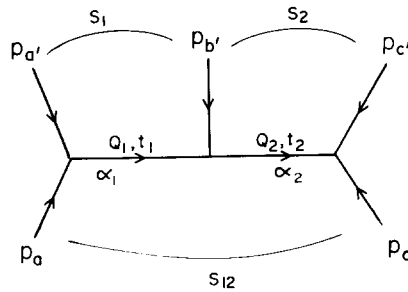
Fig. 2.1. Five-particle diagram showing notation.
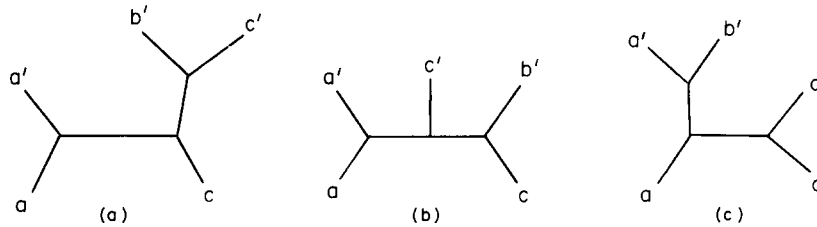
Fig. 2.2. Alternative coupling schemes for the five-particle amplitude.

transfers Q_i, we single out one, as shown in fig. 2.1, and give it a numerical subscript, corresponding to the momentum transfer(s) which it overlaps.

We intend to define the scattering angles appropriate to the partial wave decomposition in the rest frame of Q_1 and in the rest frame of Q_2. This stipulation defines a "coupling scheme" for the multiparticle amplitude. Each coupling scheme is associated with a unique kinematical diagram. There are $\frac{1}{2} \cdot 5! = 60$ unique possibilities or, excluding those related to others by reversing c.m. momenta, 15 for the five particle amplitude of which a few are shown in fig. 2.2. Each of the coupling schemes leads to a particular configuration of scattering angles, angular momenta, and helicities for the five-particle amplitude.

To illustrate the definition of the angles, we refer to the coupling scheme of fig. 2.1. First, treating $(\bar{c}\bar{c}')$ as a single particle of momentum Q_2, we define θ_1 to be the usual c.m. scattering angle for the process $aa' \rightarrow \bar{b}'(\bar{c}\bar{c}')$. Second, in the rest frame of (timelike) Q_2, let θ_2 and ω_{12} be the polar and azimuthal angles of the three-momentum $p_{\bar{c}'}$, when $p_{a'}$ is in the x-z plane and $p_{\bar{b}'}$ is along the positive z axis (fig. 2.3). The angle ω_{12} is the helicity angle or Toller angle [13]. Its

Fig. 2.3. Alignment of three-momenta in the rest frame of Q_2 showing the definition of angles θ_2 and ω_{12}.

Fig. 2.4. Six-particle amplitude.

Fourier components give the Jacob—Wick [86] helicity of the quasi-particle $(\bar{c}c')$ in the rest frame of Q_1. It also happens to give the helicity of the quasi-particle (aa') in the rest frame of Q_2, since the spinless particle b' does not change the helicity at the vertex.

Having understood the five-particle kinematics, the six-particle function presents no new difficulties, since it can be treated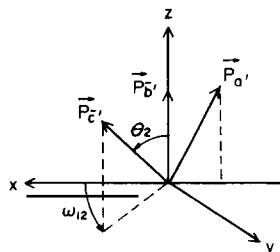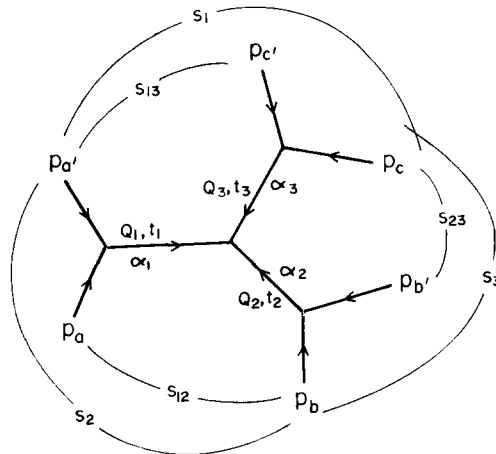 as a five-particle amplitude if we lump two of its particles together. Consider the coupling scheme shown in fig. 2.4. Lumping $(\bar{c}c')$, we follow the procedure for the five-particle amplitude described above, and define scattering angles θ_1 and θ_2 and Toller angle ω_{12}. Lumping $(\bar{b}b')$ together, we define angles θ_1 and θ_3 and Toller angle* $(-\omega_{31})$. This gives five angles, which together with the invariants t_1, t_2 and t_3 give the eight Lorentz invariants needed to describe the amplitude. Within a particular coupling scheme, the Toller angle is always associated with a particular pair of momentum transfers at a vertex.

We could make the assignment of variables symmetrical by introducing a third Toller angle ω_{23}. This angle is related to the two other by the constraint

$$\omega_{12} + \omega_{23} + \omega_{31} = 0 \ . \tag{2.1}$$

Because of the greater complexity of the three-point vertex in this coupling scheme, the relationship between the ω_{ij} and helicities is more subtle. In order to define helicity, it is necessary to have a point of reference to which rotations about the z axis are compared. If we always let $p_{a'}$ define the x-z plane as we have in the above and in fig. 2.3, then ω_{12} is the Fourier transform of λ_2, the helicity carried into the vertex by the line Q_2, and $(-\omega_{13})$ is the Fourier transform of λ_3. Since helicity is conserved at the vertex, the helicity carried in by Q_1 is λ_1 and

$$\lambda_1 + \lambda_2 + \lambda_3 = 0 \ . \tag{2.2}$$

The analysis can be made more symmetrical by choosing instead of $p_{a'}$ some arbitrary direction for the x-z plane in fig. 2.3. Then if we say that ϕ_1 gives the polar angle of $p_{a'}$ and ϕ_2, the polar angle of $p_{\bar{b}'}$ (in place of ω_{12}), etc, and if we define

---

* The minus sign is chosen to make subsequent expressions symmetric.
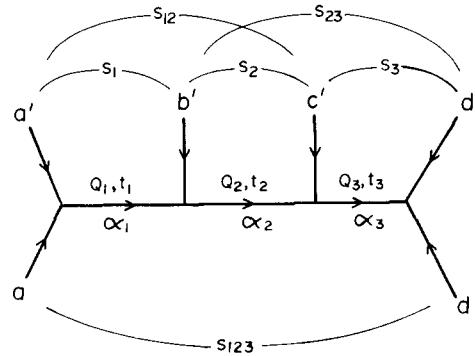
Fig. 2.5. Six-particle amplitude.

$$\omega_{12} = \phi_2 - \phi_1 ; \qquad \omega_{31} = \phi_1 - \phi_3 ; \qquad \omega_{23} = \phi_3 - \phi_2 ; \qquad (2.3)$$

then λ_1, λ_2 and λ_3 are the Fourier components of ϕ_1, ϕ_2 and ϕ_3. Because of helicity conservation, the amplitude never depends on our arbitrary choice of the x-z plane — nor do the ω_{ij}, of course — so we could just as well have put $\phi_1 = 0$, as we did in fig. 2.3, and defined λ_1 using eq. (2.2).

A second coupling scheme is shown in fig. 2.5. We consider the reaction aa' → b̄'c̄'d̄'d. We then proceed to define the scattering angles θ_1 and θ_2 appropriate to the rest frames of Q_1 and Q_2, respectively, and the Toller angle ω_{12}. We then shift one link to the right and, lumping (aa') in the rest frame of Q_3, we construct a diagram analogous to fig. 2.3 (see fig. 2.6a,b), thereby defining θ_3 and ω_{23} as the polar and azimuthal angles of $p_{d'}$.

The generalization to arbitrary amplitudes with arbitrary coupling schemes should be obvious. A systematic procedure is described in section 2.3.
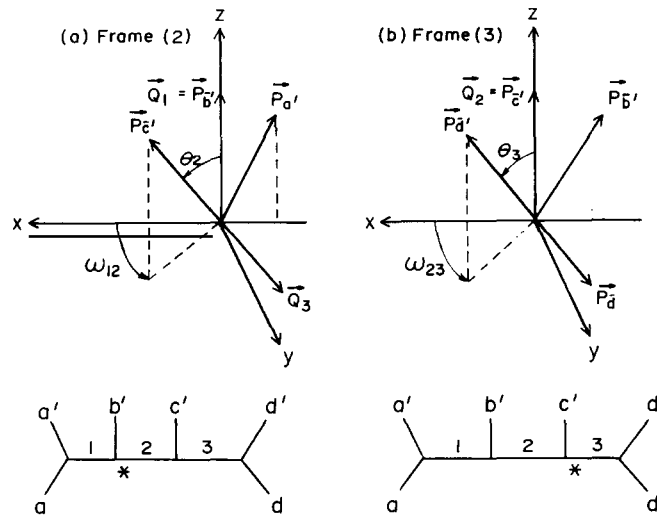
Fig. 2.6. Orientation of three momenta in various frames of reference showing definitions of angles for the six-particle amplitude.

2.2. Definition of asymptotic limits

2.2.1. Definition in terms of angles

We shall consider three types of limits.

(i) Regge asymptotic limit. In this limit the cosine of one of the c.m. scattering angles $\cos \theta_i$ is taken to infinity with all other angles and channel invariants t_j held fixed.

(ii) Helicity asymptotic limit. In this limit the cosine of one of the Toller angles $\cos \omega_{ij}$ is taken to infinity with all other angles and channel invariants t_j fixed.

(iii) Multiple limits. We shall also consider multiple limits found by taking combinations of the above. We always assume a uniformity in the amplitude that permits limits to be reached uniquely in any order.

2.2.2. Single-Regge limit in terms of channel invariants

How are these asymptotic limits expressed in terms of channel invariants? Let us consider the limit $\cos \theta_1 \to \infty$ in the five-particle amplitude of fig. 2.1. It is useful to distinguish two classes of invariants: those that overlap the channel of momentum transfer t_1, i.e. the Regge line α_1, and those that do not. The six invariants

$$s_{a'b'}, \; s_{ab'}, \; s_{a'c'}, \; s_{ac'}, \; s_{a'c}, \; s_{ac} \; , \tag{2.4}$$

all overlap, whereas the four invariants

$$t_1, \; t_2, \; s_{b'c'}, \; s_{b'c} \; , \tag{2.5}$$

do not.

All invariants overlapping t_1 have in common the property that they are linear in $\cos \theta_1$ and in $\sin \theta_1$ with coefficients in the linear expression depending on non-overlapping invariants and on ω_{12}. For example, it is straightforward to show that

$$s_{a'b'} \equiv s_1 = m_{a'}^2 + m_{b'}^2 - 2E_{a'}E_{b'}^{(1)} + 2p_a p_{b'}^{(1)} \cos \theta_1 \; ,$$

$$s_{b'c'} \equiv s_2 = m_{b'}^2 + m_{c'}^2 + 2E_{c'}E_{b'}^{(2)} - 2p_c p_{b'}^{(2)} \cos \theta_2 \; ,$$

$$s_{ac} = s_{12} = m_a^2 + m_c^2 - 2E_c E_a \cosh q_{12} + 2p_a E_c \sinh q_{12} \, \cos \theta_1 - 2p_c E_a \sinh q_{12} \cos \theta_2$$

$$+ 2p_a p_c \cosh q_{12} \cos \theta_1 \cos \theta_2 - 2p_a p_c \sin \theta_1 \sin \theta_2 \cos \omega_{12} \; ,$$

$$E_{a'} = (t_1 + m_{a'}^2 - m_a^2)/2\sqrt{t_1} \; , \qquad\qquad E_a = (t_1 + m_a^2 - m_{a'}^2)/2\sqrt{t_1} \; ,$$

$$E_{b'}^{(1)} = (t_1 + m_{b'}^2 - t_2)/2\sqrt{t_1} \; , \qquad\qquad E_{b'}^{(2)} = (t_1 - m_{b'}^2 - t_2)/2\sqrt{t_2} \; ,$$

$$E_{c'} = (t_2 + m_{c'}^2 - m_c^2)/2\sqrt{t_2} \; , \qquad\qquad E_c = (t_2 + m_c^2 - m_{c'}^2)/2\sqrt{t_2} \; ,$$

$$p_a = \lambda^{\frac{1}{2}}(t_1, m_{a'}^2, m_a^2)/2\sqrt{t_1} \; , \qquad p_{b'}^{(1)} = \lambda^{\frac{1}{2}}(t_1, t_2, m_{b'}^2)/2\sqrt{t_1} \; , \qquad p_{b'}^{(2)} = \lambda^{\frac{1}{2}}(t_1, t_2, m_{b'}^2)/2\sqrt{t_2} \; ,$$

$$p_c = \lambda^{\frac{1}{2}}(t_2, m_c^2, m_{c'}^2)/2\sqrt{t_2} \; , \qquad \cosh q_{12} = (t_2 + t_1 - m_{b'}^2)/2\sqrt{t_1}\sqrt{t_2} \; ; \tag{2.6a}$$

$$s_{ab'} = -s_1 - t_1 + t_2 + m_{b'}^2 + m_{a'}^2 + m_a^2 \,, \qquad s_{b'c} = -s_2 - t_2 + t_1 + m_{b'}^2 + m_{c'}^2 + m_c^2 \,,$$

$$s_{ac'} = -s_{12} - t_2 + s_1 + m_a^2 + m_c^2 + m_{c'}^2 \,, \qquad s_{a'c} = -s_{12} - t_1 + s_2 + m_c^2 + m_a^2 + m_{a'}^2 \,,$$

$$s_{a'c'} = -s_1 - s_2 + s_{12} + m_a^2 + m_{b'}^2 + m_{c'}^2 \,. \tag{2.6b}$$

Since $s_{b'c'}$ does not overlap t_1, $\cos\theta_2$ depends only on non-overlapping invariants. Therefore, the dependence on the overlapping invariants is as described.

Thus, as $\cos\theta_1 \to \infty$, all overlapping invariants tend to infinity with fixed ratios. All the non-overlapping invariants stay fixed. To fix ω_{12} in this limit, it suffices to fix

$$s_{ac}/s_{a'b'} \equiv s_{12}/s_1 = C \cos\omega_{12} + D \,, \tag{2.7}$$

and this ratio can be used in place of the variable ω_{12}.

Generalizing from this example, we define:

(i) Regge asymptotic limit: *Take to infinity all channel invariants that overlap the Regge line, but fix the ratios between them. Fix, also, the channel invariants that do not overlap the Regge line.*

We find that choosing a particular coupling scheme, defining the scattering angles in that scheme, and taking an asymptotic limit on the angles leads to a well-defined limit on the channel invariants. Had we chosen a second coupling scheme and taken an asymptotic limit on the angles appropriate to the second scheme, we might have obtained a different limit on the channel invariants. Suppose we turn the procedure around. Does a particular asymptotic limit on the channel invariants single out a unique coupling scheme? Not always. Consider the single-Regge limit just discussed in which the invariants (2.4) become asymptotic, while the invariants (2.5) remain fixed. There are actually three coupling schemes in which the invariants (2.4) overlap a Regge line whereas the invariants (2.5) do not. Those are shown in fig. 2.1 and fig. 2.2a, b, corresponding to whether we pair $(\bar{c}\,\bar{c}\,')$, $(\bar{b}'\bar{c}\,')$ or $(\bar{b}'\bar{c})$. The others are ruled out. Any of these three coupling schemes is suitable for analyzing the single-Regge limit.

2.2.3. Helicity asymptotic limit in terms of channel invariants

To illustrate the helicity asymptotic limit we consider, once again, the five-particle amplitude. From (2.6) as $\cos\omega_{12}$ becomes asymptotic, the only asymptotic channel invariants are those overlapping *both* lines α_1 and α_2, namely,

$$s_{ac} \sim s_{a'c'} \sim -s_{ac'} \sim -s_{a'c} \to \infty \,. \tag{2.8}$$

All other invariants remain fixed.

Generalizing from this example, we define:

(ii) Helicity limit: *Take to infinity all channel invariants that overlap both lines connected by the Toller angle. Fix their ratios. Fix all other channel invariants.*

We remark that in taking the helicity asymptotic limit of the six-particle amplitude of fig. 2.4 one must be careful to respect the constraint (2.1), which requires that at least two $\cos\omega_{ij}$'s become asymptotic together.

Specifying the helicity asymptotic limit for the five-particle amplitude in this way singles out a

unique coupling scheme, since there is only one in which the four asymptotic invariants (2.8) overlap two Regge lines and the others do not. For the six-particle amplitude, the correspondence is not unique for isolated values of the invariants, but holds otherwise [110]. We shall avoid these special configurations in our discussion.

2.2.4. Multi-Regge limit in terms of channel invariants

Let us now consider the effect upon the channel invariants of taking two Regge asymptotic limits at the same time (double-Regge limit). For the five-particle amplitude, we see from (2.6) that as $\cos\theta_1$ and $\cos\theta_2$ become asymptotic all invariants overlapping α_1 grow like $\cos\theta_1$, all those overlapping α_2, like $\cos\theta_2$, and all those overlapping both, like the product $\cos\theta_1 \cos\theta_2$,

$$s_1 \equiv s_{a'b'} \sim -s_{ab'} \propto \cos\theta_1 \to \infty , \qquad s_2 \equiv s_{b'c'} \sim -s_{b'c} \propto \cos\theta_2 \to \infty ,$$

$$s_{12} \equiv s_{ac} \sim s_{a'c'} \sim -s_{ac'} \sim -s_{a'c} \propto \cos\theta_1 \cos\theta_2 \to \infty . \tag{2.9}$$

In particular the Toller angle is found from the (fixed) ratio*

$$s_{12}/s_1 s_2 \equiv \eta_{12} = (-t_1 - t_2 + m_b^2 + 2\sqrt{t_1}\sqrt{t_2} \cos\omega_{12})/\lambda(t_1, t_2, m_b^2) . \tag{2.10}$$

Thus we write:

(iii) Multi-Regge limits: *Group the channel invariants according to the Regge lines which they overlap. Ratios of invariants in each group are fixed. Invariants which overlap several lines tend to infinity as the product of invariants overlapping each of the individual lines alone. All invariants not overlapping any asymptotic Regge line are fixed.*

Note that for the five-particle amplitude, specifying the double-Regge limit in terms of the channel invariants singles out a unique coupling scheme (fig. 2.1).

An additional complication arises in discussing limits for amplitudes with six or more particles. Consider the coupling scheme of fig. 2.5. If we follow the prescription (iii) above, the triple-Regge limit is

$$s_1 \to \infty \qquad s_2 \to \infty \qquad s_3 \to \infty ,$$

$$t_1, t_2, t_3 , \qquad \eta_{12} = s_{12}/s_1 s_2 , \qquad \eta_{23} = s_{23}/s_2 s_3 , \qquad \eta_{123} = s_{123}/s_1 s_2 s_3 \text{ fixed} . \tag{2.11}$$

Since the six-particle amplitude depends on only eight Lorentz invariants and not the nine listed here, there must be a constraint. Indeed, when we consider that the angles θ_i can each be replaced by s_i and the angles ω_{ij}, each by η_{ij}, as in (2.10), we see that the fixed ratio η_{123} must depend on the other fixed variables. It is straightforward to show that, in fact,

$$\eta_{123} = \eta_{12}\eta_{23} \quad \text{or} \quad s_{123}s_2 = s_{12}s_{23} . \tag{2.12}$$

In the coupling scheme of fig. 2.4 we would define the triple-Regge limit as

$$s_1 \to \infty \qquad s_2 \to \infty \qquad s_3 \to \infty ,$$

$$t_1, t_2, t_3 , \qquad \eta_{12} = s_{12}/s_1 s_2 , \qquad \eta_{23} = s_{23}/s_2 s_3 , \qquad \eta_{13} = s_{13}/s_1 s_3 \text{ fixed} . \tag{2.13}$$

* The Cambridge notation for η_{12} is the inverse of ours [55].

In this case the η_{ij}'s are related to the ω_{ij}'s through expressions like (2.10), and the constraint (2.1) reduces the nine variables to eight.

2.3. Kinematics for general multi-Regge limits

In this subsection we describe a systematic procedure for defining the scattering angles and working out their connection to the channel invariants for an arbitrary coupling scheme. This is the elegant group-theoretical procedure due to Toller [136] and Bali, Chew and Pignotti [13].

The idea is actually quite simple and is best illustrated by considering the six-particle amplitude in the coupling scheme of fig. 2.5. We recall that to define the angles θ_2 and ω_{12}, we considered a particular orientation of the three-momenta of particles a′, b̄′ and c̄′ in the rest frame of Q_2, shown in fig. 2.6a. Then to define the angles θ_3 and ω_{23}, we considered the analogous orientation of the three-momenta of particles b̄′, c̄′ and d̄′ in the rest frame of Q_3, which we show in fig. 2.6b. The key idea of the Toller analysis is that these frames are related by a simple combination of rotations and Lorentz boosts, and the rotation angles are precisely the same as are necessary for the partial wave analysis. In particular, we see that if we started with the momenta as in fig. 2.6a, we could put them in the configuration of fig. 2.6b by the following sequence of operations: rotate about z by $(-\omega_{12})$; rotate about y by $(-\theta_2)$; boost along the z axis so as to make $Q_3 = 0$. The magnitude of the boost is determined completely by t_1, t_2 and $(m_{c'})^2$. Let us call the Lorentz frame of fig. 2.6a, frame (2) and that of fig. 2.6b, frame (3). Then using superscripts to denote the frame in which the momenta are expressed, we have, in going from frame (3) to frame (2):

$$p^{(2)} = R_z(\omega_{12}) R_y(\theta_2) B_z [q_{c'}^{(3)\to(2)}] p^{(3)} , \qquad (2.14)$$

for any four-momentum p. The R's denote four-by-four rotation matrices, the B's boost matrices, and $q_{c'}^{(3)\to(2)}$, a boost angle. Since

$$Q_2 = Q_3 + p_{c'} , \qquad Q_2^{(2)} = (\sqrt{t_2}, 0, 0, 0) , \qquad Q_3^{(3)} = (\sqrt{t_3}, 0, 0, 0) ,$$

$$Q_3^{(2)} = (\sqrt{t_3} \cosh q_{c'}^{(3)\to(2)}, \sqrt{t_3} \sin\theta_2 \cos\omega_{12} \sinh q_{c'}^{(3)\to(2)} ,$$

$$\sqrt{t_3} \sin\theta_2 \sin\omega_{12} \sinh q_{c'}^{(3)\to(2)}, \sqrt{t_3} \cos\theta_2 \sinh q_{c'}^{(3)\to(2)}) , \qquad (2.15)$$

we find*

$$\cosh q_{c'}^{(3)\to(2)} = (t_2 + t_3 - m_{c'}^2)/2\sqrt{t_2}\sqrt{t_3} ,$$

$$\sinh q_{c'}^{(3)\to(2)} = -\lambda^{\frac{1}{2}}[t_2, t_3, m_{c'}^2]/2\sqrt{t_2}\sqrt{t_3} . \qquad (2.16)$$

The result eqs. (2.15) and (2.16) is the same as what we would have obtained had we been considering the decay of a resonance of mass $\sqrt{t_2}$ to a resonance of mass $\sqrt{t_3}$ and a particle of mass $m_{c'}$.

---

* The boost $q_k^{(j)\to(i)}$ quite generally transforms from the rest frame of p_j to that of p_i with p_k the third momentum at the vertex.
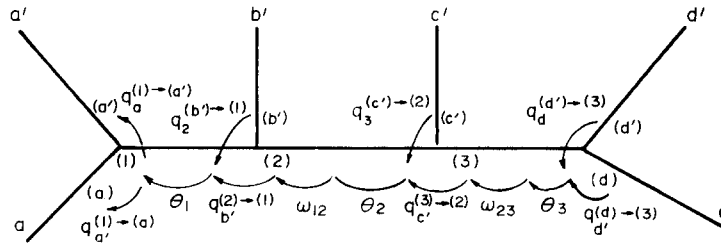
Fig. 2.7. Diagram showing the sequence of Lorentz transformations in the Toller analysis of the six-particle amplitude.

We are led naturally to a sequence of Lorentz frames for describing the orientation of the momenta of the six-particle amplitude. We can indicate the relationship among the frames by drawing the coupling scheme for the six-particle amplitude and letting a position of the diagram be associated with a frame. Thus the frames (2) and (3) are located with an asterisk on the diagrams in fig. 2.6 and the relationship among the frames is summarized in fig. 2.7. One can also define z boosts $q_a^{(1)\to(a')}$, etc., to transform to the rest frame of $p_{a'}$, etc. These are also shown in fig. 2.7.

In this way it is possible to follow a path through diagrams of arbitrary complexity by a sequence of z boosts and rotations. The various channel invariants can be defined in a straightforward manner — for example, for $s_{a'b'}$, reading the transformations from the rest frame of b' to the rest frame of a' from fig. 2.7, we have

$$s_{a'b'} = (m_{a'})^2 + (m_{b'})^2 - 2p_{a'} \cdot p_{b'}$$

$$p_{a'} \cdot p_{b'} = m_{a'} m_{b'} \{ B_z [q_a^{(1)\to(a')}] R_y(\theta_1) B_z [q_2^{(b')\to(1)}] \}_{tt} , \tag{2.17}$$

where $\{\quad\}_{tt}$ denotes the time-time component of the four-by-four Lorentz transformation matrix. Thus

$$s_{a'b'} = (m_{a'})^2 + (m_{b'})^2 - 2m_{a'} m_{b'} [\cosh q_a^{(1)\to(a')} \cosh q_2^{(b')\to(1)} + \sinh q_a^{(1)\to(a')} \sinh q_2^{(b')\to(1)} \cos \theta_1] .$$

$$\tag{2.18}$$

In this manner the expressions of eq. (2.6) can be calculated.

As a further illustration, we show the rotations and boosts for another coupling scheme of the six-point function in fig. 2.8. Note in particular the closed loop of transformations about the middle vertex. Since z boosts commute with z rotations, it follows that

$$\omega_{12} + \omega_{31} + \omega_{23} = 0 , \qquad\qquad q_1^{(3)\to(2)} + q_3^{(2)\to(1)} + q_2^{(1)\to(3)} = 0 . \tag{2.19}$$

Thus there are only two independent ω_{ij}'s at a vertex with three Q's.

Let us count variables to see if the set of $(t_i, \theta_i, \omega_{ij})$ gives the correct number of Lorentz-invariant degrees of freedom. Consider a general coupling scheme with N external lines p_i and therefore $N - 3$ momentum transfers Q_j and $N - 2$ vertices. Such an amplitude has $3N - 10$ Lorentz invariant degrees of freedom.
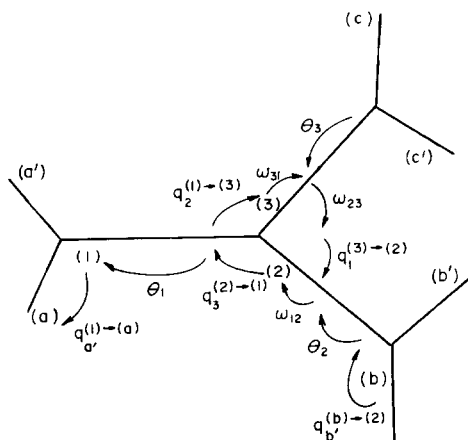
If we define

Fig. 2.8. Diagram showing the sequence of Lorentz transformations in the Toller analysis of the six-particle amplitude.

T = number of vertices with three Q's,

D = number of vertices with two Q's and one p,

S = number of vertices with one Q and two p's.

Then counting p's and vertices, we have

$$1D + 2S = N, \qquad\qquad T + D + S = N - 2. \qquad\qquad (2.20)$$

Therefore, since there are two ω_{ij}'s for each T and one for each D, there are $2T + D = N - 4$ of the ω_{ij}'s. With the addition of $N - 3$ each of t_i and θ_i there are $3N - 10$ altogether, as required.

If we consider the foregoing definition of angles in more abstract terms, we are led to a generalization. The rotations through angles θ_j and ω_{ij} are carried out in the rest frame of Q_j. The reason we chose to rotate was simply that a rotation kept us in the rest frame of Q_j, i.e. the little group of Q_j is O(3) for this case. The most general rotation depends on three Euler angles, say (μ_j, θ_j, ν_j), where μ_j and ν_j refer to z rotations. Had we used this full rotation in place of (ω_{ij}, θ_j) in the sequence of fig. 2.7, we see that each of the $q_x^{(j) \to (i)}$ z boosts would have been preceded by a z rotation of μ_j and followed by a z rotation of ν_j. Since z boosts commute with z rotations, the channel invariants would actually depend only on the sum $\nu_j + \mu_j = \omega_{ij}$. So our choice of angles is completely general.

We are generally interested in performing the above analysis for timelike Q_j. The partial wave analysis on the rotation $R_z(\mu_j) R_y(\theta_j) R_z(\nu_j)$ then gives the angular momentum in the t_j channel and a Regge pole is naturally supposed to lead to the behavior $(\cos \theta_j)^{\alpha_j}$. However, the real beauty of the Toller analysis is that it can be performed for any Q_j. In general, in place of the rotation $R_z(\mu_j) R_y(\theta_j) R_z(\nu_j)$, there should appear a transformation in the little group of Q_j. Thus, for spacelike Q_j, instead of the rest frame, we could work in the Breit frame for which

$$Q_j = (0, 0, 0, \sqrt{-t_j}), \qquad\qquad (2.21)$$

and the rotation would be replaced by the O(2,1) transformation $R_z(\mu_j) B_x(\zeta_j) R_z(\nu_j)$, which preserves Q_j. These are the variables used by Bali, Chew and Pignotti [13]. Of course the vertex z boosts $q_k^{(i) \to (j)}$ would need modification in some cases, since some of them would relate Breit

frames to rest frames. From time to time we will refer to the O(2,1) analysis since it gives a convenient means of obtaining a convenient set of independent variables in the physical region $t_j < 0$.

Whether one begins with an O(3) or O(2,1) parametrization, as long as the Regge limit is defined as $\cos \theta_j \to \infty$ or $\cosh \zeta_j \to \infty$, the channel invariant prescription for the Regge limit is the same.

2.4. Rapidity variables

It is well known that the major contribution to cross sections for particle production
$a + b \to c_1 ... + c_n$ in the (ab) c.m. system is confined to small transverse momentum ($|p_\perp| \lesssim 0.5$ GeV). Since the multi-Regge limits for the $2 \to n$ process also respect this restriction, it is convenient to choose p_a and p_b along the z axis and parametrize the momenta by their rapidity y and transverse momenta $p_\perp = (p_x, p_y)$

$$p_i = (\omega_i \cosh y_i, p_{x_i}, p_{y_i}, \omega_i \sinh y_i) \tag{2.22}$$

where $i = a, b, 1, ..., n$ for $p_a, p_b, p_{c_i} \equiv p_i$. The transverse energy ω_i is given by

$$\omega_i^2 = m_i^2 + p_{\perp i}^2 . \tag{2.23}$$

In rapidity variables, the Lorentz invariant volume element is

$$d^3 p / E = d^2 p_\perp \, dy , \tag{2.24}$$

and a Lorentz boost along the z axis is a translation $y_i \to y_i +$ const. Sometimes it is convenient to pick the lab frame for target a:

$$p_a = (m_a, 0, 0, 0) , \qquad\qquad p_b = (m_b \cosh Y, 0, 0, m_b \sinh Y) , \tag{2.25}$$

where the total rapidity $Y \to \infty$ as $s \to \infty$,

$$s = (p_a + p_b)^2 = m_a^2 + m_b^2 + 2 m_a m_b \cosh Y \sim m_a m_b \, e^Y . \tag{2.26}$$

As $s \to \infty$ the longitudinal phase space for the outgoing particles (c_i) extends from $y_i \approx y_a = 0$, to $y_i \approx y_b = Y$ [47]. Now we may define Regge limits for $a + b \to c_1 + ... + c_n$.
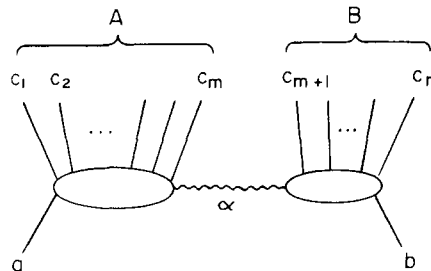
Fig. 2.9. General single-Regge diagram.
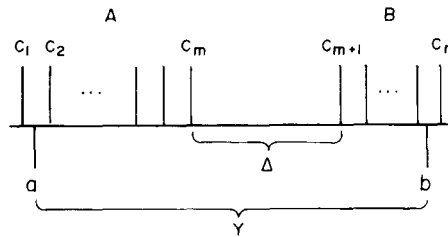
Fig. 2.10. Rapidity plot for the limit of fig. 2.9.

For simplicity consider first the single-Regge limit a + b → A + B where A is the group of particles $(c_1, c_2, ... c_m)$ on the left (see fig. 2.9) and B is the group on the right $(c_{m+1}, ..., c_n)$. According to the rule (i) in section 2.2.2 above, all channel invariants overlapping the line α must become asymptotic. All others remain fixed. Since

$$s_{ij} = (p_i + p_j)^2 = m_i^2 + m_j^2 - 2p_{\perp i} \cdot p_{\perp j} + \omega_i \omega_j \cosh(y_i - y_j) \tag{2.27}$$

we see that the cluster A must be separated from cluster B by a large gap in rapidity which grows like Y as shown in fig. 2.10. Moreover, the relative spacing of particles within a cluster is fixed. It is readily verified that all overlapping invariants must grow with fixed ratios.
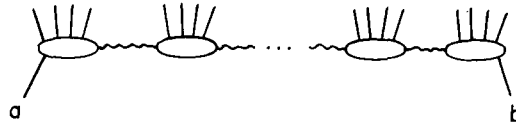
Fig. 2.11. General multi-Regge limit of the chain type.

The generalization to multi-Regge limits of the chain type shown in fig. 2.11 is obvious. There is a large rapidity gap separating each cluster. The rapidity plot is not so useful for describing helicity asymptotic limits or branching multi-Regge limits as in fig. 2.4. However, it is extremely useful for inclusive processes (section 6).

3. The five-particle amplitude

We proceed with a systematic analysis of the five-particle amplitude. It is the simplest of the multiparticle amplitudes, yet illustrates almost all of the essential complications.

3.1. Single-Regge limit

Consider the amplitude of fig. 3.1. In the physical region for aa' → $\overline{b}'\overline{c}\,\overline{c}'$ the partial-wave expansion in the t_1 channel is

$$A_5(t_1, \theta_1, \omega_{12}, \theta_2, t_2) = \sum_{J_1=0}^{\infty} \sum_{\lambda=-J_1}^{J_1} d_{0\lambda}^{J_1}(\cos\theta_1) \exp(i\lambda\omega_{12}) a(J_1, \lambda, \theta_2, t_1, t_2). \tag{3.1}$$
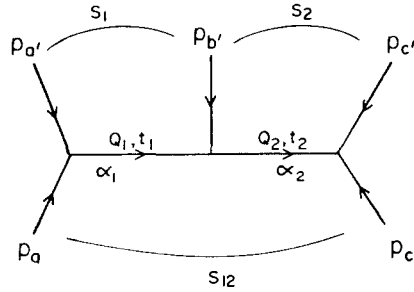
Fig. 3.1. Diagram for five-particle amplitude.

This resembles the partial wave expansion of a four-particle amplitude with one external particle (the quasi-particle $\bar{c}\bar{c}'$) with a spectrum of helicities λ. So let us suppose for the moment that the discussion of section 1.2 carries through, and a factorizable pole in complex J_1 at $\alpha_1(t_1)$ leads to the asymptotic behavior

$$A_5 \sim \Gamma[-\alpha_1(t_1)]\, \tilde{\beta}_1(t_1)\, (\cos\theta_1)^{\alpha_1(t_1)} \sum_{\lambda=-\infty}^{\infty} \exp(i\lambda\,\omega_{12})\, \tilde{R}_\lambda(\theta_2,\, t_1,\, t_2)\,, \tag{3.2}$$

or equivalently

$$A_5 \sim \Gamma[-\alpha_1(t_1)]\, \tilde{\beta}_1(t_1)\, (\cos\theta_1)^{\alpha_1(t_1)} \tilde{R}(\omega_{12},\, \theta_2,\, t_1,\, t_2)\,, \tag{3.3}$$

where $\tilde{R}_\lambda$ is the Fourier transform of $\tilde{R}(\omega_{12})$.

We can then proceed to write the asymptotic behavior (3.3) in terms of the invariants just as we did with the four-point function.

From (2.6) we see that as $\cos\theta_1 \to \infty$

$$s_1 \equiv s_{a'b'} \sim -s_{ab'} \propto \cos\theta_1 \to \infty \tag{3.4}$$

$$s_{12} \equiv s_{ac} \sim -s_{a'c} \sim -s_{ac'} \sim s_{a'c'} \propto \cos\theta_1 \to \infty\,, \qquad s_2,\, t_1,\, t_2,\, s_1/s_{12} \text{ fixed}\,. \tag{3.5}$$

We then rewrite (3.3) as

$$A_5 \sim \Gamma[-\alpha_1(t_1)]\, \beta_1(t_1)\, (s_1)^{\alpha_1(t_1)}\, R(s_1/s_{12},\, s_2,\, t_1,\, t_2)\,, \tag{3.6}$$

where we have chosen as independent variables

$$s_1,\, s_2,\, s_1/s_{12},\, t_1,\, \text{and } t_2\,. \tag{3.7}$$

Had we chosen to replace $\cos\theta_1$ with some overlapping invariant besides s_1, the result would have been merely a redefinition of R. If we analytically continue in t_1 and t_2 until they are sufficiently negative, the limit (3.5) is physical for the process $ac \to \bar{a}'\bar{b}'\bar{c}'$.

When we then proceed to study the phase of (3.6), a complication arises. The real axis singularities of $s_{ac} = s_{12}$ are mapped into the s_1 plane and the (s_1/s_{12}) plane through the constraint that ω_{12}, and therefore s_1/s_{12}, be fixed. Furthermore, the asymptotic singularities due to s_{12} can move
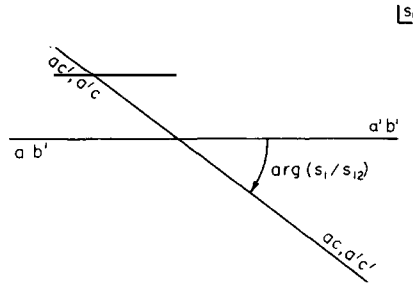
Fig. 3.2. Location of asymptotic singularities in s_1 when s_1/s_{12} is fixed. The channels contributing the singularities are indicated.

off the real axis in s_1 as s_1/s_{12} is varied. If we consider all the singularities in the various channel invariants, we find that they produce two classes of singularities in s_1 [see (3.5)]. One class remains on the real axis in the asymptotic region. The channels which produce these are

$$S_{ab'}, S_{a'b'} , \tag{3.8}$$

i.e. all invariants that grow like s_1, and so overlap only the line α_1 in fig. 3.1. The other class lies asymptotically on a line intersecting the origin in s_1, inclined at an angle to the real axis given by $\arg(s_1/s_{12})$ (see fig. 3.2). Channels producing these are

$$S_{ac}, S_{ac'}, S_{a'c}, S_{a'c'} , \tag{3.9}$$

i.e. all invariants that grow like s_{12}, and so overlap both lines α_1 and α_2 in fig. 3.1. Therefore, for an arbitrary choice of $\arg(s_1/s_{12})$ there is a discontinuity in the asymptotic phase associated with each of the four rays in fig. 3.2. From the single-Regge expression alone, it is not possible to divide the phase discontinuity into contributions from each of the two classes of singularities. Even for $\arg(s_1/s_{12}) = 0$ the phase of (3.6) is not given by the simple signature factor $\xi_1 = \exp(-i\pi\alpha_1) + \tau_1$ for s_1 just above its cut because generally there is a phase arising from the s_{12} cut, i.e. singularities in s_1/s_{12}.

The troublesome singularities in s_1/s_{12} in $R(s_1/s_{12}, s_2, t_1, t_2)$, which do not permit a complete specification of the phase of (3.6), correspond to singularities in $\cos\omega_{12}$ in (3.3). These clearly arise from a divergence of the helicity sum in (3.2). In retrospect we see that our analogy between (3.1) and the partial wave expansion of a four-particle amplitude with a particle of helicity λ is really suspect. When J_1 becomes complex, one must deal with an infinite helicity sum, which we have seen is divergent. This was a serious impediment to early attempts to generalize the Regge analysis to multiparticle amplitudes [109,10,54]. It now seems that the way to overcome it is to perform a Sommerfeld–Watson transform in the helicity λ before performing Sommerfeld–Watson transforms in angular momentum [67]. Using this technique, White [144,146,147] has recently made considerable progress in the rigorous treatment of Regge behavior of multiparticle amplitudes.

We expect from the above discussion that the singularities in s_1/s_{12} in $R(s_1/s_{12}, s_2, t_1, t_2)$ are determined by the singularities in the complex helicity plane. In section 3.5 this will be verified. However, we first wish to discuss the simpler case of the double-Regge limit of A_5, since the analysis can be carried considerably further without explicitly introducing complex helicity.

3.2. Double-Regge limit

The double-Regge limit is obtained by taking $\cos\theta_1$ and $\cos\theta_2$ to infinity, fixing ω_{12}, t_1, and t_2. Using the notation of section 3.1 and referring to (2.9), we find that this limit corresponds to taking

$$s_1 = s_{a'b'} \sim -s_{ab'} \propto \cos\theta_1 \to \infty \,, \qquad s_2 = s_{b'c'} \sim -s_{b'c} \propto \cos\theta_2 \to \infty \,, \qquad (3.10)$$

$$s_{12} = s_{ac} \sim -s_{a'c} \sim -s_{ac'} \sim s_{a'c'} \propto \cos\theta_1 \cos\theta_2 \to \infty \,, \qquad t_1, t_2, \eta_{12} = s_{12}/s_1 s_2 \text{ fixed} \,, \qquad (3.11)$$

where

$$\eta_{12} = \{2\sqrt{t_1}\sqrt{t_2}\cos\omega_{12} - t_1 - t_2 + m_b^2\}/\lambda(t_1, t_2, m_b^2) \,. \qquad (3.12)$$

As for the partial wave analysis, carrying the projection (3.1) one step further, we get

$$A_5(t_1, \theta_1, \omega_{12}, \theta_2, t_2) = \sum_{J_1 J_2} \sum_{|\lambda| \leqslant J_1, J_2} d_{0\lambda}^{J_1}(\cos\theta_1)\exp(i\lambda\omega_{12})d_{\lambda 0}^{J_2}(\cos\theta_2)a(J_1, J_2, \lambda; t_1, t_2). \quad (3.13)$$

As usual we suppose the Sommerfeld–Watson transformation carries through and factorizable poles at $J_1 = \alpha_1(t_1)$, $J_2 = \alpha_2(t_2)$ give the "double-Regge" asymptotic behavior

$$A_5 \sim \Gamma[-\alpha_1(t_1)]\,\tilde\beta_1(t_1)\,(\cos\theta_1)^{\alpha_1(t_1)} \sum_{\lambda=-\infty}^{\infty} \tilde R_\lambda(t_1, t_2)\exp(i\lambda\omega_{12})(\cos\theta_2)^{\alpha_2(t_2)}\Gamma[-\alpha_2(t_2)]\,\tilde\beta_2(t_2) \,. \tag{3.14}$$

Re-expressing (3.13) in terms of channel invariants with the replacements $\cos\theta_1 \to s_1$, $\cos\theta_2 \to s_2$, we have

$$A_5 \sim \beta_1(t_1)\,\Gamma[-\alpha_1(t_1)]\,s_1^{\alpha_1(t_1)}\bar R(t_1, t_2; \eta_{12})s_2^{\alpha_2(t_2)}\,\Gamma[-\alpha_2(t_2)]\,\beta_2(t_2) \,. \qquad (3.15)$$

With t_1 and t_2 sufficiently negative, this double-Regge expression is valid in the physical region for the process $ac \to \bar a'\bar b'\bar c'$. The asymptotic phase of the amplitude is again determined by knowing where the singularities appear in the channel invariants. Qualitatively speaking, the structure is the same as in the single Regge limit. However, as we shall see in the next section, we can now specify the phase discontinuities across all cuts in fig. 3.2!

3.3. Singularities, signature and phases

It is rather surprising that with the relatively few assumptions listed in section 1.4, it is possible to put strong restrictions on the form of the double-Regge vertex in the five-line amplitude [51, 76]. As noted in section 3.1, there are two classes of asymptotic singularities in s_1, and by the same token, there are two classes in s_2. These are shown in fig. 3.3. We invoke assumption (D) and require that the discontinuity across the singularity due to channel $a'b'$, $\text{disc}_{a'b'}A_5$, not have itself a discontinuity across the singularities due to channels $b'c$ or $b'c'$, since these channels overlap the channel $a'b'$. It may have a discontinuity due to channels ac or ac', however, since these do not
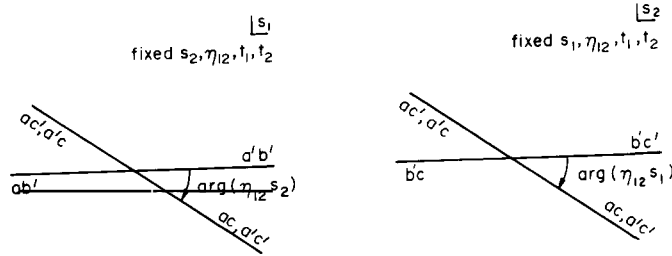
Fig. 3.3. Complex planes of s_1 and s_2 showing locations of asymptotic singularities contributed by channels indicated.

overlap the channel $a'b'$. So the part of the amplitude with a right-hand cut in s_1 may not have cuts in s_2 but may have cuts s_{12}. We can get this part of the amplitude from (3.15) by requiring $\bar{R}(\eta_{12})$ to have a term with a factor $(\eta_{12})^{\alpha_2}$ which cancels the s_2 cuts and replaces them by allowed s_{12} cuts. So we can write the part of A_5 that contributes to $\mathrm{disc}_{a'b'}A_5$ as

$$(-s_1)^{\alpha_1}(-s_{12})^{\alpha_2-\alpha_1}V_2(\eta_{12}) + (-s_1)^{\alpha_1}s_{12}^{\alpha_2-\alpha_1}V_2'(\eta_{12}), \tag{3.16}$$

where V_2 and V_2' have no discontinuities in η_{12} as η_{12} is rotated about its origin*. The singularities of the expression (3.16) are clearly contained in the set shown in fig. 3.3, if we draw the cuts of $(-s_1)^{\alpha_1-\alpha_2}$ and $(-s_{12})^{\alpha_2}$ to the right in s_1 and s_{12}. If we choose the phase to be real and positive when s_1 and s_{12} are negative, real analyticity for these terms then requires V_2 and V_2' to be real functions of η_{12}, for t_1, t_2 below their thresholds. In the physical region for ac $\to$ $\bar{a}'\bar{b}'\bar{c}'$ the phase of this term is given by the factors $(-s_{12})^{\alpha_2} = \exp(-i\pi\alpha_2)s_{12}^{\alpha_2}$ and $(-s_1)^{\alpha_1-\alpha_2} = \exp\{-i\pi(\alpha_1-\alpha_2)\}s_1^{\alpha_1-\alpha_2}$. To get the part of A_5 that contributes to $\mathrm{disc}_{ab'}A_5$ one merely replaces $(-s_1)$ by s_1 in the above expression and writes different V's. Since ab' and $a'b'$ are overlapping channels, this additive separation of left- and right-hand cuts in s_1 is required. To get the parts that contribute to $\mathrm{disc}_{b'c'}A_5$ or $\mathrm{disc}_{b'c}A_5$, one interchanges 1 and 2 in the above expressions. The whole amplitude is the sum of these parts. The sets of allowable singularities in A_5 can be neatly summarized by means of the tree diagrams shown in fig. 3.4. This exhaust all the possibilities, since for general values of $\alpha_1(t_1)$ and $\alpha_2(t_2)$ it is not possible to construct an asymptotic term consistent with (3.15) that has neither the ab, $a'b$, $b'c$ nor $b'c'$ discontinuity. (A term of the form $(-s_{12})^\delta = (-s_1)^\delta(-s_2)^\delta(-\eta_{12})^\delta$ might be considered, but then $\alpha_1(t_1)=\alpha_2(t_2)$, which is not true for moving trajectories.)

---

* This form of the amplitude must be modified for the case that there are an odd number of pseudo-scalar particles in the five-particle process, since the amplitude is analytic in the channel invariants only after removing a factor $\epsilon_{\mu\nu\rho\sigma}p_{a\mu}p_{a'\nu}p_{b'\rho}p_{c'\sigma}$.
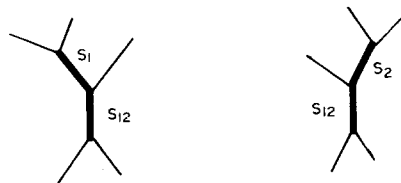

Fig. 3.4. Tree diagrams representing possible simultaneous discontinuities in asymptotic variables in the five-particle amplitude. Each heavy line can refer to a right-hand or left-hand cut.
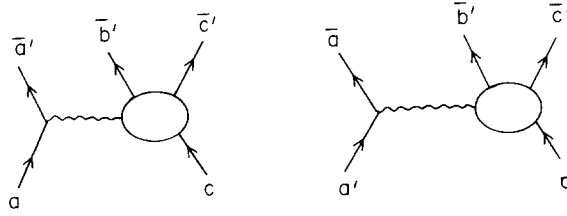
Fig. 3.5. Five-line amplitudes related by crossing.

If we introduce the assumption that Regge trajectories have definite signature, we reduce the number of independent vertex functions V, V', since signature implies a symmetry under interchanging a and a' and c and c'. How do we define signature for multiparticle amplitudes? Let us consider the trajectory α_1. We want the asymptotic amplitudes for the two processes shown in fig. 3.5 to be equal (opposite in sign) if the trajectory has positive (negative) signature. The two physical amplitudes are related by crossing, which is accomplished by continuing the amplitudes from the physical region of the first process to the physical region of the second. All channel invariants overlapping the Regge line change signs during the continuation. It is simplest to follow this continuation by examining the asymptotic form for A_5 as we have done above, term by term, and performing the appropriate change of phase in each term.

In the physical region for the process on the left in fig. 3.5, the invariants s_{ac}, $s_{a'c}$, $s_{a'b'}$ and $s_{b'c'}$ are all above their positive real axis cuts. Therefore, s_{12}, s_1 and s_2 are above their right-hand cuts. In the physical region for the process on the right, the invariants $s_{a'c}$, $s_{ac'}$, $s_{ab'}$ and $s_{b'c'}$ are all above their positive real axis cuts. Therefore s_{12} and s_1 are below their left-hand cuts and s_2 remains unchanged.

These considerations, applied to the decomposition of A_5 described above for Regge trajectories with signatures $\tau_1 = \pm 1$, $\tau_2 = \pm 1$, result in the following expression for the double-Regge asymptotic amplitude*:

$$A_5 \sim \beta_1(t_1)\,\beta_2(t_2)\,\Gamma(-\alpha_1)\,\Gamma(-\alpha_2)\,\{[(-s_2)^{\alpha_2-\alpha_1}(-s_{12})^{\alpha_1}\,V_1(\eta_{12})+(-s_1)^{\alpha_1-\alpha_2}(-s_{12})^{\alpha_2}\,V_2(\eta_{12})]$$

$$+ \tau_1[(-s_2)^{\alpha_2-\alpha_1}\,s_{12}^{\alpha_1}\,V_1(\eta_{12})+s_1^{\alpha_1-\alpha_2}\,s_{12}^{\alpha_2}\,V_2(\eta_{12})] + \tau_2[s_2^{\alpha_2-\alpha_1}\,s_{12}^{\alpha_1}\,V_1(\eta_{12})+(-s_1)^{\alpha_1-\alpha_2}\,s_{12}^{\alpha_2}\,V_2(\eta_{12})]$$

$$+ \tau_1\tau_2[s_2^{\alpha_2-\alpha_1}(-s_{12})^{\alpha_1}\,V_1(\eta_{12})+s_1^{\alpha_1-\alpha_2}(-s_{12})^{\alpha_2}\,V_2(\eta_{12})]\}\,. \tag{3.17}$$

Introducing signature has reduced the number of independent discontinuity-free functions V from eight to two. This expression can represented diagrammatically as in fig. 3.6. The first diagram corresponds to the first two terms of (3.17) with only right-hand cuts. The correspondence between diagrams with crosses and the other terms of (3.17) can be found by associating terms multiplied by τ_1, τ_2 and $\tau_1\tau_2$. A cross on a line indicates that all invariants overlapping that line have right-hand cuts changed to left-hand cuts and vice-versa.

Traditionally signature for multi-Regge amplitudes has been discussed by assuming that a generalization of (1.8) exists, that expresses the full amplitude as a sum over signatured amplitudes, which like $A^\tau(s, t)$ in (1.13) have only the right-hand cuts in the energy variables. In the case of the

---

* We have suppressed the t_1 and t_2 arguments of α_1, α_2, V_1 and V_2.
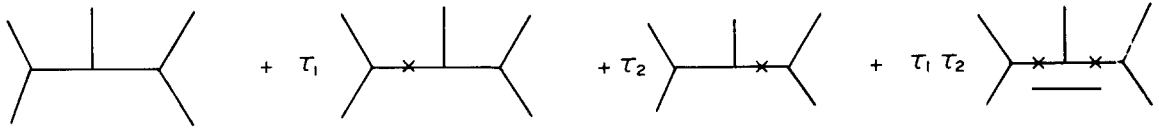
five-particle amplitude, there are three energy invariants, s_1, s_2 and s_{12}, which can have either right-hand or left-hand cuts, making altogether $2^3 = 8$ possible combinations. However, simultaneous discontinuities in all three invariants are excluded by our assumptions, thereby reducing the possible combinations to the four discussed above. Nevertheless, in addition to the signatures τ_1 and τ_2 associated with the angular momenta J_1 and J_2, it is possible to associate a third signature τ_{12} with the helicity λ (equivalently η_{12}) [67]. Thus the generalization of (1.8) is (written in a form appropriate for large energies)

$$A_5(s_1, s_2, \eta_{12}; t_1, t_2) = \sum_{\tau_1, \tau_2, \tau_{12} = \pm 1} \{[A_5^{\tau_1 \tau_2 \tau_{12}}(s_1, s_2, \eta_{12}; t_1, t_2) + \tau_1 A_5^{\tau_1 \tau_2 \tau_{12}}(-s_1, s_2, \eta_{12}; t_1, t_2)$$

$$+ \tau_2 A_5^{\tau_1 \tau_2 \tau_{12}}(s_1, -s_2, \eta_{12}; t_1, t_2) + \tau_1 \tau_2 A_5^{\tau_1 \tau_2 \tau_{12}}(-s_1, -s_2, \eta_{12}; t_1, t_2)] + \tau_{12}[\eta_{12} \leftrightarrow -\eta_{12}]\}. \quad (3.18)$$

Comparing this expression with (3.17) we see that we should associate the Regge behavior of the signatured amplitude with the first two terms of (3.17), which also have only right-hand cuts

$$A_5^{\tau_1 \tau_2 \tau_{12}} \sim \beta_1(t_1) \beta_2(t_2) \Gamma(-\alpha_1) \Gamma(-\alpha_2)[(-s_2)^{\alpha_2 - \alpha_1}(-s_{12})^{\alpha_1} V_1(\eta_{12}) + (-s_1)^{\alpha_1 - \alpha_2}(-s_{12})^{\alpha_2} V_2(\eta_{12})].$$

$$(3.19)$$

Then (3.18) and (3.19) lead to (3.17), where the introduction of vertex signature has only the effect of replacing V_i by

$$V_i(\eta_{12}) = V_i(\eta_{12}) + \tau_i \tau_{12} V_i(-\eta_{12}). \quad (3.20)$$

Thus, requiring a definite vertex signature has the trivial effect of making V_i even odd or in η_{12}. Although the unitary equation for A_5 is diagonal in τ_{12} [145], we do not know if vertex signature remains a good quantum number when all unitarity equations are considered. Actually models do not usually produce Regge poles with a definite vertex signature. For example, in the ordinary dual-resonance model, there are only right-hand cuts in η_{12} whereas in Mandelstam's [100] nonplanar dual model, there are only left-hand cuts [119]. In what follows, we shall often use the traditional signature language and suppress the vertex signature. We will, however, discuss its role in the Sommerfeld–Watson transform in section 3.4.3.

Due to the complicated singularity structure of fig. 3.3 the phase of (3.17) cannot in general be factored into pieces associated with the Regge propagators and vertices. However, when all energy invariants are real, as in the physical region $ac \to \bar{a}'\bar{b}'\bar{c}'$ we may rewrite (3.17) as*

---

* In all of these expressions the t_1 and t_2 arguments have been suppressed in $\alpha_1(t_1)$, $\alpha_2(t_2)$, $\xi_1(t_1)$, $\xi_2(t_2)$, $\xi_{ij}(t_1, t_2)$.

$$A_5 \sim \beta_1(t_1) \, s_1^{\alpha_1} \Gamma(-\alpha_1)[\xi_1 \xi_{21} \eta_{12}^{\alpha_1} V_1(t_1, t_2; \eta_{12}) + \xi_2 \xi_{12} \eta_{12}^{\alpha_1} V_2(t_1, t_2; \eta_{12})]\Gamma(-\alpha_2) s_2^{\alpha_2} \beta_2(t_2) \qquad (3.21)$$

where

$$\xi_i = \exp(-i\pi\alpha_i) + \tau_i \,, \qquad\qquad \xi_{ij} = \exp\{-i\pi(\alpha_i - \alpha_j)\} + \tau_i\tau_j \,.$$

We have used the relation $(-s) \to s \exp(-i\pi)$ above the right-hand cut. Also applicable in the physical region is the expression

$$A_5 \sim \beta_1(t_1) \, s_1^{\alpha_1} \Gamma(-\alpha_1)[\exp(-i\pi\alpha_1) \exp(-i\pi\alpha_2) V(t_1, t_2; \eta_{12} - i\epsilon) + \tau_1 \exp(-i\pi\alpha_2) V(t_1, t_2; \eta_{12} - i\epsilon)$$

$$+ \exp(-i\pi\alpha_1) \tau_2 V_1(t_1, t_2; \eta_{12} - i\epsilon) + \tau_1\tau_2 V(t_1, t_2; \eta_{12} + i\epsilon)]\Gamma(-\alpha_2) s_2^{\alpha_2} \beta_2(t_2) \,, \qquad (3.22)$$

where

$$V(t_1, t_2; \eta_{12}) = (-\eta_{12})^{\alpha_1} V_1(t_1, t_2; \eta_{12}) + (-\eta_{12})^{\alpha_2} V_2(t_1, t_2; \eta_{12}) \,.$$

In order to compare with the Regge behavior of A_4 it is useful to extract the Regge propagators $\xi_i \Gamma(-\alpha_i) s_i^{\alpha_i}$ from (3.21)

$$A_5 \sim \beta_1(t_1)[\xi_1 \Gamma(-\alpha_1) \, s_1^{\alpha_1}] R_{12}^{b'}(t_1, t_2; \eta_{12})[\xi_2 \Gamma(-\alpha_2) s_2^{\alpha_2}] \beta_2(t_2) \qquad (3.23)$$

so that

$$R_{12}^{b'}(t_1, t_2; \eta_{12}) = \xi_2^{-1} \xi_{21} \eta_{12}^{\alpha_1} V_1(t_1, t_2; \eta_{12}) + \xi_1^{-1} \xi_{12} \eta_{12}^{\alpha_2} V_2(t_1, t_2; \eta_{12}) \,.$$

The double-Regge residue R is, of course, not real. The extraction of the signature factors ξ_1, ξ_2 is therefore purely a convention.

The singularity structure (3.17) of the double-Regge vertex was first found in a large class of models by Drummond [55] and Drummond, Landshoff and Zakrewski [56]. The proper treatment of signature leading to the above expressions was first obtained by Drummond, Landshoff and Zakrewski [57]. White [147] has demonstrated the factorization of the Regge pole residues, which allows us to factor out the single-Regge couplings $\beta_1(t_1)$ and $\beta_2(t_2)$ in (3.17).

3.4. Mellin representation

3.4.1. Description and properties of the Mellin representation

The aim of this section is to obtain a Mellin representation of the five-particle amplitude analogous to the representation (1.17) of the four-particle amplitude. This representation will provide a compact summary of the properties of the five-particle amplitude obtained above and also a convenient language for discussing a number of additional properties.

We first discuss the representation and its properties [141] and then discuss its connection to the usual Sommerfeld–Watson transform. The representation for the signatured amplitude is*

---

* Vertex signature is suppressed. We deliberately use the same notation for the Mellin transform parameters as angular momentum and helicity. Even though they are not precisely the same, they serve the same function to leading order in asymptotic expansions.
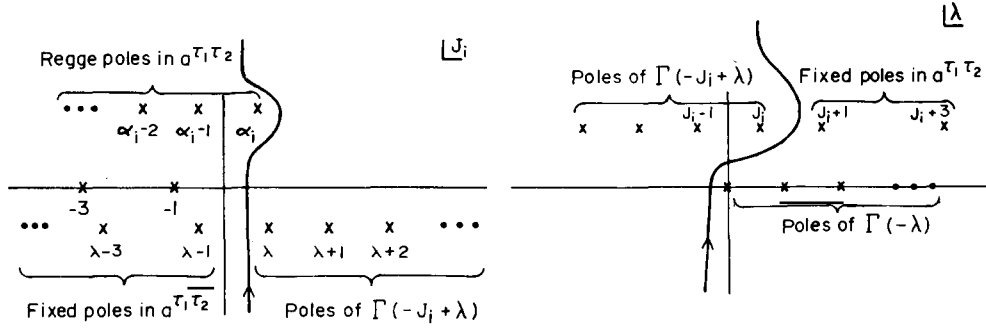
Fig. 3.7. Integration contours for the Mellin representation.

$$A_5^{\tau_1 \tau_2} = \left(\frac{1}{2\pi i}\right)^3 \int d\lambda \int dJ_1 \int dJ_2 \; \Gamma(-\lambda)\, \Gamma(-J_1 + \lambda)\, \Gamma(-J_2 + \lambda)$$

$$\times \; (-s_1)^{J_1 - \lambda} (-s_2)^{J_2 - \lambda} (-s_{12})^\lambda \, a^{\tau_1 \tau_2}(J_1, J_2, \lambda; t_1, t_2) \,. \tag{3.24}$$

The integration contours are shown in fig. 3.7. Let us disregard the fixed poles for the moment. The contours are such that the poles in the Γ functions, which are necessary for the recovery of the partial wave series, lie to the right, whereas all the other singularities lie to the left. Thus closing the λ contour to the right and then the J_i contours to the right yields

$$A_5^{\tau_1 \tau_2} = \sum_{\lambda=0}^{\infty} \sum_{J_1 = \lambda}^{\infty} \sum_{J_2 = \lambda}^{\infty} s_1^{J_1} s_2^{J_2} \left(\frac{s_{12}}{s_1 s_2}\right)^\lambda \frac{a^{\tau_1 \tau_2}(J_1, J_2, \lambda; t_1, t_2)}{\lambda!(J_1 - \lambda)!(J_2 - \lambda)!} \,. \tag{3.25}$$

Recalling (2.6), this is easily seen to agree with the partial wave expansion where a term of given J_1, J_2, λ in (3.25) contributes to angular momenta and helicity equal to or less than that value*. Equation (3.25) can also be obtained by first closing J_i contours to the right. The poles in $\Gamma(-J_i + \lambda)$ pinch the helicity contour against the poles in $\Gamma(-\lambda)$ and produce the poles for integer J_i.

We now compare the double-Regge behavior obtained from the Mellin representation (3.24) with that deduced in sections 3.2 and 3.3. Suppose the partial wave amplitude has the behavior

$$a^{\tau_1 \tau_2} \approx \beta(\lambda; t_1, t_2)/[J_1 - \alpha_1(t_1)][J_2 - \alpha_2(t_2)] \,. \tag{3.26}$$

Shifting the J_i contours to the left and collecting the residues of these poles, we obtain

$$A_5^{\tau_1 \tau_2} \underset{s_1, s_2 \to \infty}{\sim} \frac{1}{2\pi i} \int d\lambda \, \Gamma(-\lambda)\, \Gamma(-\alpha_1 + \lambda)\, \Gamma(-\alpha_2 + \lambda)\, (-s_1)^{\alpha_1 - \lambda} (-s_2)^{\alpha_2 - \lambda} (-s_{12})^\lambda \beta(\lambda; t_1, t_2) \,. \tag{3.27}$$

---

* The representation (3.24) is valid only for an amplitude with all external particles scalar ($J^P = 0^+$) since the polynomial (3.25) is an even function of ω_{12}. For amplitudes with an odd number of pseudoscalar particles, it is necessary to multiply by an overall factor $\epsilon_{\mu\nu\rho\sigma} p_{a\mu} p_{a'\nu} p_{b'\rho} p_{c'\sigma}$ which is odd in ω_{12}.

Comparing with section 3.3, we find

$$V(t_1, t_2; \eta_{12}) = \frac{1}{\Gamma(-\alpha_1)\,\Gamma(-\alpha_2)} \frac{1}{2\pi i} \int d\lambda\, \Gamma(-\lambda)\, \Gamma(-\alpha_1 + \lambda)\, \Gamma(-\alpha_2 + \lambda)\, (-\eta_{12})^\lambda\, \beta(\lambda; t_1, t_2). \quad (3.28)$$

If the behavior of β as $|\lambda| \to \infty$ is less than $|\lambda|^{|\lambda|}$, the λ contour can be closed to the left, yielding

$$V(t_1, t_2; \eta_{12}) = (-\eta_{12})^{\alpha_1} V_1(t_1, t_2; \eta_{12}) + (-\eta_{12})^{\alpha_2} V_2(t_1, t_2; \eta_{12}), \quad (3.29)$$

in complete agreement with (3.21), where

$$V_1(t_1, t_2; \eta_{12}) = \frac{1}{\Gamma(-\alpha_1)\,\Gamma(-\alpha_2)} \sum_{i=0}^{\infty} \frac{1}{i!}\, \Gamma(-\alpha_1 + i)\, \Gamma(-\alpha_2 + \alpha_1 - i)\, \eta_{12}^{-i}\, \beta(\alpha_1 - i, t_1, t_2),$$

$$V_2(t_1, t_2; \eta_{12}) = \frac{1}{\Gamma(-\alpha_1)\,\Gamma(-\alpha_2)} \sum_{i=0}^{\infty} \frac{1}{i!}\, \Gamma(-\alpha_2 + i)\, \Gamma(-\alpha_1 + \alpha_2 - i)\, \eta_{12}^{-i}\, \beta(\alpha_2 - i, t_1, t_2). \quad (3.30)$$

We could have obtained the expressions (3.30) for the double-Regge vertex functions by direct arguments, rather than relying on the Mellin transform [51]. The arguments are based on the following requirements that are satisfied by (3.30):

(i) At the poles in the full five-particle amplitude corresponding to the physical recurrences $\alpha_1(t_1) = J_1$ and $\alpha_2(t_2) = J_2$, the residue must be a polynomial in η_{12} of degree $\min(J_1, J_2)$, since the powers of η_{12} determine the helicity content of the residue through (3.12). It is straightforward to verify that the Γ function arguments in (3.30) must be as shown in order to obtain this result.

(ii) The residue at the physical recurrences $\alpha_1(t_1) = J_1$ and $\alpha_2(t_2) = J_2$ must be the same, regardless of the direction in t_1 and t_2 the pole is approached. This condition also guarantees that the "spurious" poles at $\alpha_1 - \alpha_2 =$ integer but $\alpha_i \neq$ integer cancel between each other in (3.29) in analogy with the identity

$$\frac{1}{\alpha_1 \alpha_2} \equiv \frac{1}{\alpha_1(\alpha_2 - \alpha_1)} + \frac{1}{\alpha_2(\alpha_1 - \alpha_2)}. \quad (3.31)$$

(iii) The discontinuity of the full five-particle amplitude in s_1 must not have poles in t_1, since that invariant overlaps s_1. Since cuts in s_1 come from the term

$$(-s_1)^{\alpha_1 - \alpha_2} (-s_{12})^{\alpha_2} \Gamma(-\alpha_1)\, \Gamma(-\alpha_2)\, V_2, \quad (3.32)$$

taking the discontinuity introduces a factor $\sin\pi(\alpha_1 - \alpha_2)$, which nicely removes poles in t_1 from V_2.

The beauty of (3.24) is that it is a succinct expression of so many necessary features!

From (3.28) we see that the singularities in η_{12} of the double-Regge vertex are directly related to presence of singularities in the complex helicity λ. The two term structure (3.29) arises from helicity poles associated with the two reggeons α_1 and α_2 [67]. Further singularities in λ

would give a double-Regge vertex inconsistent with our general arguments in section 3.3.
The absence of such singularities in (3.28) is traced back to our assumption that the only singularities in λ in (3.24) are those explicitly exhibited by the gamma functions, i.e. there are no "dynamical" helicity singularities in $a^{\tau_1\tau_2}$.* We believe this is a general property of $a^{\tau_1\tau_2}$ and not just the part which has a double-Regge pole. This will be discussed further in section 3.5 below. Here we remark only that the integrand of (3.24) behaves like

$$(-s_1)^{J_1-\lambda} (-s_2)^{J_2-\lambda} (-s_{12})^{\lambda} . \tag{3.33}$$

If the λ contour can be closed to the left, only contributions for $J_i - \lambda = 0, 1, 2, ...$ will lead to an amplitude free of forbidden simultaneous discontinuities in s_1 and s_2.** On the other hand, extra singularities in λ to the right of the contour other than the fixed poles in fig. 3.7 would spoil the partial wave series.

3.4.2. Fixed poles

The above discussion has ignored fixed poles. In the four-particle amplitude these can exist at nonsense-wrong-signature angular momenta

$$J = N \quad \text{for} \quad N = -1, -2, -3, ... \text{ with } \tau = (-)^{N+1} . \tag{3.34}$$

They have the interesting effect that if they occur multiplicatively with Regge poles, they remove nonsense-wrong-signature zeros. Thus

$$A(s, t) \sim \beta(t) \Gamma[-\alpha(t)] (e^{-i\pi\alpha} + \tau)s^{\alpha} , \tag{3.35}$$

normally vanishes for α satisfying (3.34), but if

$$a^{\tau}(J, t) \approx \beta(t)/[J - \alpha(t)] (J - N) , \tag{3.36}$$

eq. (3.35) is replaced by

$$A(s, t) \sim \frac{\beta(t) \Gamma[-\alpha(t)]}{\alpha(t) - N} (e^{-i\pi\alpha} + \tau)s^{\alpha} , \tag{3.37}$$

which is finite at $\alpha(t) = N$.

Analogous fixed poles are expected in the five-particle amplitude. Combining (3.21) and (3.30) we see contributions to the double-Regge limit proportional to

$$(\exp(-i\pi\alpha_1) + \tau_1) \Gamma(-\alpha_1)[\exp\{-i\pi(\alpha_2 - \alpha_1)\} + \tau_1\tau_2] \Gamma(-\alpha_2 + \alpha_1)\beta(\alpha_1; t_1, t_2) \tag{3.38}$$

and

$$(\exp(-i\pi\alpha_2) + \tau_2) \Gamma(-\alpha_2)[\exp\{-i\pi(\alpha_1 - \alpha_2)\} + \tau_1\tau_2] \Gamma(-\alpha_1 + \alpha_2)\beta(\alpha_2; t_1, t_2) . \tag{3.39}$$

Each of these terms exhibits two sets of nonsense-wrong-signature zeros analogous to those in (3.35). We thus expect fixed poles at

---

* Aside from the fixed pole singularities discussed below.

** Contributions for $J_i - \lambda = -1, -2, ...$ are excluded since terms s_i^{-1}, s_i^{-2}, should be interpreted as asymptotic representations of cuts for finite values of s_i. Such helicity singularities are called "nonsense" singularities, since they correspond to helicity greater than angular momentum.

$$J_1 = N_1 \quad \text{for} \quad N_1 = -1, -2, -3, \ldots \text{ with } \tau_1 = (-)^{N_1 + 1}$$

$$J_1 = \lambda + N_1 \quad \text{for} \quad N_1 = -1, -2, -3, \ldots \text{ with } \tau_1 \tau_2 = (-)^{N_1 + 1}, \tag{3.40}$$

and similarly for J_2. These two sets of fixed poles are naturally interpreted as being at nonsense angular momenta with respect to the vertices on either end (the former associated with the two external particles with helicity zero and the latter, with the central vertex with helicity λ).

The possibility of nonsense-wrong-signature fixed poles in the four-particle amplitude is tied to the existence of cuts in angular momentum, which shield them to keep them from violating unitarity. We anticipate a similar connection in the five-particle amplitude. However, the analysis of the five-particle amplitude is not yet sufficiently developed to allow us to investigate these questions and so eqs. (3.40) are conjectural at present. Some support can be obtained from the study of models — we refer the reader to Weis [141] for a discussion.

Let us consider the effect of multiplicative fixed poles in more detail. Suppose

$$a^{\tau_1 \tau_2} \approx \beta(\lambda; t_1, t_2)/(J_1 - N_1)(J_1 - \alpha_1)(J_2 - \alpha_2), \tag{3.41}$$

then

$$A_5^{\tau_1 \tau_2} \sim \frac{1}{\alpha_1 - N_1} \{ \Gamma(-\alpha_1) \Gamma(\alpha_1 - \alpha_2)(-s_{12})^{\alpha_1}(-s_2)^{\alpha_2 - \alpha_1} \beta(\alpha_1; t_1, t_2)$$

$$+ \Gamma(-\alpha_2) \Gamma(\alpha_2 - \alpha_1)(-s_{12})^{\alpha_2}(-s_1)^{\alpha_1 - \alpha_2} \beta(\alpha_2; t_1, t_2)$$

$$- \Gamma(-N_1) \Gamma(N_1 - \alpha_2)(-s_{12})^{N_1}(-s_2)^{\alpha_2 - N_1} \beta(N_1; t_1, t_2)$$

$$- \Gamma(-\alpha_2) \Gamma(\alpha_2 - N_1)(-s_{12})^{\alpha_2}(-s_1)^{N_1 - \alpha_2} \beta(\alpha_2; t_1, t_2) \} + \text{ terms of lower order in } \eta_{12}, \tag{3.42}$$

whereas if

$$a^{\tau_1 \tau_2} \approx \beta(\lambda; t_1, t_2)/(J_1 - \lambda - N_1)(J_1 - \alpha_1)(J_2 - \alpha_2) \tag{3.43}$$

$$A_5^{\tau_1 \tau_2} \sim \frac{\Gamma(-\alpha_2)}{\alpha_1 - \alpha_2 - J_1} [\Gamma(\alpha_2 - \alpha_1)(-s_{12})^{\alpha_2}(-s_1)^{\alpha_1 - \alpha_2} - \Gamma(-N_1)(-s_{12})^{\alpha_2}(-s_1)^{N_1}] \beta(\alpha_2; t_1, t_2)$$

$$+ \frac{\Gamma(-\alpha_1) \Gamma(\alpha_1 - \alpha_2)}{N_1} (-s_{12})^{\alpha_1}(-s_2)^{\alpha_2 - \alpha_1} \beta(\alpha_1; t_1, t_2) + \text{ terms of lower order in } \eta_{12}. \tag{3.44}$$

These behaviors are seen to have the desired effect of removing the nonsense-wrong-signatures zeros, and furthermore the parts of (3.42) and (3.44) with fixed power behavior in the energies drop out in the full amplitude.

3.4.3. Relationship to the Sommerfeld–Watson transform

We now discuss the relationship of the simplified Mellin representation (3.24) to the Sommerfeld–Watson transform. Our dicussion of the Sommerfeld–Watson transform follows Goddard and White [67] and White [145,147]. We refer the reader to these papers for further details.

The double partial-wave expansion for the signatured amplitude is (re-introducing the vertex signature)

$$A_5^{\tau_1\tau_2\tau_{12}} = \sum_{\lambda=-\infty}^{\infty} \sum_{J_1=|\lambda|}^{\infty} \sum_{J_2=|\lambda|}^{\infty} (2J_1+1)(2J_2+1)d_{0\lambda}^{J_1}(\cos\theta_1)d_{\lambda 0}^{J_2}(\cos\theta_2)\exp(i\lambda\omega_{12})a^{\tau_1\tau_2\tau_{12}}(J_1,J_2,\lambda;t_1,t_2).$$

(3.45)

The Sommerfeld—Watson transform proceeds in two steps. First the helicity λ is transformed. We have, suppressing irrelevant labels,

$$A_5(z) = \sum_{\lambda=0}^{\infty} a^>(\lambda)z^\lambda - \sum_{\lambda=-\infty}^{-1} a^<(\lambda)z^\lambda$$

$$= -\frac{1}{2i}\int_{C^>} d\lambda\,\frac{a^>(\lambda)(-z)^\lambda}{\sin\pi\lambda} - \frac{1}{2i}\int_{C^<} d\lambda\,\frac{a^<(\lambda)(-z)^\lambda}{\sin\pi\lambda},$$

(3.46)

where $z = e^{i\omega}$ and the contours are shown in fig. 3.8. A dispersion relation in s_{12}, equivalently z, has been assumed

$$A_5(z) = \int_0^{1-\epsilon} \frac{\text{Im}\,A(z')}{z'-z}\,dz' + \int_{1+\epsilon}^{\infty} \frac{\text{Im}\,A(z')}{z'-z}\,dz',$$

(3.47)

which gives

$$a^>(\lambda) = \int_{1+\epsilon}^{\infty} (z')^{-\lambda-1}\,\text{Im}\,A(z')\,dz'$$
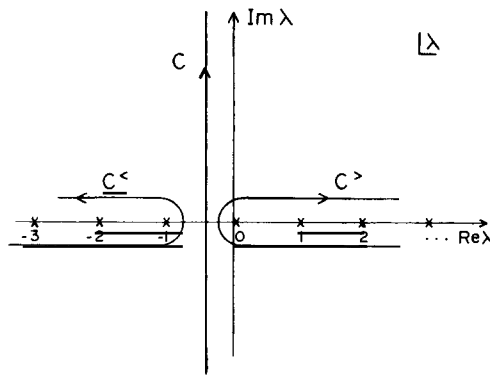
(3.48a)

and

Fig. 3.8. Integration contours in the complex helicity plane.

$$a^<(\lambda) = \int\limits_0^{1-\epsilon} (z')^{-\lambda-1} \operatorname{Im} A(z') \, dz' \ . \tag{3.48b}$$

Right-hand cuts in s_{12} normally map onto positive z and left-hand cuts, onto negative z. An amplitude with definite vertex signature has only right-hand cuts and so permits the integral (3.48) to range only over positive z'. This is crucial for obtaining good behavior as $\lambda \to \infty$ just as in the well-known case of the Sommerfeld–Watson transform of A_4. The amplitudes $a^>(\lambda)$ and $a^<(\lambda)$ have good asymptotic behaviors in the right-half and left-half λ planes respectively. We may thus write (see fig. 3.8)

$$A_5(z) = -\frac{1}{2i} \int\limits_C d\lambda \, \frac{a^>(\lambda) + a^<(\lambda)}{\sin \pi\lambda} \, (-z)^\lambda \ . \tag{3.49}$$

In the second step Sommerfeld–Watson transforms in J_1 and J_2 are performed on the $a^\gtrless(\lambda, s_1, s_2, t_1, t_2)$. The correct complete set of functions is the $d_{0\lambda}^{J_1}(\cos\theta_i)$ [equivalently the Jacobi polynomials $P_{J_i-\lambda}^{(\lambda,\lambda)}(\cos\theta_i)$]. Then

$$a^\gtrless(\lambda) = \sum_{J_1=\lambda}^{\infty} \sum_{J_2=\lambda}^{\infty} (2J_1+1)(2J_2+1) d_{0\lambda}^{J_1}(\cos\theta_1) \, d_{\lambda 0}^{J_2}(\cos\theta_2) \, a^\gtrless(J_1, J_2, \lambda; t_1, t_2) \ , \tag{3.50}$$

which becomes

$$a^\gtrless(\lambda) = \left(-\frac{1}{2i}\right)^2 \int dJ_1 \int dJ_2 \, \frac{d_{0\lambda}^{J_1}(-\cos\theta_1) \, d_{\lambda 0}^{J_2}(-\cos\theta_2)}{\sin \pi(J_1-\lambda) \sin \pi(J_2-\lambda)} \, a^\gtrless(J_1, J_2, \lambda; t_1, t_2) \ . \tag{3.51}$$

The definition of Froissart–Gribov continuations of the $a^\gtrless(J_1, J_2, \lambda; t_1, t_2)$ to complex J_1 and J_2 presents considerable difficulty. White [145] has been able to obtain a satisfactory continuation for one angular momentum and the helicity, but not for J_1, J_2 and λ simultaneously. (His treatment for the most part considered only normal thresholds and thus parallels our assumptions.) We shall however assume that such a continuation exists in the following.

It is clear that there is a close correspondence between (3.49) and (3.51) and the Mellin representation (3.24). In (3.24) when η_{12} is taken to infinity the λ contour should be moved to the left and only singularities at $\lambda = J_i + n_i$ ($n_i = 0, -1, -2, \ldots$) are picked up. In (3.49) $\eta_{12} \to \infty$ corresponds to $z \to \infty$ or $z \to 0$. In either case, one appears to get contributions for integral λ from the $\sin \pi\lambda$ as well. However, White [147] has argued that the symmetry

$$a^>(I) = -a^<(-I) \tag{3.52}$$

holds for integer I so that these poles actually cancel. Taking also into account the symmetry

$$a^>(I) = a^<(-I) \ , \tag{3.53}$$

which follows from the fact that A_5 is a function of $\cos \omega = \frac{1}{2}(z + z^{-1})$, we see that the representation

$$A_5(\eta_{12}) = \frac{1}{2\pi i} \int d\lambda \, \Gamma(-\lambda) \, (-\eta_{12})^\lambda \, a(\lambda) \tag{3.54}$$

seems to exhibit all the essential features of (3.49). The variable λ in (3.54) is (to leading order) the absolute value of the helicity. Eq. (3.51) can be rewritten as*

$$a(\lambda) = \left(\frac{1}{2\pi i}\right)^2 \int dJ_1 \int dJ_2 \, \Gamma(-J_1+\lambda) \, \Gamma(-J_2+\lambda) \, (-s_1)^{J_1} (-s_2)^{J_2} a(J_1, J_2, \lambda; t_1, t_2) \,, \tag{3.55}$$

in the same way that (1.9) was rewritten as (1.17). We have thus obtained the Mellin representation (3.24). A considerable reordering of series is of course involved in this process and one does not know a priori that if one representation is good, the other one is also. The fact that the Mellin representation is consistent with results of models is perhaps our greatest source of confidence in it.

3.5. Helicity limits

All of the limits discussed so far refer to asymptotic limits in the cosine of the angle which is conjugate to the angular momentum. One might ask, what happens if we take one of the helicity angles to infinity instead? We consider the five-point function. When $\cos \omega_{12} \to \infty$ with $\cos \theta_1$ and $\cos \theta_2$ fixed, we recall from (2.8) that

$$s_{12} \equiv s_{ac}, \, s_{ac'}, \, s_{a'c}, \, s_{a'c'} \to \infty \,, \tag{3.56a}$$

with

$$s_1 \equiv s_{a'b'}, \, s_{ab'}, \qquad s_2 \equiv s_{b'c'}, \, s_{b'c}, \, t_1, \, t_2 \quad \text{fixed} \,. \tag{3.56b}$$

Let us refer to the Mellin representation (3.24) to see what we can say about the helicity limit if we know that there are leading Regge poles at $J_1 = \alpha_1$ and $J_2 = \alpha_2$. Shifting the J_1 and J_2 contours to the left to isolate these poles, we have

$$A_5^{\tau_1 \tau_2} = \frac{1}{2\pi i} \int d\lambda \, \Gamma(\lambda - \alpha_1) \, \Gamma(\lambda - \alpha_2) \, \Gamma(-\lambda) \, (-s_{12})^\lambda (-s_1)^{\alpha_1 - \lambda} (-s_2)^{\alpha_2 - \lambda} \beta(\lambda; t_1, t_2) + \underbrace{\int \int \int}_{\text{Background}} \cdots \tag{3.57}$$

The background integral must be kept since we are not taking s_1 or s_2 large. To obtain the large s_{12} behavior, we shift the λ contour to the left. The λ singularities are given explicitly in the Γ functions and we obtain the leading behaviors $(-s_{12})^{\alpha_1}$ and $(-s_{12})^{\alpha_2}$. To take proper account of the background contribution, we look back at (3.24). The singularities in λ are seen to arise from the pinching of the J_1 and J_2 contours between the "kinematic" poles in $\Gamma(-J_1+\lambda) \, \Gamma(-J_2+\lambda)$ and the "dynamical" Regge poles in $a^{\tau_1 \tau_2}$. Thus if $a^{\tau_1 \tau_2}$ has the Regge pole singularities

---

* The partial wave amplitude $a(J_1, J_2, \lambda; t_1, t_2)$ is of course redefined and there is a one-to-one correspondence of J_1 and J_2 with angular momenta only in leading order.

$$a^{\tau_1 \tau_2} \approx R(J_2, \lambda; t_1, t_2)/(J_1 - \alpha_1) \tag{3.58a}$$

and

$$a^{\tau_1 \tau_2} \approx R(J_1, \lambda; t_1, t_2)/(J_2 - \alpha_2), \tag{3.58b}$$

we have [6,141]

$$A_5^{\tau_1 \tau_2} \underset{s_{12} \to \infty}{\sim} \Gamma(-\alpha_1) (-s_{12})^{\alpha_1} \frac{1}{2\pi i} \int dJ_2 \Gamma(-J_2 + \alpha_1) (-s_2)^{J_2 - \alpha_1} R(J_2, \alpha_1; t_1, t_2)$$

$$+ \Gamma(-\alpha_2) (-s_{12})^{\alpha_2} \frac{1}{2\pi i} \int dJ_1 \Gamma(-J_1 + \alpha_2) (-s_1)^{J_1 - \alpha_2} R(J_1, \alpha_2; t_1, t_2). \tag{3.59}$$

We see that the behavior in the helicity limit is determined completely by the angular momentum singularities. This follows from our assertion that there are no dynamical helicity poles but only helicity poles in the "kinematic" factors $\Gamma(-J_1 + \lambda) \Gamma(-J_2 + \lambda)$. These kinematic factors tie the helicity to the two angular momenta J_1 and J_2 at the vertex. Both J_1 and J_2 are involved because the z component of angular momentum is conserved at the vertex, i.e., the helicity is the same on both sides.

The reason why no dynamical helicity singularities can appear in our treatment is easy to trace to our discussion of (3.27) and the absence of simultaneous discontinuities in overlapping channels. Thus the two terms in (3.59) correspond to the two possible sets of simultaneous discontinuities. (see fig. 3.4) — the first term has discontinuities in s_2 and s_{12} and the second in s_1 and s_{12}.

The helicity limit is not in the physical region for the five-particle amplitude (clearly one of the final state sub-energies must grow if the total energy s_{12} grows) so we must assume simultaneous discontinuities in overlapping variables are forbidden even in the unphysical region of this limit. In the absence of rigorous axiomatic support for such an assumption (see section 1.4) we seek further backing for the absence of dynamical helicity singularities. We mention the following arguments:

(i) Intuitive: Since helicity is not a Casimir operator of the Poincare group, as are spin and mass, one does not classify particles according to their helicities. Since "dynamical" poles usually correspond to particles, there should be no dynamical helicity poles. Neither do the residues of kinematical helicity poles necessarily factor as do Regge pole residues, nor does it make any sense to draw a vertex with a helicity pole dangling out one side.

(ii) Contribution to discontinuities: Consider the discontinuity in $s_2(s_{b'c'})$ of the five-particle amplitude in fig. 3.9. Each term in the sum over intermediate states has the Regge behavior shown for $s_{12} \to \infty$; thus, we expect

$$\mathrm{disc}_{b'c'} A_5 \underset{s_{12} \to \infty}{\sim} s_{12}^{\alpha_1} f(s_1/s_{12}, s_2, t_1, t_2), \tag{3.60}$$

where f is a polynomial in s_1/s_{12} for a state in the s_2 channel of finite spin. The leading term in the polynomial gives the first term in (3.59) for $s_{12}/s_1 \to \infty$. Similarly $\mathrm{disc}_{a'b} A_5$ gives the second term. Unfortunately this argument is not rigorous. Since $s_{12}/s_1 \to \infty$ is not inside the physical region, the
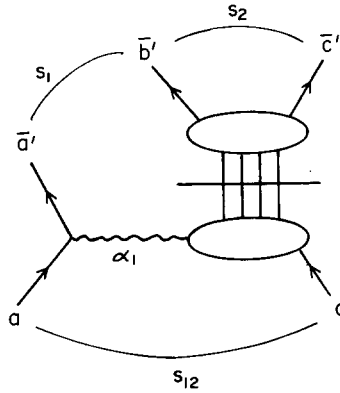
Fig. 3.9. A. discontinuity of A_5.

sum over intermediates states could conceivably diverge giving a behavior different from (3.60). For the six-particle amplitude, helicity limits can be taken inside the physical region and this argument can be used [49] (see section 4).

(iii) Models: The behavior (3.59) holds in the dual resonance model (see the Appendix, eq. (A.14)).

(iv) For further discussion and arguments we refer the reader to Abarbanel and Schwimmer [6] and Brower, Einhorn, Green, Patrascioiu and Weis [23].

Complex helicity is interesting for reasons other than obtaining the asymptotic behavior in the helicity limit. Indeed it seems first to have been introduced in the study of Regge cuts [75]. We shall return to this application in section 8. Representations of $O(2,1)$ in a complex helicity basis have found use in the study of the multiperipheral integral equation [43,42,105]. For group theoretical expansions of the scattering amplitude in the physical region, e.g. $O(2,1)$, involving complex helicity, we refer to Goddard and White [67] and Jones, Low and Young [89–92].

3.6. Reggeon scattering amplitudes

In section 3.1 we discussed briefly the single-Regge limit of the five-particle amplitude — see fig. 3.5. By factoring off the Regge residue $\beta_1^{a\bar{a}'}(t_1)$ and propagator $\xi_1\Gamma(-\alpha_1)s_1^{\alpha_1}$, we can define a scattering amplitude with one external reggeon — see fig. 3.10. It is very interesting to study the
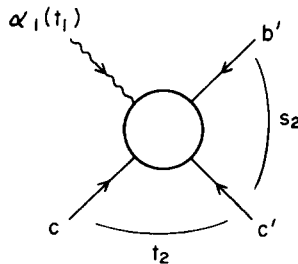
Fig. 3.10. Scattering amplitude with one external reggeon.

analytic structure and unitarity properties of such amplitudes and see how they differ from those of the ordinary four-particle amplitude.

The essential complication of the reggeon amplitude as opposed to the four-particle amplitude is its dependence on the helicity variable s_1/s_{12}. We study this dependence using the Mellin representation (3.24) which gives*

$$A_5 \underset{s_1 \to \infty}{\sim} (-s_1)^{\alpha_1} \left(\frac{1}{2\pi i}\right)^2 \int d\lambda \int dJ_2 \, \Gamma(-\lambda) \, \Gamma(-\alpha_1+\lambda) \, \Gamma(-J_2+\lambda) (-s_2)^{J_2-\lambda} \left(\frac{s_{12}}{s_1}\right)^\lambda R(J_2, \lambda; t_1, t_2) .$$

$$(3.61)$$

In the physical region for the process $ac \to \bar{a}'\bar{b}'\bar{c}'$ where $0 \leqslant s_1/s_{12} \leqslant 1$ we expect to be able to close the λ contour to the left since $(s_{12}/s_1)^\lambda$ vanishes rapidly. We then obtain

$$A_5 \sim \Gamma(-\alpha_1)(-s_{12})^{\alpha_1} \left\{ \sum_{i=0}^\infty \frac{\Gamma(-\alpha_1+i)}{\Gamma(-\alpha_1)i!} \left[\left(\frac{1}{2\pi i}\right) \int dJ_2 \, \Gamma(-J_2+\alpha_1-i) (-s_2)^{J_2-\alpha_1+i} R(J_2, \alpha_1-i; t_1, t_2) \right] \right.$$

$$\times \left(-\frac{s_1}{s_{12}} \right)^i + \left(\frac{s_1}{s_{12}}\right)^{\alpha_1-\alpha_2} \sum_{i=0}^\infty \frac{\Gamma(-\alpha_2+i) \, \Gamma(-\alpha_1+\alpha_2-i)}{\Gamma(-\alpha_1)i!} \, \beta(\alpha_2-i; t_1, t_2) \left(\frac{s_1 s_2}{s_{12}}\right)^i \right\} , \qquad (3.62)$$

where R and β are defined by (3.58a) and (3.26) respectively. In the second sum of (3.62) only the contribution of one Regge pole at $J_2 = \alpha_2$ has been explicitly written; actually the infinite sum over all Regge poles in J_2 should be included.

Each term in the first sum in (3.62) has the structure of a four-particle amplitude – compare with (1.12). However the t_2-channel singularities are shifted since $J_2 \to J_2 - \alpha_1 + i$. Thus a singularity in R at $J_2 = \alpha_2$ produces poles at $\alpha_2 - \alpha_1 + i = N$ rather than at $\alpha_2 = N$. Since the second sum is a series in s_2, all the physical singularities in s_2 appear in the first sum and are represented in (3.62) by the cuts $(-s_2)^{J_2-\alpha_1+n}$. The first sum thus has simultaneous discontinuities in s_2 and s_{12} and the second term in s_1 and s_{12}.

Since (3.62) is rather complicated it is useful to have at hand the explicit form in the dual resonance model (DRM) for comparison. From eq. (A.7) we have

$$B_5 \sim \Gamma(-\alpha_1)(-s_{12})^{\alpha_1} \left\{ \sum_{i=0}^\infty \frac{\Gamma(-\alpha_1+i)}{\Gamma(-\alpha_1)i!} \left[\frac{\Gamma(-\alpha_2+\alpha_1-i) \, \Gamma[-\alpha(s_2)+i]}{\Gamma[-\alpha(s_2)+\alpha_1-\alpha_2]} \right] \left(-\frac{s_1}{s_{12}} \right)^i \right.$$

$$+ \left(\frac{s_1}{s_{12}}\right)^{\alpha_1-\alpha_2} \sum_{i=0}^\infty \frac{\Gamma(-\alpha_2+i)}{\Gamma(-\alpha_1)i!} \left[\frac{\Gamma(-\alpha_1+\alpha_2-i) \, \Gamma[-\alpha(s_2)+\alpha_1-\alpha_2+i]}{\Gamma[-\alpha(s_2)+\alpha_1-\alpha_2]} \right] \left(-\frac{s_1}{s_{12}} \right)^i \right\} . \quad (3.63)$$

Each of the sums in (3.63) is proportional to a hypergeometric function of argument s_1/s_{12} and

---

* Throughout this subsection we consider for simplicity an amplitude with only right-hand cuts. Also for convenience we discuss the properties of the full amplitude A_5 in the limit which exposes the Regge pole α_1, rather than factoring out the residue and propagator to get the four-point amplitude.
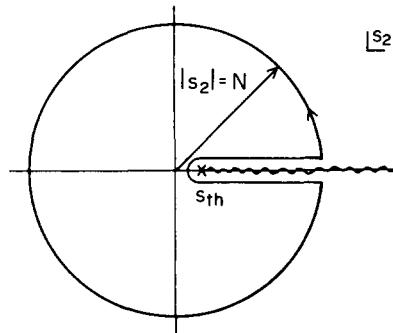
Fig. 3.11. Integration contour for FESR.

thus is singular for $s_1/s_{12} \geq 1$. When $s_1/s_{12} \geq 1$ we can be in the physical region for the crossed process $a'b' \rightarrow \bar{a}\bar{c}\bar{c}'$. The appropriate convergent expansion then has the roles of s_2 and t_2 exchanged.

We first discuss analyticity in s_2. Suppose t_2 and s_1/s_{12} (and, of course, t_1) are held fixed. Then as discussed above all the physical singularities in s_2 occur in the square brackets in the first sum in (3.62) or (3.63). We cannot write a dispersion relation in s_2 since the second sum clearly represents an infinite number of subtractions. In the case of (3.63) the discontinuity in s_2 can be seen to have the behavior $\exp [s_2 s_1/s_{12}]$ as $s_2 \rightarrow +\infty$. The analyticity can be exploited, however, with finite energy sum rules (FESR). Integrating A_5 along the contour of fig. 3.11 gives*

$$\int_{s_{th}}^{N} ds_2' \operatorname{disc}_{s_2} A_5^{(1)}(s_1, s_2', s_{12}; t_1, t_2)$$

$$= -2i(-s_{12})^{\alpha_1} N^{\alpha_2 - \alpha_1 + 1} \sum_{i=0}^{\infty} \frac{\Gamma(-\alpha_1 + i)\,\beta(\alpha_1 - i; t_1, t_2)}{\Gamma(1 - \alpha_1 + \alpha_2 + i)(\alpha_2 - \alpha_1 + i + 1)\,i!} \left(\frac{N s_1}{s_{12}}\right)^i \tag{3.64}$$

where the superscript (1) indicates the first sum in (3.61). FESR are often used to determine the Regge pole parameters (in this case double-Regge vertex) from the low energy data. Eq. (3.64) is probably not too useful from this point of view since the cutoff (N) dependence is not just the simple Regge power $N^{\alpha_2 - \alpha_1 + 1}$.

Instead of fixing s_1/s_{12}, we can fix $\eta_{12} = s_{12}/s_1 s_2$. Both sums now have singularities in s_2. To isolate as much as possible the singularities in s_2 due to intermediate states in the s_2 channel we consider the first sum in (3.62) or (3.63). The asymptotic behavior is $s_2^{\alpha_2 - \alpha_1}$ so a dispersion relation can be written. However, in addition to the singularities in s_2 arising from the term in brackets, there are singularities for $s_1/s_{12} \geq 1$, i.e., $0 \leq s_2 \leq 1/\eta_{12}$ which must be included in the dispersion integral. These are outside the physical region for the process $ac \rightarrow \bar{a}'\bar{b}'\bar{c}'$ and are a reflection of the existence of the second sum [in the DRM the discontinuity for $0 \leq s_2 \leq 1/\eta_{12}$ cancels between the two sums since the full amplitude does not have this discontinuity; see (A.5) and (A.6)] and

---

* Fixed poles in J_2 [(3.39) and (3.40)] also contribute to the right-hand side. These have been omitted for simplicity.
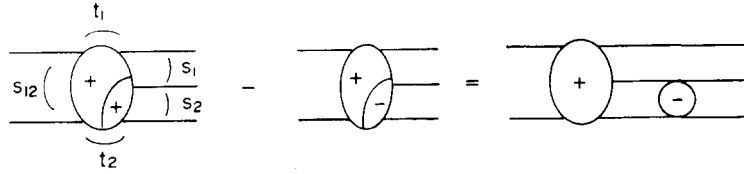
Fig. 3.12. Unitarity equation for A_5 giving discontinuity across two-body threshold in s_2.

of the crossed process $a'b' \to \bar{a}\bar{c}\bar{c}'$.* For the FESR we have [82] neglecting fixed poles

$$
\int_{s_{th}}^{N} ds_2' \, \mathrm{disc}_{s_2} A_5^{(1)}(s_1, s_2', \eta_{12}; t_1, t_2) = - \int_0^{1/\eta_{12}} ds_2' \, \mathrm{disc}_{s_2} A_5^{(1)}(s_1, s_2', \eta_{12}; t_1, t_2)
$$

$$
+ 2i \sin \pi(\alpha_2 - \alpha_1)(-s_{12})^{\alpha_1} \frac{N^{\alpha_2 - \alpha_1 + 1}}{\alpha_2 - \alpha_1 + 1} \sum_{i=0}^{\infty} \frac{\Gamma(-\alpha_1 + i)\,\Gamma(-\alpha_2 + \alpha_1 - i)}{i!} \beta(\alpha_1 - i; t_1, t_2)\eta_{12}^i. \quad (3.65)
$$

Another possibility is to consider the coefficient of each power $(s_1/s_{12})^i$ in the first sum rather than the full sum. These amplitudes are essentially amplitudes of definte t_2 channel helicity and bear the greatest resemblance to ordinary four-body amplitudes. They have only physical discontinuities in s_2 and the asymptotic behavior $s_2^{\alpha_2 - \alpha_1 + i}$. Dispersion relations for larger i thus require more subtractions.

The above discussion has indicated how the s_1/s_{12} dependence of the reggeon amplitudes complicates the analyticity properties in s_2. Neither fixed s_1/s_{12} nor fixed η_{12} is completely satisfactory. The former does not allow a dispersion relation to be written whereas the latter necessitates the inclusion of unphysical singularities or the contributions of singularities in s_1 and s_{12} in addition to those in s_2. For practical applications of FESR it appears that (3.65) is the most useful. We refer the reader to Hoyer and Kwiecinski [82] for further discussion. They note that in the unphysical limit $\eta_{12} \to \infty$ the unphysical region contribution vanishes. Then eqs. (3.64), (3.65) and a FESR for the coefficient of $(s_1/s_{12})^0$ are all equivalent.

We now discuss unitarity in the s_2 channel. The natural way to obtain an unitarity relation for the reggeon amplitude of fig. 3.10 is to take the Regge limit of the unitarity equation in fig. 3.12. When the Regge propagator (including the signature factor $\exp(-i\pi\alpha_1) + \tau_1$) is factored off, the discontinuity on the left-hand side is purely imaginary. The phase of the reggeon amplitude below the three-body threshold must then be the same as that of the elastic amplitude [149].

We note that only the first sum in (3.62) contributes to the left-hand side. Both sums can in principle contribute to the right-hand side. Therefore we cannot obtain a linear unitarity equation for one of the sums alone. Thus, if, as discussed above, dispersion relations are written for the coefficients of the powers $(s_1/s_{12})^i$, information about the other sum will still be necessary to evaluate the discontinuity. The first sum is a series in s_1/s_{12}. Since

$$
s_1/s_{12} \sim \frac{m_{b'}}{\sqrt{s_2}} \left[\cosh q_c^{(b') \to (s_2)} - \{ \tanh q_c^{(s_2) \to (1)} \cos \theta + \sin \theta \cos \phi \} \sinh q_c^{(b') \to (s_2)} \right], \quad (3.66)
$$

_____

* If a dispersion relation is written for the full amplitude, there is no unphysical discontinuity but a discontinuity arises from the second sum in (3.61) due to thresholds in s_1 and s_{12}.
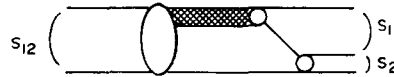
Fig. 3.13. Analytic structure of right-hand side of unitarity equation due to second sum in eq. (3.61).

where θ and ϕ are the polar angles of c' in the s_2 center of mass with a, a' and c in the x-z plane and the boosts q are given by (2.16), this is equivalent to a series in $\cos \phi$. It is convenient to rewrite the first sum as a series in $[\exp(i\lambda_s\phi) + \exp(-i\lambda_s\phi)]$ since the unitarity equation is diagonal in the s_2 helicity λ_s conjugate to ϕ. This sum has t_2 channel helicity $\lambda_t = \lambda$ (conjugate to the Toller angle ω) equal to $\alpha_1, \alpha_1 - 1, \alpha_1 - 2, \dots$. The diagonalized equation will thus relate linear combinations of t_2 channel helicity amplitudes of helicities $\alpha_1, \alpha_1 - 1, \dots$. The second sum in (3.62) gives an analytic structure of the right-hand side of the unitarity equation described by fig. 3.13 due to the singularity in s_1. Such a diagram has anomalous threshold and box singularities in s_1 and s_2. We do not know if it survives in the Regge limit and if so how its structure matches with that of the left-hand side — for further comments see section 8.2. It is amusing to note that in the special case of only narrow resonance singularities in s_2, to leading order in resonance widths only the first sum contributes on the right-hand side of fig. 3.12.* The unitarity equation is then linear in this sum, e.g. in a sum of amplitudes with $\lambda_t = \alpha_1, \alpha_1 - 1, \dots$.

Finally we discuss briefly the structure in t_2. The first sum in (3.62) has shifted singularities in t_2 as discussed above. The physical singularities are contained entirely in the second sum. We cannot discuss unitarity in t_2 as we did above for s_2 since (3.62) does not converge in the physical region for $t_2 > t_{th}(a'b' \to \bar{a}c\bar{c}')$. Nevertheless White [147] has argued that the amplitudes of definite t_2 channel helicity $\alpha_1, \alpha_1 - 1, \alpha_1 - 2, \dots$ (e.g., linear combinations of the coefficients of $(s_1/s_{12})^{\alpha_1 - i}$ in the first sum) satisfy a linear t_2-channel unitarity equation. This remarkable result is obtained at the cost of having a contribution to the right-hand side which cannot be written as a sum over intermediate states in addition to the usual intermediate state sum. In the special case where the only singularities are narrow resonances, to leading order in resonance widths only the non-intermediate state piece contributes — in the reggeon amplitude the t_2 channel singularities are at $\alpha_2 = N + \alpha_1$ whereas in the four particle amplitude they are at $\alpha_2 = N$ so there is no overlap.

Much remains to be understood concerning the analyticity and unitarity of reggeon amplitudes. An intimately related problem is the nature of the crossing relation between the s_2 and t_2 channels. The non-integral spin of the reggeon is a non-trivial complication. For further discussion and a somewhat different point of view, we refer the reader to White [147]. See also Hoyer and Trueman [149].

4. The six-particle amplitude

In this section we extend the type of analysis given in section 3 to the six-particle amplitude. We discuss here the triple-Regge limit of fig. 4.1 and related helicity asymptotic limits. The linear triple-Regge limit of fig. 2.5 will be discussed in section 5.

---

* This can be verified for the DRM amplitude (3.63) using the interpretation of Di Giacomo, Fubini, Sertorio and Veneziano [53].
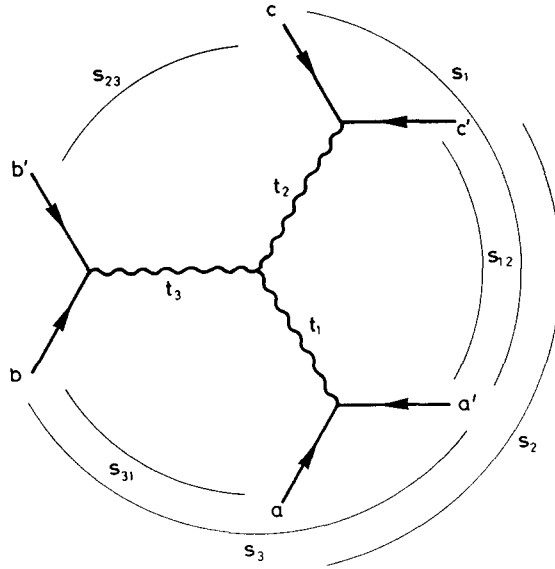
Fig. 4.1. Triple-Regge limit of six-particle amplitude.

4.1. Triple-Regge limit and the triple-Regge vertex

According to the general definitions of section 2.2, the triple-Regge limit shown in fig. 4.1 is [96,101,66]

$$s_1, s_2, s_3, s_{12}, s_{23}, s_{31} \to \infty ,$$ (4.1a)

with

$$t_1, t_2, t_3, \eta_{12}, \eta_{23}, \eta_{31} \text{ fixed} .$$ (4.1b)

Each η_{ij} is given by

$$\eta_{ij} = s_{ij}/s_i s_j \sim \frac{t_k - t_i - t_j + 2\sqrt{t_i t_j} \cos \omega_{ij}}{\lambda(t_i, t_j, t_k)} ,$$ (4.2)

with the Toller angles satisfying

$$\omega_{12} + \omega_{23} + \omega_{31} = 0 .$$ (4.3)

Eq. (4.3) gives a complicated nonlinear constraint between the η_{ij} which reduces the total number of independent invariants to eight. For reasons which will soon become clear we will generally write the amplitude as a function of all three η_{ij}, however.

In the Regge limit (4.1) we expect the behavior

$$A_6 \sim \beta_1(t_1)[\xi_1 \Gamma(-\alpha_1) s_1^{\alpha_1}] \beta_2(t_2) [\xi_2 \Gamma(-\alpha_2) s_2^{\alpha_2}] \beta_3(t_3) [\xi_3 \Gamma(-\alpha_3) s_3^{\alpha_3}] R_{123}(t_1, t_2, t_3; \eta_{12}, \eta_{23}, \eta_{31}).$$

(4.4)
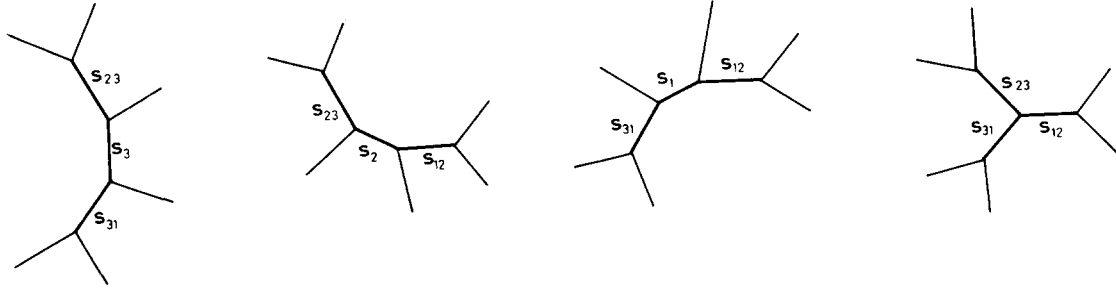
Fig. 4.2. Tree diagrams representing possible simultaneous discontinuities in energy invariants in triple-Regge limit.

However, this form does not exhibit the singularity structure of the amplitude and does not give the phase of the amplitude (R_{123}, like the double-Regge vertex, is not real). To treat these questions correctly we need to perform an analysis analogous to that of section 3.3.

In order to reduce the singularities in the channel invariants to a manageable number, let us consider the signatured amplitude which has only right-hand cuts in the six energy invariants (4.1a). We argued in section 3.3 that our assumption of the independence of overlapping channel singularities permits an additive separation of right- and left-hand cuts and allows the definition of a signatured amplitude. The only sets of simultaneous discontinuities allowed in the signatured amplitude are easily seen to be those of fig. 4.2. Thus, if we write the signatured amplitude as*

$$A_6^{\tau_1\tau_2\tau_3} \sim \beta_1(t_1)\, \Gamma(-\alpha_1)\, \Gamma(-s_1)^{\alpha_1}\beta_2(t_2)\, \Gamma(-\alpha_2)\, (-s_2)^{\alpha_2}\beta_3(t_3)\, \Gamma(-\alpha_3)\, (-s_3)^{\alpha_3}\, V(t_1, t_2, t_3; \eta_{12}, \eta_{23}, \eta_{31}),$$

(4.5)

consistency with fig. 4.2 requires that the vertex has the structure [51]

$$V(t_1, t_2, t_3; \eta_{12}, \eta_{23}, \eta_{31}) = (-\eta_{31})^{\alpha_1}(-\eta_{23})^{\alpha_2}\, V_{12}(t_1, t_2, t_3; \eta_{12}, \eta_{23}, \eta_{31})$$

$$+ (-\eta_{12})^{\alpha_2}(-\eta_{31})^{\alpha_3}\, V_{23}(t_1, t_2, t_3; \eta_{12}, \eta_{23}, \eta_{31}) + (-\eta_{23})^{\alpha_3}(-\eta_{12})^{\alpha_1}\, V_{31}(t_1, t_2, t_3; \eta_{12}, \eta_{23}, \eta_{31})$$

$$+ (-\eta_{12})^{(\alpha_1+\alpha_2-\alpha_3)/2}(-\eta_{23})^{(\alpha_2+\alpha_3-\alpha_1)/2}(-\eta_{31})^{(\alpha_3+\alpha_1-\alpha_2)/2}\, V_{123}(t_1, t_2, t_3; \eta_{12}, \eta_{23}, \eta_{31}),$$

(4.6)

where the V_{ij} and V_{ijk} introduce no further cuts. Combining (4.5) and (4.6) we see the signatured amplitude has the form

$$A_6^{\tau_1\tau_2\tau_3} \sim \beta_1(t_1)\, \Gamma(-\alpha_1)\beta_2(t_2)\, \Gamma(-\alpha_2)\beta_3(t_3)\, \Gamma(-\alpha_3)\, \{(-s_3)^{\alpha_3-\alpha_1-\alpha_2}(-s_{31})^{\alpha_1}(-s_{23})^{\alpha_2}\, V_{12}$$

$$+ (-s_1)^{\alpha_1-\alpha_2-\alpha_3}(-s_{12})^{\alpha_2}(-s_{31})^{\alpha_3}\, V_{23} + (-s_2)^{\alpha_2-\alpha_3-\alpha_1}(-s_{23})^{\alpha_3}(-s_{12})^{\alpha_1}\, V_{31}$$

$$+ (-s_{12})^{(\alpha_1+\alpha_2-\alpha_3)/2}(-s_{23})^{(\alpha_2+\alpha_3-\alpha_1)/2}(-s_{31})^{(\alpha_3+\alpha_1-\alpha_2)/2}\, V_{123}\}.$$

(4.7)

---

* We again assume all external particles have $J^P = 0^+$ so all internal trajectories have natural parity and the amplitude is only a function of the channel invariants.

One could, if he wished, choose one of the η_{ij} to be a dependent variable and eliminate it from the above expressions. The singularities which arise from normal thresholds in s_{ij} would then occur in the other variables as a result of the nonlinear constraint (4.3). Clearly, in order to exclude simultaneous singularities in overlapping channels properly we have to know the origin of the various singularities in the independent variables as thresholds in specific channels. Using the overcomplete set of variables makes this explicit; thus a complicated singularity in the independent variables arising from a term of the form $(-\eta_{ij})^a$ is to be interpreted as arising from thresholds in s_{ij} (and s_i and s_j), and continuing around such a singularity is to be done in such a way that η_{ij} is continued around its singularity.

The contribution of the triple-Regge behavior (4.5) to the full amplitude can now be straightforwardly obtained. The full amplitude is the sum of eight terms analogous to fig. 3.6. For all s_i and s_{ij} positive and above their cuts we obtain*

$$R_{123}(t_1, t_2, t_3; \eta_{12}, \eta_{23}, \eta_{31}) = \xi_3^{-1} \xi_{312} \overline{V}_{12} + \xi_1^{-1} \xi_{123} \overline{V}_{23} + \xi_2^{-1} \xi_{231} \overline{V}_{31}$$

$$+ \xi_1^{-1} \xi_2^{-1} \xi_3^{-1} \exp\{-\tfrac{1}{2}i\pi(\alpha_1 + \alpha_2 + \alpha_3)\} (1 + \tau_1 \exp(i\pi\alpha_1) + \tau_2 \exp(i\pi\alpha_2) + \tau_3 \exp(i\pi\alpha_3)) \overline{V}_{123},$$

(4.8)

where**

$$\overline{V}_{ij} = \eta_{ki}^{\alpha i} \eta_{jk}^{\alpha j} V_{ij},$$

$$\overline{V}_{ijk} = \eta_{ij}^{(\alpha_i + \alpha_j - \alpha_k)/2} \eta_{jk}^{(\alpha_j + \alpha_k - \alpha_i)/2} \eta_{ki}^{(\alpha_k + \alpha_i - \alpha_j)/2} V_{ijk}$$

(4.9)

and

$$\xi_{ijk} = \exp\{-i\pi(\alpha_i - \alpha_j - \alpha_k)\} + \tau_i \tau_j \tau_k.$$

(4.10)

The structure of the vertex parts V_{ij} and V_{ijk} will be discussed in section 4.2. We should remark that there actually is no physical region in which all six energy invariants are positive. This is easily seen from fig. 4.1; there is no way to put arrows on the lines such that each momentum transfer is formed from lines with arrows in opposite directions and each energy is formed from lines with arrows in the same direction.

The relation (4.2) of the η_{ij} to the Toller angle ω_{ij} is only meaningful for $\lambda(t_1, t_2, t_3) \geq 0$ [101,66]. When all three t_i have the same sign it is possible to have $\lambda(t_1, t_2, t_3) \leq 0$. If all three t_i are negative, the vertex transformations $q_k^{(i) \to (j)}$, eq. (2.16), become rotations about the x axis and the convenient O(2,1) little group transformations become $R_z(\mu_i) B_y(\zeta_i) B_x(\lambda_i)$.*** We then have

$$\eta_{ij} \sim \frac{t_k - t_i - t_j + 2\sqrt{-t_i}\sqrt{-t_j}\cosh\delta_{ij}}{-\lambda(t_i, t_j, t_k)},$$

(4.11)

---

* Vertex signatures are neglected throughout this section. They cause no essential modification of the following expressions just as in the case of the double-Regge vertex.

** Actually we shall see later that V_{ijk} has some square-root singularities in the η_{ij} which causes a slight modification of the relation of $\overline{V}_{ijk}$ to V_{ijk}; see (4.21) and fig. 5.8.

*** The standard forms are $Q_i = (0,0,0,\sqrt{-t_i})$.

where $\delta_{ij} = \lambda_i - \lambda_j$ and the analog to (4.3) is

$$\delta_{12} + \delta_{23} + \delta_{31} = 0 .$$

(4.12)

Eq. (4.11) is particularly interesting because it means the helicity limit $\eta_{ij} \to \infty$ can be inside the physical region in this case as it is just the boost $\delta_{ij} \to \infty$. We return to helicity limits in section 4.3.

4.2. Mellin representation

In this subsection we discuss a proposal for a Mellin representation for the six-particle amplitude associated with the coupling scheme of fig. 4.1 [41]. This representation is a recasting of the multiple Sommerfeld–Watson transform which exhibits its essential features.

The triple partial wave analysis of the signatured amplitude corresponding to fig. 4.1 is

$$A_6^{\tau_1\tau_2\tau_3} = \sum_{\lambda_1=-\infty}^{\infty} \sum_{\lambda_2=-\infty}^{\infty} \exp(i\lambda_1\varphi_1) \exp(i\lambda_2\varphi_2) \exp(i\lambda_3\varphi_3)$$

$$\times \left\{ \sum_{J_1=|\lambda_1|}^{\infty} \sum_{J_2=|\lambda_2|}^{\infty} \sum_{J_3=|\lambda_3|}^{\infty} (2J_1+1)(2J_2+1)(2J_3+1) d_{0\lambda_1}^{J_1}(\cos\theta_1) d_{0\lambda_2}^{J_2}(\cos\theta_2) d_{0\lambda_3}^{J_3}(\cos\theta_3) \right.$$

$$\left. \times a(J_1, J_2, J_3; \lambda_1, \lambda_2, \lambda_3; t_1, t_2, t_3) \right\} ,$$

(4.13)

where

$$\lambda_3 = -\lambda_1 - \lambda_2$$

(4.14)

and

$$\omega_{ij} = \varphi_i - \varphi_j .$$

The z component of angular momentum conservation constraint (4.14) means that (4.13) can be written in terms of the ω_{ij} as was done in section 4.1. As we stressed there, in order to exhibit the singularities in all six energy channels clearly, it is useful to use an overcomplete set of variables, namely all three ω_{ij}. This can be done by introducing the variables λ_{ij} defined by

$$\lambda_1 = \lambda_{12} - \lambda_{31} , \qquad \lambda_2 = \lambda_{23} - \lambda_{12} , \qquad \lambda_3 = \lambda_{31} - \lambda_{23} ,$$

(4.15)

since then

$$\exp(i\lambda_1\varphi_1) \exp(i\lambda_2\varphi_2) \exp(i\lambda_3\varphi_3) = \exp(i\lambda_{12}\omega_{12}) \exp(i\lambda_{23}\omega_{23}) \exp(i\lambda_{31}\omega_{31}) .$$

Furthermore the amplitude must be an even function of the λ_{ij}, since it is a function only of the η_{ij} and thus is even in the ω_{ij}. (This is a consequence of the assumption that all six particles have $J^P = 0^+$.) We can therefore rewrite (4.13) as

$$A_6^{\tau_1 \tau_2 \tau_3} = \sum_{\lambda_1 = -\infty}^{\infty} \sum_{\lambda_2 = -\infty}^{\infty} \exp(i\lambda_1 \varphi_1) \exp(i\lambda_2 \varphi_2) \exp(i\lambda_3 \varphi_3) \, a(\lambda_1, \lambda_2, \lambda_3)$$

$$\rightarrow \sum_{\lambda_{12}=0}^{\infty} \sum_{\lambda_{23}=0}^{\infty} \sum_{\lambda_{31}=0}^{\infty} (\exp(i\lambda_{12}\omega_{12}) + \exp(-i\lambda_{12}\omega_{12}))$$

$$\times (\exp(i\lambda_{23}\omega_{23}) + \exp(-i\lambda_{23}\omega_{23}))(\exp(i\lambda_{31}\omega_{31}) + \exp(-i\lambda_{31}\omega_{31})) \, a(\lambda_{12}, \lambda_{23}, \lambda_{31}) , \quad (4.16)$$

where a represents the quantity in large brackets in (4.13). In this form with $\lambda_{ij} \geq 0$ we see that $a(\lambda_{12}, \lambda_{23}, \lambda_{31})$ contributes to helicities $\lambda_1 = \pm\lambda_{12} \pm \lambda_{31}$, etc. Because sense values of the helicities are $J_i \geq \lambda_i$, for each value of the λ_{ij} in (4.16) we must have

$$J_1 \geq \lambda_{12} + \lambda_{31}, \qquad\qquad J_2 \geq \lambda_{23} + \lambda_{12}, \qquad\qquad J_3 \geq \lambda_{31} + \lambda_{23} . \qquad (4.17)$$

Thus collecting the essential gamma-functions from the $d_{0\lambda_i}^{J_i}$ and sweeping inessential factors into the partial wave amplitude, we obtain the representation

$$A_6^{\tau_1 \tau_2 \tau_3}(s_1, s_2, s_3, \eta_{12}, \eta_{23}, \eta_{31}; t_1, t_2, t_3)$$

$$= \left(\frac{1}{2\pi i}\right)^6 \int d\lambda_{12} \int d\lambda_{23} \int d\lambda_{31} \int dJ_1 \int dJ_2 \int dJ_3 \, \Gamma(-\lambda_{12}) \, \Gamma(-\lambda_{23}) \, \Gamma(-\lambda_{31}) \, \Gamma(-J_1 + \lambda_{12} + \lambda_{31})$$

$$\times \Gamma(-J_2 + \lambda_{23} + \lambda_{12}) \, \Gamma(-J_3 + \lambda_{31} + \lambda_{23}) \, (-s_1)^{J_1} (-s_2)^{J_2} (-s_3)^{J_3} (-\eta_{12})^{\lambda_{12}} (-\eta_{23})^{\lambda_{23}} (-\eta_{31})^{\lambda_{31}}$$

$$\times a^{\tau_1 \tau_2 \tau_3}(J_1, J_2, J_3, \lambda_{12}, \lambda_{23}, \lambda_{31}; t_1, t_2, t_3) . \qquad (4.18)$$

The above discussion should only be regarded as a plausibility argument for the representation (4.18) since converting a standard Sommerfeld–Watson transform of (4.13) to this form requires reordering infinite sums, etc.* However, as we now discuss, this representation expresses in a compact form the essential behaviors of A_6; e.g. the partial wave expansion (4.13) and the singularity structure (4.6) of the triple-Regge vertex. This latter feature of (4.18) is indeed one of the strongest motivations for it. Furthermore this form for the triple-Regge vertex is found in models studied thus far; this can be shown for the hybrid Gribov model, the ordinary dual resonance model and a large class of related models** [96] using the results of DeTar and Weis [51] and was shown for the nonlinear dual model [12] by Sukhatme [128].

Let us consider the contribution of a triple-Regge pole to (4.18),

$$a^{\tau_1 \tau_2 \tau_3} \approx \beta_1(t_1) \, \beta_2(t_2) \, \beta_3(t_3) \, \beta(\lambda_{12}, \lambda_{23}, \lambda_{31}; t_1, t_2, t_3)/(J_1 - \alpha_1)(J_2 - \alpha_2)(J_3 - \alpha_3) . \qquad (4.19)$$

We find comparing with (4.7),

---

* For the standard Sommerfeld–Watson transformation see White [144] and Abarbanel and Schwimmer [6].
** For further discussion of these models see section 5.3.

$$V(t_1, t_2, t_3; \eta_{12}, \eta_{23}, \eta_{31}) = \frac{1}{\Gamma(-\alpha_1) \, \Gamma(-\alpha_2) \, \Gamma(-\alpha_3)} \left(\frac{1}{2\pi i}\right)^3 \int d\lambda_{12} \int d\lambda_{23} \int d\lambda_{31}$$

$$\times \; \Gamma(-\lambda_{12}) \, \Gamma(-\lambda_{23}) \, \Gamma(-\lambda_{31}) \, \Gamma(-\alpha_1 + \lambda_{12} + \lambda_{31}) \, \Gamma(-\alpha_2 + \lambda_{23} + \lambda_{12}) \, \Gamma(-\alpha_3 + \lambda_{31} + \lambda_{23})$$

$$\times \; (-\eta_{12})^{\lambda_{12}} \, (-\eta_{23})^{\lambda_{23}} \, (-\eta_{31})^{\lambda_{31}} \, \beta(\lambda_{12}, \lambda_{23}, \lambda_{31}; t_1, t_2, t_3) \, . \tag{4.20}$$

This is analogous to the representation (3.28) for the double-Regge vertex and clearly reduces to it at $\alpha_3 = 0$, where we must also have $\lambda_{31} = \lambda_{23} = 0$. In order to extract the singularities in the η_{ij} we essentially close the λ_{ij} contours to the left.* This calculation is involved and we will not go into the details here but refer the reader to DeTar and Weis [51] for further discussion. We indeed obtain just the four terms of (4.6) with the following explicit forms for the V_{ij} and V_{ijk}:

$$V_{ij} = \frac{1}{\Gamma(-\alpha_i) \, \Gamma(-\alpha_j) \, \Gamma(-\alpha_k)} \sum_{m,n,p=0}^{\infty} \Gamma(-\alpha_i + m + p) \, \Gamma(-\alpha_j + n + p) \, \Gamma(-\alpha_k + \alpha_i + \alpha_j - m - n - 2p)$$

$$\times \; \frac{1}{m! \, n! \, p!} \; \eta_{ki}^{-m} \eta_{jk}^{-n} \left(\frac{\eta_{ki}\eta_{jk}}{\eta_{ij}}\right)^{-p} \beta(p, \alpha_j - n - p, \alpha_i - m - p; t_i, t_j, t_k) \, ,$$

$$V_{ijk} = \frac{1}{2 \, \Gamma(-\alpha_i) \, \Gamma(-\alpha_j) \, \Gamma(-\alpha_k)}$$

$$\times \sum_{m,n,p=0}^{\infty} \Gamma[\tfrac{1}{2}(\alpha_i - \alpha_j - \alpha_k - m + n + p)] \, \Gamma[\tfrac{1}{2}(\alpha_j - \alpha_k - \alpha_i - n + p + m)] \; \Gamma[\tfrac{1}{2}(\alpha_k - \alpha_i - \alpha_j - p + m + n)]$$

$$\times \; \frac{(-1)^{m+n+p} \exp\{-\tfrac{1}{2} i\pi(m + n + p)\}}{m! \, n! \, p!} \left(\frac{\eta_{ki}\eta_{ij}}{\eta_{jk}}\right)^{-m/2} \left(\frac{\eta_{ij}\eta_{jk}}{\eta_{ki}}\right)^{-n/2} \left(\frac{\eta_{jk}\eta_{ki}}{\eta_{ij}}\right)^{-p/2}$$

$$\times \; \beta[\tfrac{1}{2}(\alpha_i + \alpha_j - \alpha_k - m - n + p), \tfrac{1}{2}(\alpha_j + \alpha_k - \alpha_i - n - p + m), \tfrac{1}{2}(\alpha_k + \alpha_i - \alpha_j - p - m + n); t_i, t_j, t_k] \, . \tag{4.21}$$

The functions V_{ij} can be seen to have the expected behavior for α_i integral. For example, V_{ij} is nonvanishing for α_i and α_j integral. The triple-pole arises since then the factor $\Gamma(-\alpha_k + \alpha_i + \alpha_j - m - n - 2p)$ can also be singular. Furthermore, the particular ratios of η_{ij}'s present are just the ones needed to give a polynomial residue at poles. The V_{ijk} term plays a peculiar but essential role. It does not contribute for any α_i integral but allows cancellation of the spurious singularities in the V_{ij} terms for integral $\alpha_k - \alpha_i - \alpha_j$.

In addition to Regge pole singularities like (4.19) in the angular momenta we expect fixed pole singularities of two types: fixed poles of the form (3.39) corresponding to nonsense with respect to the external lines and fixed poles corresponding to nonsense at the central vertex which are extensions of the singularities in $\Gamma(-J_i + \lambda_{ij} + \lambda_{ki})$ but lie on the opposite side of the integration contour, e.g.

---

* For some contributions we actually close contours to right. The correct direction is always that for which the contour at infinity vanishes, assuming at most exponential behavior for β.

$$a^{\tau_1 \tau_2 \tau_3} \approx \beta / \{ J_1 - \lambda_{12} - \lambda_{31} - N_1 \},$$

(4.22)

with

$$N_1 = -1, -2, -3, \ldots \qquad \text{and} \qquad \tau_1 \tau_2 \tau_3 = (-1)^{N_1}.$$

The wrong-signature rule is a natural generalization of the usual one to spinning particles and assures that there is no fixed power behavior in the full amplitude. We shall not work out in detail here the contributions of additive or multiplicative fixed poles of the form (3.39) or (4.22) since they are straightforward generalizations of the results of section 3.4. As yet only a few model studies have been made of fixed poles [69], for further discussion see Weis [141]. While the results are completely in agreement with the discussion given here it would clearly be of interest to study further models to gain further confidence in the above proposals.

4.3. Helicity asymptotic limits

There are clearly a large number of helicity asymptotic limits of the six-particle amplitude analogous to those of section 3.5 which can be studied. There is one essential difference from the five-particle amplitude, however. For $\lambda(t_1, t_2, t_3) \leq 0$ helicity asymptotic limits of the six-particle amplitude can be in the physical region as we noted at the end of section 4.1*.

We shall discuss here only one helicity limit, namely the one which is directly accessible in inclusive cross sections [49]. Here we discuss the general form of the amplitude in this limit; the application will be discussed in detail in section 6.3. The limit of interest is actually a mixed Regge-helicity limit since it is

$$s_3 \to \infty \quad \text{(Regge)}, \qquad \qquad \eta_{31}, \eta_{23} \to \infty \quad \text{(Helicity)},$$

(4.23)

with $s_1, s_2, \eta_{12}, t_1, t_2, t_3$ fixed.

From (4.12) we note that η_{31} and η_{23} actually must grow at the same rate. From (4.18) we obtain four terms analogous to the case of the triple-Regge vertex

$$A_6^{\tau_1 \tau_2 \tau_3} \sim (-s_3)^{\alpha_3 - \alpha_1 - \alpha_2} (-s_{31})^{\alpha_1} (-s_{23})^{\alpha_2} \Gamma(-\alpha_3 + \alpha_1 + \alpha_2) \Gamma(-\alpha_1) \Gamma(-\alpha_2)$$

$$\times \beta_1(t_1) \beta_2(t_2) \beta_3(t_3) \beta(0, \alpha_2, \alpha_1; t_1, t_2, t_3) + (-s_{31})^{\alpha_3} U_1(s_1, s_{12}; t_1, t_2, t_3)$$

(4.24)

$$+ (-s_{23})^{\alpha_3} U_2(s_2, s_{12}; t_1, t_2, t_3) + (-s_{31})^{(\alpha_3 + \alpha_1 - \alpha_2)/2} (-s_{23})^{(\alpha_2 + \alpha_3 - \alpha_1)/2} U_{12}(s_1, s_2, s_{12}; t_1, t_2, t_3).$$

The functions U are analogous to the coefficients of the asymptotic powers in the helicity limit (3.59). In section 6.3 we shall give several independent arguments for the behavior of the form (4.24) and discuss its structure in some detail.

We close this section with a technical remark [110]. The limit (4.23) does not always uniquely define the coupling scheme of fig. 4.1. The diagram with a and c interchanged is equally good for certain isolated values of the invariants — for example the "forward" configuration $p_b = -p_{b'}$, $p_a = -p_c$, $p_{a'} = -p_{c'}$. This nonuniqueness of coupling schemes is a complication to be generally

---

* This point is emphasized by Abarbanel and Schwimmer [6].

expected in helicity limits of amplitudes with more than five particles. It means there are contributions not explicitly exhibited in (4.18), i.e. $a^{\tau_1 \tau_2 \tau_3}$ has singularities in helicity or, alternatively, there are other contributions to $A_6^{\tau_1 \tau_2 \tau_3}$ not of this form. These further contributions are not expected to have a discontinuity in $s_3 = (p_b + p_a + p_{a'})^2$ (which will interest us in section 6.3) but to have a discontinuity in $(p_b + p_a + p_{c'})^2$.

For the O(2,1) analysis of these limits, see Jones, Low and Young [90–92] and Mak [98]. For the O(3) Sommerfeld–Watson analysis, see also Abarbanel and Schwimmer [6].

5. Multi-Regge amplitudes

We discuss general multi-Regge asymptotic limits. The problem of reconciling the factorizability of Regge pole contributions with the analytic structure of the amplitude is stressed.

5.1. Introduction

In section 2 we have defined the general multi-Regge limit by studying the multiple O(3) partial wave analysis. Thus, for example, the multi-Regge limit of fig. 5.1 is all the single-reggeon energies, s_i, going to infinity with the energies across several reggeons growing like

$$s_{ij...k} \propto s_i s_j ... s_k .$$
(5.1)

As a complete set of independent variables we choose the t_i, the s_i and

$$\eta_{ij} = s_{ij}/s_i s_j .$$
(5.2)

We have verified in section 2 that this is precisely a complete set after application of the constraint reducing the three η_{ij} at a triple-Regge vertex to two.

The essential complication of amplitudes containing more than one double- or triple-Regge vertex concerns the energies across more than two reggeons. As discussed in section 2 these can be expressed in terms of the s_i and η_{ij} in the Regge limit since

$$s_{ij...kl} s_{j...k}/s_{ij...k} s_{j...kl} = 1 .$$
(5.3)

Normal thresholds in the channels corresponding to the $s_{i...j}$ produce singularities which occur in the independent variables by virtue of these nonlinear constraints. The singularity structure in the independent variables is thus quite complicated since it must reflect the thresholds (as well as other singularities) in several channels. Therefore one does not expect that the singularity structure of multi-particle amplitudes can be represented simply as a product of Regge propagators (with cuts in the s_i) and Regge vertices (with cuts in the η_{ij}).

On the other hand, the physical picture of a reggeon as an exchanged object in a well-defined state leads naturally to the idea of factorization of reggeon couplings. Thus a multi-Regge exchange amplitude should be somehow expressible in terms of the basic single-, double-, and triple-Regge vertices. In order to focus on this apparent conflict, we recall the situation for the four-particle and five-particle amplitudes.
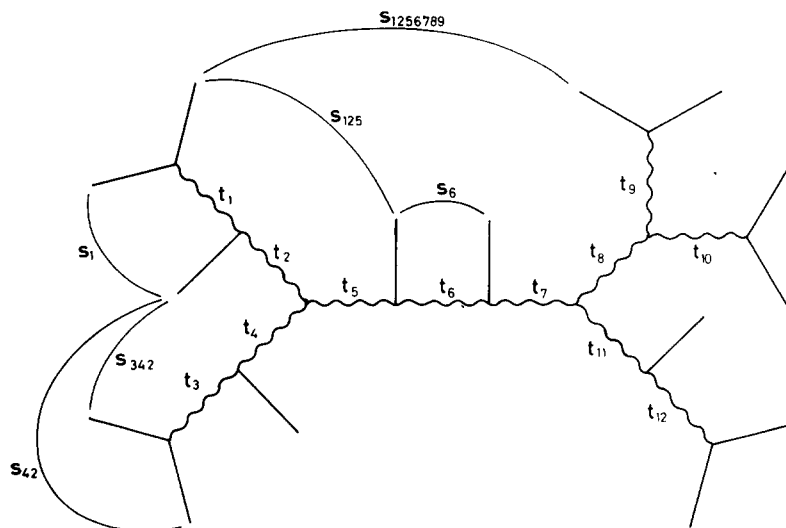
Fig. 5.1. Example of multi-Regge amplitude.

The fundamental statement of factorization is that the residue of the Regge pole at $J = \alpha(t)$ in the signatured partial-wave amplitude should factor,

$$a^\tau(J, t) \approx \beta^{aa'}(t)\, \beta^{bb'}(t)/\{J - \alpha(t)\} \,, \tag{5.4}$$

where the particles are labeled as in fig. 1.1. In the case of the four-particle amplitude factorization can be proven from t-channel unitarity. The Regge-pole contribution to the signatured amplitude then has the factorized form [see eq. (1.15)],

$$A_4^\tau(s, t) \sim \beta^{aa'}(t)\, \Gamma(-\alpha)\,(-s)^\alpha\, \beta^{bb'}(t) \,. \tag{5.5}$$

The full amplitude also factorizes

$$A_4(s, t) \sim \beta^{aa'}(t)\, [\xi(t)\, \Gamma(-\alpha)\, s^\alpha]\beta^{bb'}(t) \,. \tag{5.6}$$

Therefore factorization of the Regge-pole residue implies factorization of the Regge-pole contribution to the signatured and full amplitudes*. Furthermore the phase of the amplitude is entirely

---

* If the external particles have spin, eq. (5.5) becomes

$$A^\tau_{\lambda_a\lambda_a';\lambda_b\lambda_b'}(s, t) \sim \tilde\beta_{\lambda_a\lambda_a'}(t)\, \tilde\beta_{\lambda_b\lambda_b'}(t)\, e_{\lambda\lambda'}^{-\alpha-1}(-z_t) \,,$$

where $\lambda = \lambda_a - \lambda_a'$, $\lambda' = \lambda_b - \lambda_b'$. In general this is not a factorized form, but to leading order in $z_t(s)$,

$$e_{\lambda\lambda'}^{-\alpha-1}(-z_t) \sim \sqrt{\pi}\{[\Gamma(\lambda - \alpha)\,\Gamma(-\lambda - \alpha)\,\Gamma(\lambda'-\alpha)\,\Gamma(-\lambda'-\alpha)]^{\frac{1}{2}}/\Gamma(-\alpha)\,\Gamma(-\alpha+\tfrac{1}{2})\}\,(-2z_t)^\alpha \,,$$

and thus, $A^\tau_{\lambda_a\lambda_a';\lambda_b\lambda_b'}(s, t) \sim \beta_{\lambda_a\lambda_a'}(t)\,\Gamma(-\alpha)\,(-s)^\alpha\,\beta_{\lambda_b\lambda_b'}(t)$.

Thus the spin correlation carried by the exchanged reggeon does not spoil factorization to leading order in s. Similarly, for many-particle amplitudes factorization can only be expected in leading order since the reggeon transmits information about the relative orientation of the groups of particles between which it is exchanged.

Fig. 5.2. A double discontinuity of a multi-Regge amplitude.

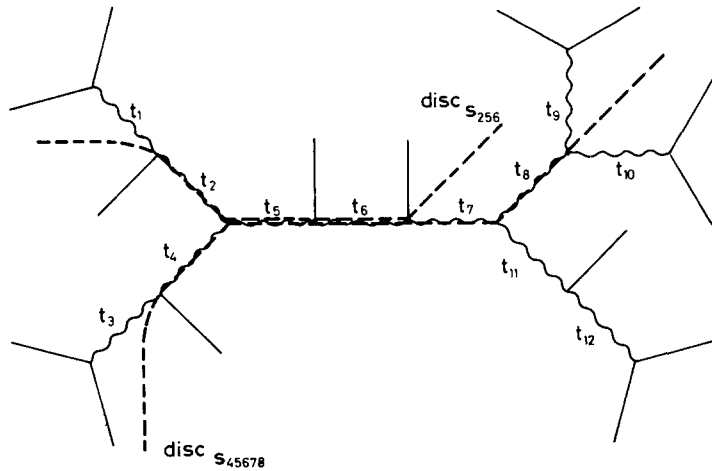associated with the Regge propagator, $\xi(t)\Gamma(-\alpha)s^\alpha$, and the factorized form can be continued throughout the first sheet of the complex s-plane if care is taken to interpret correctly $\xi(t)s^\alpha = (-s)^\alpha + \tau s^\alpha$ as representing right-hand and left-hand cuts as described in section 1.2.

Factorization of the double-Regge residue in the five particle amplitude (fig. 3.1),

$$a^{\tau_1\tau_2}(J_1, J_2, \lambda; t_1, t_2) \approx \beta^{aa'}(t_1)\, \beta_{12}^{b'}(\lambda; t_1, t_2)\, \beta^{cc'}(t_2)/(J_1 - \alpha_1)(J_2 - \alpha_2)\,, \tag{5.7}$$

leads to the asymptotic behavior (3.19),

$$A_5^{\tau_1\tau_2}(s_1, s_2, s_{12}; t_1, t_2) \sim \beta^{aa'}(t_1)\, \Gamma(-\alpha_1)\, (-s_1)^{\alpha_1}\, V_{12}^{b'}(t_1, t_2; \eta_{12})\, \Gamma(-\alpha_2)\, (-s_2)^{\alpha_2}\, \beta^{cc'}(t_2)\,. \tag{5.8}$$

The phase of the amplitude cannot be factored into separate pieces associated with the Regge propagators and double-Regge vertex because it does not represent independent cuts in s_1, s_2 and η_{12} but rather cuts in s_1, s_2 and s_{12} in eq. (3.19). Thus the requirement that s_1, s_2 and s_{12} be on their first sheets restricts the range of application of (5.8) in s_1 (for fixed η_{12} and s_2) to $-\pi \leqslant \arg(-s_1) \leqslant \pi - \arg(1/\eta_{12}s_2)$ [for $\arg(1/\eta_{12}s_2) \geqslant 0$] — see fig. 3.3 — which is a nonfactorized restriction. Due to this complication we were content in section 3 to give a factorized expression for the full amplitude only for physical s_1, s_2 and s_{12} (i.e. positive and above their cuts),

$$A_5(s_1, s_2, s_{12}; t_1, t_2) \sim \beta^{aa'}(t_1)[\xi_1\Gamma(-\alpha_1)s_1^{\alpha_1}]\, R_{12}^{b'}(t_1, t_2; \eta_{12})\,[\xi_2\Gamma(-\alpha_2)s_2^{\alpha_2}]\, \beta^{cc'}(t_2)\,. \tag{5.9}$$

The consequences of factorization of Regge-pole residues for the asymptotic behavior of amplitudes are therefore weaker for the five-particle amplitude than for the four-particle amplitude.

In the discussion of the factorization properties of multi-Regge exchange amplitudes the complication of singularities in dependent variables (5.3) plays an essential role. Indeed, contrary to one's first expectations discussed above, it is precisely this complication which allows a generalization of the physical region factorization (5.9). More remarkably, any discontinuity or multiple discontinuity of the amplitude (see fig. 5.2) also factors in the physical region.
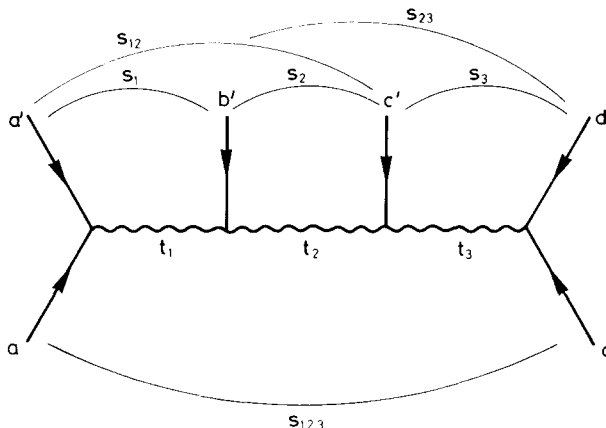
Fig. 5.3. Linear triple-Regge limit of six-particle amplitude.

In section 5.2 we discuss in detail the simplest nontrivial case — the linear triple-Regge limit of the six-particle amplitude of fig. 5.3. The form of the signatured amplitude required by the singularity structure of the amplitude described in section 1.3 is established. Then its intimate connection to the factorization of the full amplitude and its discontinuities is elucidated. The discussion follows the treatment of Weis [140,142.]

In section 5.3 we give the rules for writing down an arbitrary multi-Regge amplitude or discontinuity [142,143]. These rules are natural generalizations of the results for the six-particle amplitude and have been proven in certain models.

5.2. Factorization and the six-particle amplitude

Here we discuss in detail the linear triple-Regge limit of the amplitude for six scalar particles shown in fig. 5.3. We first want to demonstrate that in the physical region the six-particle amplitude has the factorized form

$$A_6 \sim \beta^{aa'}(t_1) [\xi_1 \Gamma(-\alpha_1) s_1^{\alpha_1}] R_{12}^{b'}(t_1, t_2; \eta_{12}) [\xi_2 \Gamma(-\alpha_2) s_2^{\alpha_2}] R_{23}^{c'}(t_2, t_3; \eta_{23}) [\xi_3 \Gamma(-\alpha_3) s_3^{\alpha_3}] \beta^{dd'}(t_3).$$

(5.10)

Since a detailed study of the Mellin or Sommerfeld—Watson transform of the six-particle amplitude has not yet been given, we do not know the appropriate statement of factorization of Regge-pole residues in partial wave amplitudes, so we discuss directly the full amplitude.

We begin by considering the contribution to (5.10) representing right-hand cuts in the energy variables. Equivalently, we assume the existence of a signatured amplitude* with only right-hand cuts in the energy variables of fig. 5.3. One might first believe that factorization of Regge-pole residues would lead to the behavior

---

* Vertex signatures are neglected.

Fig. 5.4. Allowable simultaneous discontinuities in linear triple-Regge limit.

$$A_6^{\tau_1 \tau_2 \tau_3} \sim \beta(t_1)\, \Gamma(-\alpha_1)\, (-s_1)^{\alpha_1}\, V(t_1, t_2; \eta_{12})\, \Gamma(-\alpha_2)(-s_2)^{\alpha_2}\, V(t_2, t_3; \eta_{23})\, \Gamma(-\alpha_3)\, (-s_3)^{\alpha_3}\, \beta(t_3)\,.$$

$$(5.11)$$

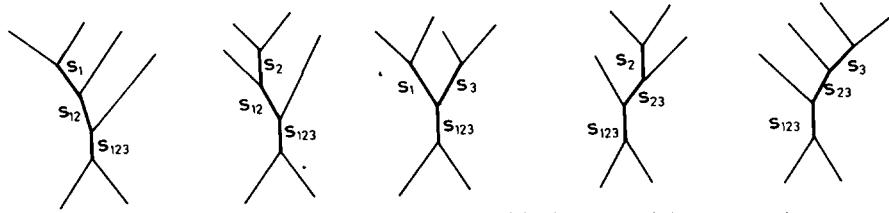As it stands, (5.11) is obviously inconsistent with the required analytic structure of A_6 discussed in section 1.3. It has simultaneous discontinuities in overlapping channel invariants. The only allowable sets of simultaneous singularities are shown in fig. 5.4. For each of the terms in the figure the nature of the singularity in each of the energies is uniquely determined by consistency with the asymptotic behavior $s_1^{\alpha_1} s_2^{\alpha_2} s_3^{\alpha_3}$ and the constraints

$$s_{12} = s_1 s_2 \eta_{12}\,, \qquad\qquad s_{23} = s_2 s_3 \eta_{23}\,, \qquad\qquad s_{123} = s_1 s_2 s_3 \eta_{12} \eta_{23}\,. \qquad (5.12)$$

For example, the first term has the behavior

$$(-s_1)^a\, (-s_{12})^b\, (-s_{123})^c$$

where

$$a + b + c = \alpha_1\,, \qquad\qquad b + c = \alpha_2\,, \qquad\qquad c = \alpha_3\,.$$

We thus find instead of (5.11) the correct structure,

$$A_6^{\tau_1 \tau_2 \tau_3} \sim \Gamma(-\alpha_1)\, \Gamma(-\alpha_2)\, \Gamma(-\alpha_3)\{(-s_1)^{\alpha_1 - \alpha_2}(-s_{12})^{\alpha_2 - \alpha_3}(-s_{123})^{\alpha_3}\, W_{23}^3$$

$$+ (-s_2)^{\alpha_2 - \alpha_1}(-s_{12})^{\alpha_1 - \alpha_3}(-s_{123})^{\alpha_3}\, W_{13}^3 + (-s_1)^{\alpha_1 - \alpha_2}(-s_3)^{\alpha_3 - \alpha_2}(-s_{123})^{\alpha_2}\, W_{22}^2$$

$$+ (-s_2)^{\alpha_2 - \alpha_3}(-s_{23})^{\alpha_3 - \alpha_1}(-s_{123})^{\alpha_1}\, W_{13}^1 + (-s_3)^{\alpha_3 - \alpha_2}(-s_{23})^{\alpha_2 - \alpha_1}(-s_{123})^{\alpha_1}\, W_{12}^1\}\,. \qquad (5.13)$$

The functions $W_{ij}^k(t_1, t_2, t_3; \eta_{12}, \eta_{23})$ are free of cuts in η_{12} and η_{23}.

The natural choice of independent energy variables for the factorized expression (5.10) is the set s_1, s_2, s_3, η_{12} and η_{23}. However, the constraints (5.12) complicate the singularity structure of the amplitude in terms of these invariants. In particular with all other variables fixed, the cuts in s_1 are those shown in fig. 5.5. Comparing with fig. 3.3, one notes the presence of an additional set of singularities arising from the dependent energy s_{123}. A factorized expression like (5.11) is incapable of representing the intricate structure of fig. 5.5 and formula (5.13). Factorization implies that the amplitude is an independent function of η_{12} and η_{23}, whereas the singularities in s_{123} are mapped into the s_1 plane (and other complex energy planes) in a way which depends on both
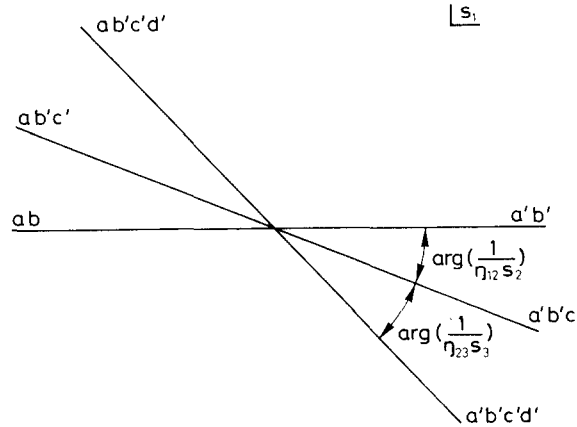
Fig. 5.5. Complex s_1 plane showing locations of asymptotic singularities contributed by channels indicated for fixed s_2, s_3, η_{12}, η_{23}.

η_{12} and η_{23}. In the special configuration,

$$\text{Im } s_1 = \text{Im } s_2 = \text{Im } s_3 = \text{Im } s_{12} = \text{Im } s_{23} = \text{Im } s_{123} = 0 \,, \tag{5.14}$$

all cuts coalesce on the real axis, simplifying the analytic structure considerably. All physical regions are included in this configuration. So we are led to look for a restricted form of factorization holding for (5.14).

We first consider the signatured amplitude for all the energies negative. Since we are away from the cuts we expect no effects of the complicated singularity structure (5.13). We therefore might expect that factorization of Regge-pole residues would lead to (5.11) in this region. Then we tentatively have, using (5.12),

$$W_{23}^3 = \beta(t_1)\, V_2(t_1, t_2; \eta_{12})\, V_3(t_2, t_3; \eta_{23})\, \beta(t_3) \,,$$

$$W_{22}^2 = \beta(t_1)\, V_2(t_1, t_2; \eta_{12})\, V_2(t_2, t_3; \eta_{23})\, \beta(t_3) \,,$$

$$W_{12}^1 = \beta(t_1)\, V_1(t_1, t_2; \eta_{12})\, V_2(t_2, t_3; \eta_{23})\, \beta(t_3) \,,$$

$$W_{13}^3 + W_{13}^1 = \beta(t_1)\, V_1(t_1, t_2; \eta_{12})\, V_3(t_2, t_3; \eta_{23})\, \beta(t_3) \,, \tag{5.15}$$

where the V_i are the parts of the double-Regge vertices defined by (3.19).

We now consider whether the structure (5.13) is compatible with factorization (5.10) of the full amplitude which is given by a sum of eight terms analogous to fig. 3.6. We shall find that it is, given (5.15) and one further condition which determines uniquely the W_{13}^3 and W_{13}^1. Let us work in the physical region for $ad \rightarrow \bar{a}'\bar{b}'\bar{c}'\bar{d}'$ so s_1, s_2, s_3, s_{12}, s_{23} and s_{123} are above their right-hand cuts.

The eight terms in the full amplitude arising from the W_{23}^3 term in (5.13) are

$$[(-s_1)^{\alpha_1-\alpha_2}(-s_{12})^{\alpha_2-\alpha_3}(-s_{123})^{\alpha_3}+\tau_1 s_1^{\alpha_1-\alpha_2}s_{12}^{\alpha_2-\alpha_3}s_{123}^{\alpha_3}+\tau_2(-s_1)^{\alpha_1-\alpha_2}s_{12}^{\alpha_2-\alpha_3}s_{123}^{\alpha_3}$$

$$+\tau_3(-s_1)^{\alpha_1-\alpha_2}(-s_{12})^{\alpha_2-\alpha_3}s_{123}^{\alpha_3}+\tau_1\tau_2 s_1^{\alpha_1-\alpha_2}(-s_{12})^{\alpha_2-\alpha_3}(-s_{123})^{\alpha_3}+\tau_1\tau_3 s_1^{\alpha_1-\alpha_2}s_{12}^{\alpha_2-\alpha_3}(-s_{123})^{\alpha_3}$$

$$+\tau_2\tau_3(-s_1)^{\alpha_1-\alpha_2}s_{12}^{\alpha_2-\alpha_3}(-s_{123})^{\alpha_3}+\tau_1\tau_2\tau_3 s_1^{\alpha_1-\alpha_2}(-s_{12})^{\alpha_2-\alpha_3}s_{123}^{\alpha_3}]\,W_{23}^3\,. \tag{5.16}$$

As usual we start with all the energies negative and continue the asymptotic form in large semi-circles $[(-s)\to e^{\pm i\pi}s$ as we go above/below the cut].* The phase of (5.16) is therefore

$$[\exp(-i\pi\alpha_1)+\tau_1+\tau_2\exp\{-i\pi(\alpha_1-\alpha_2)\}+\tau_3\exp\{-i\pi(\alpha_1-\alpha_3)\}+\tau_1\tau_2\exp\{-i\pi\alpha_2\}$$

$$+\tau_1\tau_3\exp\{-i\pi\alpha_3\}+\tau_2\tau_3\exp\{-i\pi(\alpha_1-\alpha_2+\alpha_3)\}+\tau_1\tau_2\tau_3\exp\{-i\pi(\alpha_2-\alpha_3)\}]\,. \tag{5.17}$$

Since $W_{23}^3\propto V_1(t_1,t_2;\eta_{12})\,V_3(t_2,t_3;\eta_{23})$ this phase should be the same as that multiplying $V_2(t_1,t_2;\eta_{12})\,V_3(t_2,t_3;\eta_{23})$ in (5.10) which from (3.23) is

$$\xi_1[\xi_1^{-1}\xi_{12}]\xi_2[\xi_2^{-1}\xi_{23}]\xi_3\,. \tag{5.18}$$

Eqs. (5.17) and (5.18) are indeed equal. The same procedure can be applied to the other terms in (5.13). The only complication arises for the contributions proportional to $V_1(t_1,t_2;\eta_{12})\times V_3(t_2,t_3;\eta_{23})$. In addition to (5.15), the condition

$$\exp\{i\pi(\alpha_1-\alpha_2-\alpha_3)\}\,W_{13}^3+\exp\{i\pi(-\alpha_1-\alpha_2+\alpha_3)\}\,W_{13}^1=\frac{1}{-2i\sin\pi\alpha_2}$$

$$\times\,[\exp\{i\pi(\alpha_1-2\alpha_2+\alpha_3)\}+\exp\{i\pi(-\alpha_1-\alpha_3)\}-\exp\{i\pi(-\alpha_1+\alpha_3)\}-\exp\{i\pi(\alpha_1-\alpha_3)\}]$$

$$\times\,\beta(t_1)\,V_1(t_1,t_2;\eta_{12})\,V_3(t_2,t_3;\eta_{23})\,\beta(t_3)\,, \tag{5.19}$$

must hold to obtain factorization. Eqs. (5.15) and (5.19) can be solved to determine W_{13}^3 and W_{13}^1,

$$W_{13}^3=\frac{\sin\pi(\alpha_2-\alpha_3)\sin\pi\alpha_1}{\sin\pi\alpha_2\sin\pi(\alpha_1-\alpha_3)}\,\beta(t_1)\,V_1(t_1,t_2;\eta_{12})\,V_3(t_2,t_3;\eta_{23})\,\beta(t_3)\,,$$

$$W_{13}^1=\frac{\sin\pi(\alpha_2-\alpha_1)\sin\pi\alpha_3}{\sin\pi\alpha_2\sin\pi(\alpha_3-\alpha_1)}\,\beta(t_1)\,V_1(t_1,t_2;\eta_{12})\,V_3(t_2,t_3;\eta_{23})\,\beta(t_3)\,. \tag{5.20}$$

Several remarks should be made about the above discussion: (i) Factorization holds in all the physical regions of all crossed processes. The computation in each physical region is identical to that above with a permutation of the terms. (ii) Factorization cannot be imposed if the correct singularity structure (5.13) is not taken into account. The form (5.11) which neglects the cuts

---

* This is most simply implemented by choosing for each term in (5.13) a set of independent variables containing the energies with singularities – each singularity then occurs in only one independent variable. For example, in this term we choose s_1, s_3, s_{12}, s_{23} and s_{123}. Then as, say, s_{123} varies with the others fixed, s_2 will vary but, since there are no singularities in s_2 in this term, the only phase comes from the singularity in s_{123}.
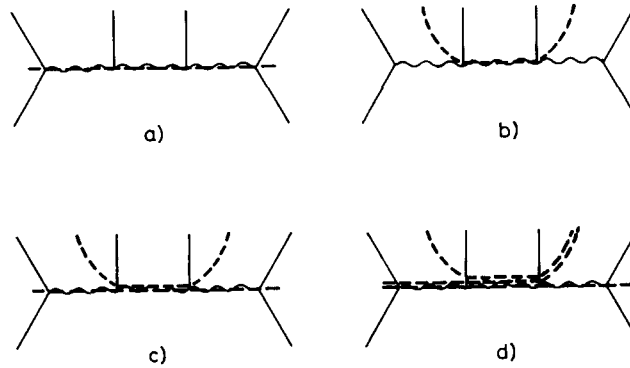
in s_{123} does not yield (5.10) [46]. Therefore the complicated singularity structure allows factorization of the amplitude rather than spoiling it [76,139,140]. (iii) The signaturization of the center reggeon α_2 is essential. If either of the end reggeons is unsignatured, the amplitude still factorizes. However, it is essential that the combination of right-hand cut in s_2 plus τ_2 times left-hand cut in s_2 be formed since it is only this combination which give factorization of the terms in A_6 proportional to $\tau_1\tau_3$. In other words, when a reggeon couples two states each with more than two particles it must be signaturized to give a factorized contribution. (iv) Finally, we re-emphasize the restricted validity of (5.10). It cannot be used for continuing the amplitude between physical regions. Doing so gives the wrong phases. The proper formula for continuation is the non-factorizable expression (5.16) (plus the other four similar expressions according to (5.13)).

In a physical region discontinuity of A_6, the energy variables also satisfy (5.14). We now show that these discontinuities have the remarkable property that they also factorize.

We first identify the basic elements by computing the discontinuities of the four-particle and five-particle amplitudes. From $\mathrm{disc}_s A_4$ we find

$$\underline{-\!\!\!-\!\!\!\curvearrowright\!\!\!\curvearrowright\!\!\!-\atop t} \quad = \frac{2\pi i}{\Gamma(\alpha+1)}\, s^\alpha\ ; \qquad \searrow\!\!\curvearrowright\!\!\nwarrow_t = \beta(t)\ . \tag{5.21}$$

Taking the discontinuity of A_5 in $s_{12} = (p_a + p_c)^2$ we find from (3.18) and (3.19),

$$\mathrm{disc}_{s_{12}} A_5 = 2i\Gamma(-\alpha_1) s_1^{\alpha_1} \{\exp\{i\pi(\alpha_1-\alpha_2)\}\sin\pi(-\alpha_1)\,\eta_{12}^{\alpha_1} V_1 + \exp\{i\pi(\alpha_2-\alpha_1)\}\sin\pi(-\alpha_2)\,\eta_{12}^{\alpha_2} V_2\}$$

$$\times \Gamma(-\alpha_2) s_2^{\alpha_2}\beta_1(t_1)\beta_2(t_2)$$

and hence from (5.21)

$$\underset{t_1 \qquad\qquad t_2}{\longrightarrow\!\!\curvearrowright\!\!\curvearrowright\!\!\downarrow\!\!\curvearrowleft\!\!\curvearrowleft\!\!\longrightarrow} \quad = -\frac{\exp\{i\pi(\alpha_1-\alpha_2)\}}{2i\sin\pi\alpha_2}\,\eta_{12}^{\alpha_1} V_1 - \frac{\exp\{i\pi(\alpha_2-\alpha_1)\}}{2i\sin\pi\alpha_1}\,\eta_{12}^{\alpha_2} V_2\ . \tag{5.22}$$

Similarly from $\mathrm{disc}_{s_1} A_5$ we obtain

$$\underset{t_1 \qquad\qquad t_2}{\longrightarrow\!\!\curvearrowright\!\!\curvearrowright\!\!\downarrow\!\!\nearrow\!\!\curvearrowleft\!\!\curvearrowright} \quad = \frac{\sin\pi(\alpha_1-\alpha_2)}{\sin\pi\alpha_1}\,\eta_{12}^{\alpha_2} V_2\ . \tag{5.23}$$

Now consider the discontinuity in $s_{123} = (p_a + p_d)^2$ of A_6 as shown in fig. 5.6(a). Only the first term of the eight forming the full amplitude has singularities in this channel and using (5.13) we obtain

$$\mathrm{disc}_{s_{123}} A_6 \sim 2i\Gamma(-\alpha_1) s_1^{\alpha_1} \Gamma(-\alpha_2) s_2^{\alpha_2} \Gamma(-\alpha_3) s_3^{\alpha_3} \{\exp\{i\pi(-\alpha_1+\alpha_3)\}\sin\pi(-\alpha_3)\,\eta_{12}^{\alpha_2}\eta_{23}^{\alpha_3} W_{23}^3$$

$$+ \exp\{i\pi(-\alpha_2+\alpha_3)\}\sin\pi(-\alpha_3)\,\eta_{12}^{\alpha_1}\eta_{23}^{\alpha_3} W_{13}^3 + \exp\{i\pi(-\alpha_1+2\alpha_2-\alpha_3)\}\sin\pi(-\alpha_2)\,\eta_{12}^{\alpha_2}\eta_{23}^{\alpha_2} W_{22}^2$$

$$+ \exp\{i\pi(\alpha_1-\alpha_2)\}\sin\pi(-\alpha_1)\,\eta_{12}^{\alpha_1}\eta_{23}^{\alpha_3} W_{13}^1 + \exp\{i\pi(\alpha_1-\alpha_3)\}\sin\pi(-\alpha_1)\,\eta_{12}^{\alpha_1}\eta_{23}^{\alpha_2} W_{12}^1\}\ . \tag{5.24}$$

Fig. 5.6. Examples of discontinuities of A_6: (a) discontinuity in s_{123}, (b) discontinuity in s_2, (c) double discontinuity in s_{123} and s_2, (d) triple discontinuity in s_{123}, s_{12} and s_2.

Using (5.15), (5.20) and the identity

$$\exp\{i\pi(-\alpha_2+\alpha_3)\}\sin\pi(\alpha_2-\alpha_3) - \exp\{i\pi(\alpha_1-\alpha_2)\}\sin\pi(\alpha_2-\alpha_1) = \exp\{i\pi(\alpha_1-2\alpha_2+\alpha_3)\}\sin\pi(\alpha_1-\alpha_3),$$

to combine the W_{13}^3 and W_{13}^1 terms, we have

$$\text{disc}_{s_{123}}A_6 \sim 2i\beta(t_1)\sin\pi(-\alpha_1)\,\Gamma(-\alpha_1)\,s_1^{\alpha_1}$$

$$\times \left[-\frac{\exp\{i\pi(\alpha_1-\alpha_2)\}}{\sin\pi\alpha_2}\eta_{12}^{\alpha_1}V_1 - \frac{\exp\{i\pi(\alpha_2-\alpha_1)\}}{\sin\pi\alpha_1}\eta_{12}^{\alpha_2}V_2\right]\sin\pi(-\alpha_2)\,\Gamma(-\alpha_2)\,s_2^{\alpha_2}$$

$$\times \left[-\frac{\exp\{i\pi(\alpha_2-\alpha_3)\}}{\sin\pi\alpha_3}\eta_{23}^{\alpha_2}V_2 - \frac{\exp\{i\pi(\alpha_3-\alpha_2)\}}{\sin\pi\alpha_2}\eta_{23}^{\alpha_3}V_3\right]\sin\pi(-\alpha_3)\,\Gamma(-\alpha_3)\,s_3^{\alpha_3}\beta(t_3)\,. \quad (5.25)$$

The discontinuity clearly factorizes into the product of the appropriate propagators and vertices (5.21) and (5.22). The factorization of the other single discontinuities of A_6 can similarly be easily checked. (One should note that four terms out of the eight contribute to the discontinuity in fig. 5.6(b), for example.)

This rather remarkable factorization also extends to multiple discontinuities such as those shown in fig. 5.6(c) and (d). We must first identify the basic double-Regge vertex with two discontinuities taken through it. From $\text{disc}_{s_1}\text{disc}_{s_{12}}A_5$ we easily find

  $= \dfrac{\sin\pi(\alpha_1-\alpha_2)}{\sin\pi\alpha_1}\eta_{12}^{\alpha_2}V_2\,.$

$$(5.26)$$

For fig. 5.6(c) we find, using formula (5.13),

$$\mathrm{disc}_{s_2}\, \mathrm{disc}_{s_{123}} A_6 \sim \Gamma(-\alpha_1)\, s_1^{\alpha_1}\, \Gamma(-\alpha_2)\, s_2^{\alpha_2}\, \Gamma(-\alpha_3)\, s_3^{\alpha_3}$$

$$\times\ (2\mathrm{i})^2 \{\exp\{i\pi(-\alpha_1+\alpha_3)\}\, \sin\pi(\alpha_1-\alpha_2)\, \sin\pi\alpha_3\, W_{13}^3$$

$$+ \exp\{i\pi(\alpha_1-\alpha_3)\}\, \sin\pi(\alpha_3-\alpha_2)\, \sin\pi\alpha_1\, W_{13}^1 \}\ ,$$

and then (5.20),

$$\mathrm{disc}_{s_2}\, \mathrm{disc}_{s_{123}} A_6 \sim (2\mathrm{i})^3\, \beta(t_1)\, \sin\pi(-\alpha_1)\, \Gamma(-\alpha_1)\, s_1^{\alpha_1} \left[\frac{\sin\pi(\alpha_2-\alpha_1)}{\sin\pi\alpha_2}\, \eta_{12}^{\alpha_1} V_1\right]$$

$$\times\ \sin\pi(-\alpha_2)\, \Gamma(-\alpha_2)\, s_2^{\alpha_2} \left[\frac{\sin\pi(\alpha_2-\alpha_3)}{\sin\pi\alpha_2}\, \eta_{23}^{\alpha_3} V_3\right] \sin\pi(-\alpha_3)\, \Gamma(-\alpha_3)\, s_3^{\alpha_3}\, \beta(t_3)\ ,$$

which has the required factorized form. The factorization of the other multiple discontinuities is similarly checked with the rule that further cutting of a propagator or vertex does not change it — see fig. 5.7.

The above discussion has shown how intimately the factorization of multi-Regge amplitudes and their discontinuities is related to the singularity structure of the amplitude. Without the somewhat complicated structure of (5.13), there would be little hope of obtaining factorization. We have seen that this structure, constrained by the requirement of factorization of the signatured and full amplitudes with energies above their cuts, implies the factorization of all discontinuities. One feels that the factorization of the signatured and full amplitudes is a natural consequence of the definition of a Regge-pole as a simple pole in the complex angular momentum plane and should be provable from *t-channel* unitarity*. The factorization of discontinuities then appears to be a somewhat mysterious consequence of the singularity structure of the amplitude.

On the other hand, the above argument could have been made in the reverse direction. The factorization of all single discontinuities implies the basic relations (5.15) and (5.20) and thus factorization of the full amplitude. At least within the context of the multiperipheral model there is a close connection between factorization of discontinuities and *s-channel* unitarity (see Halliday [76]). In this model the discontinuity is expressed as a sum over (*s*-channel) intermediate states of

---

* For example, White [147] has proven the factorization of the double-Regge exchange in the five-particle amplitude in this way.
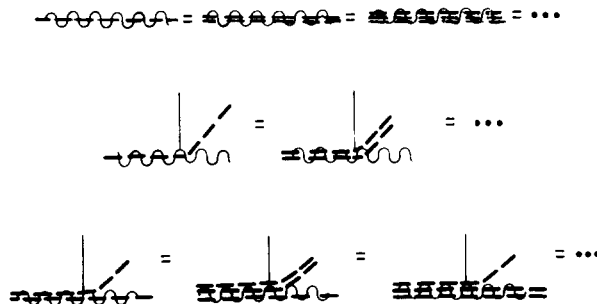

Fig. 5.7. Equality of propagator and vertices under several identical cuttings.

peripheral nature. Factorization of the "output" Regge exchanges follows because they are generated by an infinite number of peripheral links which essentially decouple the two ends of the Regge exchange. Therefore the s-channel picture of reggeons makes the factorization of discontinuities seem natural and the factorization of the full amplitude appears to be a mysterious consequence of the singularity structure.

The above discussion hints at the existence of a deeper reason for the validity of the factorization properties discussed above and a deeper connection with unitarity which, of course, is expected to imply the singularity structure exploited here. It may be that at least a partial deeper understanding of these factorization properties can arise from deriving them as a consequence of factorization of amplitudes of definite (complex) helicity as suggested by White [147]*.

In conclusion, we note that the general properties discussed above have indeed been found in explicit models. Factorization of the full amplitude has been shown in Gribov's hybrid model [31], the ladder model [76], and the dual resonance model [139]. Factorization of total energy discontinuity appropriate for inclusive cross sections has been shown in the ladder and Gribov model [77] and the dual-resonance model [80,83,84,87,120,139]. For an example of factorization for amplitudes involving pseudoscalar particles, see Moen, Montonen and Zakrzewski [102]. In this case the analysis leading to (5.13) must be applied to appropriate invariant amplitudes.

5.3. Rules for multi-Regge amplitudes

One naturally expects that the discussion of the preceding subsection can be generalized to an arbitrary multi-Regge amplitude or discontinuity thereof — see figs. 5.1 and 5.2. Thus these amplitudes should be expressible as products of the basic uncut and cut propagators and vertices. In fig. 5.8 we show these basic objects. The propagators and single- and double-Regge vertices have been discussed above. The triple-Regge vertices can easily be obtained from the results of section 4.1. For completeness we also collect here the expressions for the vertex parts of definite helicity:

$$V_i = \frac{1}{\Gamma(-\alpha_i)\Gamma(-\alpha_j)} \sum_{m=0}^{\infty} \Gamma(-\alpha_i+m)\,\Gamma(-\alpha_i+\alpha_j-m)\,\frac{\eta_{ij}^{-m}}{m!}\,\beta(\alpha_i-m;t_i,t_j)\ ,$$

$$V_{ij} = \frac{1}{\Gamma(-\alpha_i)\,\Gamma(-\alpha_j)\,\Gamma(-\alpha_k)} \sum_{m,n,p=0}^{\infty} \Gamma(-\alpha_i+m+p)\,\Gamma(-\alpha_j+n+p)\,\Gamma(-\alpha_k+\alpha_i+\alpha_j-m-n-2p)$$

$$\times\ \frac{1}{m!\,n!\,p!}\ \eta_{ki}^{-m}\,\eta_{jk}^{-n}\,\left(\frac{\eta_{ki}\eta_{jk}}{\eta_{ij}}\right)^{-p}\,\beta(p,\alpha_j-n-p,\alpha_i-m-p;t_i,t_j,t_k)\ ,$$

$$V_{ijk} = \frac{1}{2\Gamma(-\alpha_i)\,\Gamma(-\alpha_j)\,\Gamma(-\alpha_k)} \sum_{m,n,p=0}^{\infty} \Gamma[\tfrac{1}{2}(\alpha_i-\alpha_j-\alpha_k-m+n+p)]\,\Gamma[\tfrac{1}{2}(\alpha_j-\alpha_k-\alpha_i-n+p+m)]$$

$$\times\ \Gamma[\tfrac{1}{2}(\alpha_k-\alpha_i-\alpha_j-p+m+n)]\,\frac{(-1)^{m+n+p}\exp\{-\tfrac{1}{2}i\pi(m+n+p)\}}{m!\,n!\,p!}\left(\frac{\eta_{ki}\eta_{ij}}{\eta_{jk}}\right)^{-m/2}\left(\frac{\eta_{ij}\eta_{jk}}{\eta_{ki}}\right)^{-n/2}\left(\frac{\eta_{jk}\eta_{ki}}{\eta_{ij}}\right)^{-p/2}$$

$$\times\ \beta[\tfrac{1}{2}(\alpha_i+\alpha_j-\alpha_k-m-n+p),\tfrac{1}{2}(\alpha_j+\alpha_k-\alpha_i-n-p+m),\tfrac{1}{2}(\alpha_k+\alpha_i-\alpha_j-p-m+n);t_i,t_j,t_k]\ ,\quad (5.27)$$

---

* Note that discontinuities tend to extract amplitudes of definite helicity. For example, the discontinuity in (5.23) extracts the amplitudes of helicity $\lambda = \alpha_2 - N$ $(N = 0,1,2,...)$.

a) t_i ⟨propagator diagram⟩ $= \xi_i \Gamma(-\alpha_i) s^{\alpha_i}$

b) t_i ⟨propagator diagram⟩ $= \dfrac{2\pi i}{\Gamma(\alpha_i + 1)} s^{\alpha_i}$

c) t_i ⟨vertex diagram⟩ $= \beta(t_i)$

d) t_i ⟨vertex diagram⟩ $= \beta(t_i)$

e) t_i ⟨diagram⟩ t_j $= R(t_i, t_j; \eta_{ij}) = \xi_j^{-1} \xi_{ji} \bar{V}_i + \xi_i^{-1} \xi_{ij} \bar{V}_j$

f) t_i ⟨diagram⟩ t_j $= \dfrac{\sin\pi(\alpha_i - \alpha_j)}{\sin\pi\alpha_i} \bar{V}_j$

g) t_i ⟨diagram⟩ t_j $= -\dfrac{e^{i\pi(\alpha_i - \alpha_j)}}{2 i \sin\pi\alpha_j} \bar{V}_i - \dfrac{e^{i\pi(\alpha_j - \alpha_i)}}{2 i \sin\pi\alpha_i} \bar{V}_j$

h) t_i ⟨diagram⟩ t_j $= \dfrac{\sin\pi(\alpha_i - \alpha_j)}{\sin\pi\alpha_i} \bar{V}_j$

Fig. 5.8. Basic propagators and vertices; $\xi_i = \exp\{-i\pi\alpha_i\} + \tau_i$, $\xi_{ij} = \exp\{-i\pi(\alpha_i - \alpha_j)\} + \tau_i\tau_j$, $\xi_{ijk} = \exp\{-i\pi(\alpha_i - \alpha_j - \alpha_k)\} + \tau_i\tau_j\tau_k$. The dependence of the functions $\bar{V}_i = \eta_{ij}^{\alpha_i} V_i$, $\bar{V}_{ij} = \eta_{ki}^{\alpha_i}\eta_{jk}^{\alpha_j} V_{ij}$, etc, on the t_i and η_{ij} has been suppressed. In the expansion (5.27) for V_{ijk} the following factors must be inserted:

for (i), $[1 + (-1)^{m+n+p}\tau_i\tau_j\tau_k]$;

for (k), $[\sin\frac{1}{2}\pi(\alpha_i + \alpha_j - \alpha_k - m - n + p)/\sin\frac{1}{2}\pi(\alpha_i + \alpha_j - \alpha_k)]$;
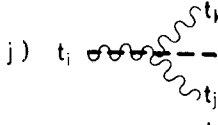
for (n), $[\sin\frac{1}{2}\pi(\alpha_i + \alpha_j - \alpha_k - m - n + p)\sin\frac{1}{2}\pi(\alpha_k + \alpha_i - \alpha_j - p - m + n)/\sin\frac{1}{2}\pi(\alpha_i + \alpha_j - \alpha_k)\sin\frac{1}{2}\pi(\alpha_k + \alpha_i - \alpha_j)]$;
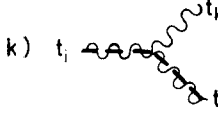
for (o), $[\sin\frac{1}{2}\pi(\alpha_i + \alpha_j - \alpha_k - m - n + p)\sin\frac{1}{2}\pi(\alpha_j + \alpha_k - \alpha_i - n - p + m)\sin\frac{1}{2}\pi(\alpha_k + \alpha_i - \alpha_j - p - m + n)/\sin\frac{1}{2}\pi(\alpha_i + \alpha_j - \alpha_k)$

$\times \sin\frac{1}{2}\pi(\alpha_j + \alpha_k - \alpha_i)\sin\frac{1}{2}\pi(\alpha_k + \alpha_i - \alpha_j)]$.
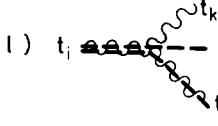
where the real functions β have no singularities in their arguments below thresholds in the t_i in the absence of multiplicative fixed poles.
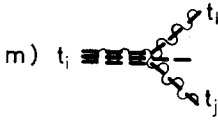
Factorization of arbitrary multi-Regge amplitudes has thus far been shown only in certain models as we discuss below. However it is expected to hold on the same general grounds as the discussion in the preceding subsection. We note that this requires the existence of signatured amplitudes with singularities in a complete set of planar channels (channels formed from several adjacent lines for a fixed ordering of the external lines — see fig. 5.1). It is expected that Regge
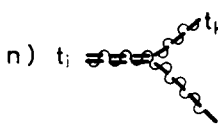
i) t_i ... t_k ... t_j

$$= R(t_i, t_j, t_k; n_{ij}, n_{jk}, n_{ki}) =$$

$$\xi_k^{-1} \xi_{kij} \bar{V}_{ij} + \xi_i^{-1} \xi_{ijk} \bar{V}_{jk} + \xi_j^{-1} \xi_{jki} \bar{V}_{ki} +$$

$$+ \xi_i^{-1} \xi_j^{-1} \xi_k^{-1} e^{-i\frac{\pi}{2}(\alpha_i + \alpha_j + \alpha_k)} \left\{ 1 + \tau_i e^{i\pi\alpha_i} + \tau_j e^{i\pi\alpha_j} + \tau_k e^{i\pi\alpha_k} \right\} \bar{V}_{ijk}$$

j) t_i ... t_k ... t_j

$$= \frac{\sin\pi(\alpha_i - \alpha_j - \alpha_k)}{\sin\pi\alpha_i} \bar{V}_{jk}$$

k) t_i ... t_k ... t_j

$$= -\frac{e^{i\pi(\alpha_j + \alpha_k - \alpha_i)}}{2i\sin\pi\alpha_i} \bar{V}_{jk} - \frac{e^{i\pi(\alpha_k + \alpha_i - \alpha_j)}}{2i\sin\pi\alpha_j} \bar{V}_{ki} - \frac{\sin\frac{\pi}{2}(\alpha_i + \alpha_j - \alpha_k)}{2i\sin\pi\alpha_i \sin\pi\alpha_j} \bar{V}_{ijk}$$

l) t_i ... t_k ... t_j

$$= \frac{\sin\pi(\alpha_i - \alpha_j - \alpha_k)}{\sin\pi\alpha_i} \bar{V}_{jk}$$

m) t_i ... t_k ... t_j

$$= \frac{\sin\pi(\alpha_i - \alpha_j - \alpha_k)}{\sin\pi\alpha_i} \bar{V}_{jk}$$

n) t_i ... t_k ... t_j

$$= -\frac{e^{i\pi(\alpha_j + \alpha_k - \alpha_i)}}{2i\sin\pi\alpha_i} \bar{V}_{jk} + \frac{e^{i\frac{\pi}{2}(\alpha_i - \alpha_j - \alpha_k)} \sin\frac{\pi}{2}(\alpha_j + \alpha_i - \alpha_k) \sin\frac{\pi}{2}(\alpha_k + \alpha_i - \alpha_j)}{2i\sin\pi\alpha_i \sin\pi\alpha_j \sin\pi\alpha_k} \bar{V}_{ijk}$$

o) t_i ... t_k ... t_j

$$= \frac{\sin\frac{\pi}{2}(\alpha_i + \alpha_j - \alpha_k) \sin\frac{\pi}{2}(\alpha_j + \alpha_k - \alpha_i) \sin\frac{\pi}{2}(\alpha_k + \alpha_i - \alpha_j)}{\sin\pi\alpha_i \sin\pi\alpha_j \sin\pi\alpha_k} \bar{V}_{ijk}$$

Fig. 5.8. For caption see last page.

behaved nonplanar amplitudes can be decomposed into such signatured amplitudes with only the added complication of the introduction of multiplicative nonsense wrong-signature fixed poles (see sections 3.4 and 4.2). This type of analysis also requires the simple singularity structure assumed in (D) of section 1.4. For some discussion of the possible effects of more complicated singularities, see the end of section 8.2.

Finally we also note that the specific forms of the vertices given in fig. 5.8 and eq. (5.27) are appropriate for amplitudes with all scalar particles and thus all trajectories of natural parity. They also have the behavior at $t = 0$ corresponding to nondegenerate, e.g. Toller quantum number $M = 0$, trajectories. To treat other cases the analysis should be applied to appropriate invariant amplitudes.

Most of the factorization results embodied in the rules stated above have been proven in the dual resonance model — for discussion, see Weis [143]. These results can be extended to a large class of models which are essentially integrals over the dual-resonance model of the form

$$A_N \sim \prod_{i,j} \int dz_{ij} \prod f(t_i, t_j, t_k; z_{ij}, z_{jk}, z_{ki}) B_N(\{\alpha_i\}, \{s_i\}, \{z_{ij}\eta_{ij}\}, \{\phi_{ij\ldots l}\}) , \tag{5.28}$$

where $\phi_{ij\ldots l}$ is the ratio in (5.3) and there is one smearing function f for each vertex*. As long as the z_{ij} integrals do not create any further singularities in the η_{ij} or $\phi_{ij\ldots k}$, the results for the dual-resonance model carry over directly. Representations of this form were originally introduced by the Cambridge group [56,96]. They found that all models they studied had double- and triple-Regge vertices of this form. We believe that (5.28) may be the most general form consistent with the singularity structure assumed here and factorization of the full amplitude.

Finally, we note that in this section we have discussed multi-Regge amplitudes with only vertices with three lines. Amplitudes involving reggeon couplings with more than three lines are also of interest, particularly in inclusive cross sections as discussed in section 6 (see fig. 6.2). We expect the factorization properties discussed above to generalize to these more complicated amplitudes as is the case in models studied thus far (see the end of section 5.2). It should also be emphasized that the rules given above are for all $s_{ij\ldots k} > 0$; to treat the case of some $s_{ij\ldots k} < 0$ (as is the case in inclusive cross sections) an analysis like that of section 5.2 must be carried out.

6. Applications to inclusive cross sections

The multi-Regge limits of particular *exclusive* processes, e.g. $a + b \rightarrow c_1 + \ldots + c_n$ (see fig. 2.11), give small cross sections in restricted regions of phase space and are therefore difficult to confront with experiment. Consequently, interest in multi-Regge theory for a long time was confined to a small band of devotees. However, Mueller [104] realized that the theory could be applied to the larger *inclusive* cross sections for $a + b \rightarrow c_1 + \ldots + c_n + X$, where X is any (undetected) state. For no detected particles ($n = 0$) this is just the familiar total cross section. Unitarity relates the sum over X to the s discontinuity of the elastic amplitude $A_4^{ab}(s, t = 0)$ (optical theorem). Regge behavior of A_4^{ab} then gives a Regge expansion for the total cross section (see fig. 6.1).

---

* We have given the form for triple-Regge vertices. Double-Regge vertices have factors $f(t_i, t_j; z_{ij})$.
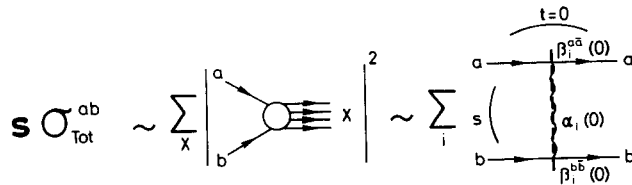

Fig. 6.1. The Regge limit for the totally inclusive reaction $a + b \rightarrow X$ (i.e. total cross section) as a discontinuity (dashed line) of the forward ($t = 0$) elastic amplitude for $a + b \rightarrow a + b$.
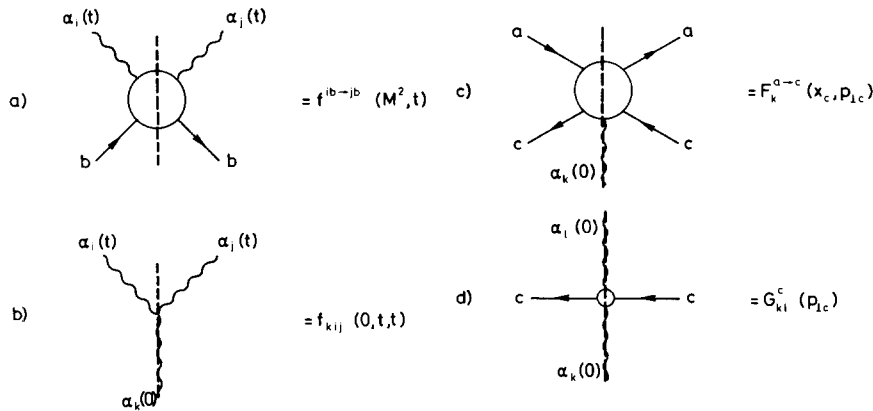
Fig. 6.2. Notation for vertices encountered in single-particle inclusive cross sections, $a + b \to c + X$: $f^{ib \to jb}$, f_{kij}, F and G contribute to the phase space regions with $M^2 = \text{const.}$, $M^2/s \to 0$, $0 \leqslant M^2/s \leqslant 1$, and $M^2/s \to 1$, respectively, as $s = (p_a + p_b)^2 \to \infty$. The dashed line indicates a discontinuity in $M^2 = (p_a + p_b - p_c)^2$.

In section 6.1 we generalize the optical theorem to express the inclusive cross sections for $a + b \to c_1 + \ldots + c_n + X$ as appropriate discontinuities of the forward $a + b + c_1 + \ldots + c_n \to a + b + c_1 + \ldots + c_n$ amplitudes. Then in sections 6.2 and 6.3 we apply multi-Regge theory to obtain Regge expansions of the cross sections in various regions of phase space. Some of the Regge couplings involved are shown in fig. 6.2. In section 6.4 we return to the unitarity equations to give sum rules relating different inclusive cross sections (e.g. different Regge couplings).

We restrict ourselves to those aspects of inclusive Regge theory which illustrate the basic concepts of multi-Regge theory. For reviews of the vast literature on inclusive phenomenology we refer the reader to Frazer et al. [64], Roberts [118], and Slansky [125].

6.1. Generalized optical theorems

For the total cross section ($a + b \to X$), the unitarity equation,*

$$\tag{6.1}$$

for $p_a = p_{a'}$, $p_b = p_{b'}$, converts the cross section

$$\sigma_{\text{Tot}}^{ab} = \frac{1}{2\sqrt{\lambda}} \sum_{n=2}^{\infty} \prod_{t} \frac{1}{n_t!} \int \prod_{i=1}^{n} dp_i (2\pi)^4 \delta^4(p_a + p_b - \Sigma p_i) |A_{n+2}(p_a, p_b; p_1, \ldots, p_n)|^2 \tag{6.2}$$

into the optical theorem

---

* In this section we use a mixed convention for momenta since it is more convenient than the all-incoming convention used elsewhere in this work.
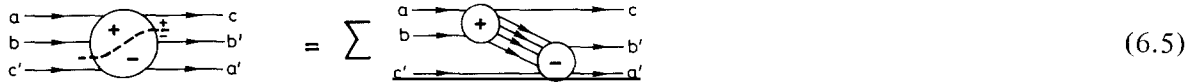
$$\sigma_{\text{Tot}}^{\text{ab}} = \frac{1}{\sqrt{\lambda}} \, \frac{1}{2i} \, \text{disc}_s A_4^{\text{ab}}(s, 0) \, . \tag{6.3}$$

In the above, $s = (p_a + p_b)^2$, $\lambda = \lambda(s, m_a^2, m_b^2)$, $dp_i = d^3 p_i / 2 E_i (2\pi)^3$, and $1/n_t!$ is the statistical factor for n_t identical particles of type t.

We would like to use a similar unitarity equation to relate the inclusive cross section for $a + b \rightarrow c + X$,

$$(2\pi)^3 \, 2 E_c \frac{d^3 \sigma^{\text{ab}}}{d^3 p_c} = \frac{1}{2\sqrt{\lambda}} \sum_{n=1}^{\infty} \prod_t \frac{1}{n_t!} \int \prod_{i=1}^{n} dp_i (2\pi)^4 \delta^4(p_a + p_b - p_c - \Sigma p_i)$$

$$\times \, |A_{n+3}(p_a, p_b; p_c, p_1, \dots, p_n)|^2 \, , \tag{6.4}$$

to the forward six-particle amplitude. The appropriate equation is (for $p_a = p_{a'}$, $p_b = p_{b'}$, $p_c = p_{c'}$)

$$\tag{6.5}$$

We define $s = (p_a + p_b)^2$, $t = (p_a - p_c)^2$, $u = (p_b - p_c)^2$ and $M^2 = (p_a + p_b - p_c)^2 = m_X^2$. The dashed line in (6.5) indicates a discontinuity in M^2 so the generalized optical theorem is

$$(2\pi)^3 \, 2 E_c \, d^3 \sigma^{\text{ab}} / d^3 p_c = \frac{1}{\sqrt{\lambda}} \, \frac{1}{2i} \, \text{disc}_{M^2} A_6^{\text{ab} \rightarrow \text{c}}(s, t, M^2) \, . \tag{6.6}$$

The definition of the discontinuity in (6.5) involves some subtle points which are not present in (6.1) [126,113,129,29,30]. The signs inside the bubble on the left-hand side give the location of the subenergy invariants on each side of the discontinuity with respect to their cuts; most importantly, $s_{\text{ab}} = (p_a + p_b)^2$ is above its cut and $s_{a'b'} = (p_{a'} + p_{b'})^2$ is below its cut [the reason for this is clearly seen from the right-hand side of (6.5)]. One might believe that for variables which overlap the discontinuity the location relative to their cuts should also be specified. In particular, the variable $(p_a + p_b + p_{c'})^2$ is above its threshold (and linearly related to M^2). However, the Steinmann relations discussed in section 1.4 guarantee that the discontinuity is independent of the locations of these overlapping variables so they need not be specified. We should remark, however, that there are anomalous thresholds present in M^2 in general in addition to the usual normal thresholds [113,129,111]. If we assume the simplified singularity structure discussed in section 1.4 as we have in preceding sections, none of these subtle points arise, of course.

The above optical theorems can be generalized with no more difficulty to the n-particle inclusive reaction, $a + b \rightarrow c_1 + \dots + c_n + X$,

$$\frac{d^n \sigma^{\text{ab}}}{dp_{c_1} \dots dp_{c_n}} = \frac{1}{\sqrt{\lambda}} \, \frac{1}{2i} \, \text{disc}_{M^2} A_{2(n+2)}(p_a, p_b; p_{c_1}, \dots, p_{c_n}) \, , \tag{6.7}$$
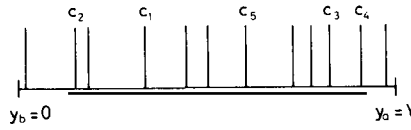
where $M^2 = (p_a + p_b - p_{c_1} \dots - p_{c_n})^2$.

Fig. 6.3. Rapidity plot for a particular event in the reaction $a + b \to c_1 + \ldots + c_5 + X$, with 7 particles in state X.

6.2. Mueller–Regge limits

We wish to consider the high energy or Regge limits of the inclusive process $a + b$ $\to c_1 + \ldots + c_n + X$ [104]. The central lesson of experiment is that particle production is confined to a region of phase space where p_i ($i = c_1, \ldots, c_n$) have small *transverse* momentum ($|p_{\perp i}| \sim 0.5$ GeV) relative to the longitudinal momentum along p_a and p_b. Consequently, we use the rapidity y_i and the transverse momentum $p_{\perp i}$ variables introduced in section 2.4. Fig. 6.3 gives the rapidity plot for a typical final state $c_1 + \ldots + c_n + X$ in the rest frame of particle b ($y_b = 0$, $y_a = Y \sim \ln s$).

6.2.1. Single particle inclusive cross section

First we consider the Regge limits for the single particle inclusive reaction, $a + b \to c + X$, where we use the total rapidity Y, the rapidity ($y = y_c$) of c, and the transverse momentum ($p_\perp = p_{\perp c}$) of c to replace s, t, M^2 invariants in (6.6). As $Y \to \infty$, the physical region is the interval $y_{\min} \leqslant y \leqslant y_{\max}$, where

$$y_{\min} \sim y_b - \ln(m_b/\omega_c), \qquad y_{\max} \sim y_a + \ln(m_a/\omega_c). \tag{6.8}$$

This interval can be divided up into a number of regions as shown in fig. 6.4. These regions, to be discussed in sequence below, are for $p_\perp$ fixed and $Y \to \infty$:

Fixed M^2	$y - y_{\min} \to \infty$;	$y_{\max} - y \to 0$
Triple-Regge	$y - y_{\min} \to \infty$;	$y_{\max} - y \ll 1$
Fragmentation of a into c ($a \to c|b$)	$y - y_{\min} \to \infty$;	$y_{\max} - y$ finite
Central ($a|c|b$)	$y - y_{\min} \to \infty$;	$y_{\max} - y \to \infty$
Fragmentation of b into c ($a|c \to b$)	$y - y_{\min}$ finite;	$y_{\max} - y \to \infty$
Triple-Regge	$y - y_{\min} \ll 1$;	$y_{\max} - y \to \infty$
Fixed M^2	$y - y_{\min} \to 0$;	$y_{\max} - y \to \infty$.

$$\tag{6.9}$$

The slash in ($a \to c|b$), etc., indicates the large rapidity gap.

In the fragmentation region it is sometimes convenient to use Feynman's x variable,
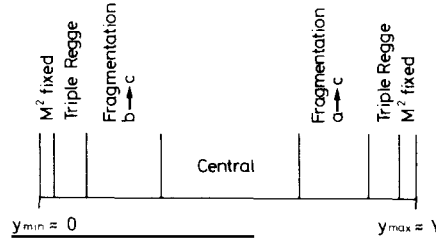
$$x = 2p_\parallel^{cm}/\sqrt{s}, \tag{6.10}$$

Fig. 6.4. Phase space regions in rapidity for the single-particle inclusive reaction a + b → c + X.

which is the fractional longitudinal momentum of c ($p_{\parallel}^{cm}$) in the center of mass of a and b. In this variable the fragmentation region of a(b) is $1 \geqslant x > 0$ ($-1 \leqslant x < 0$), and the invariant volume element is

$$d^3 p/E = d^2 p_{\perp} \, dy = d^2 p_{\perp} \, dx/\sqrt{x^2 + 4\omega_c^2/s} \approx d^2 p_{\perp} \, dx/x .$$ (6.11)

For the fragmentation region (a → c|b) or $x > 0$, we have the connection to the invariants

$$s \sim m_a m_b e^Y , \qquad M^2 \sim s(1 - e^{-\delta y}) \sim s(1 - x) , \qquad t \sim m_a^2 + m_c^2 - m_a^2 e^{-\delta y} - \omega_c^2 e^{\delta y} , \quad (6.12)$$

where

$$\delta y = y_{max} - y .$$

Just at the phase space boundary $\delta y = y_{max} - y \to 0$ there is a fixed M^2 region. Since only a fixed set of states occur in the sum over X

$$d^3\sigma/d^2 p_{\perp} \, dy \sim \frac{1}{s} \sum_X |A^{ab \to cX}|^2 ,$$ (6.13)

presumably we may take the $s \to \infty$ limit inside the sum. Each exclusive channel may be analyzed by Regge pole exchange in the $t = (p_a - p_c)^2$ channel [fig. 6.5(a,b)]

$$A^{ab \to cX} \sim \sum_i \xi_i \, \beta_i^{a\bar{c}}(t) \, s^{\alpha_i(t)} V_i^{bX} ,$$ (6.14)
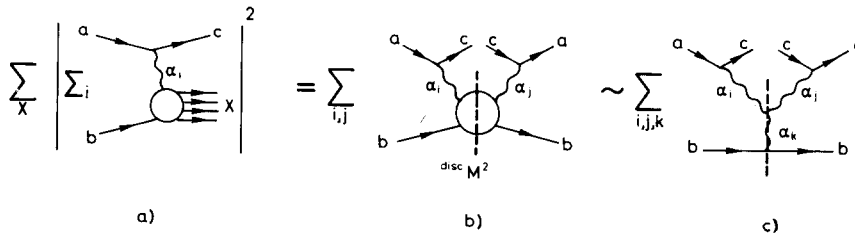

Fig. 6.5. Regge limit of inclusive reaction a + b → c + X for (b) fixed M^2 and (c) $s \gg M^2 \gg 1$.

to obtain the inclusive cross section:

$$d^3\sigma/d^2p_\perp \, dy \sim \frac{1}{s} \sum_{i,j} \xi_i \xi_j^* \, \beta_i^{a\bar{c}}(t) \, \beta_j^{a\bar{c}}(t) s^{\alpha_i(t)+\alpha_j(t)} f^{ib \to jb}(M^2, t) \,. \tag{6.15}$$

The function $f^{ib \to jb}(M^2, t)$ can be interpreted as the absorptive part of a reggeon i + b $\to$ reggeon j + b scattering amplitude in the forward direction $t_{b\bar{b}} = 0$.

As we move further away from the phase space boundary, M^2 becomes large and

$$f^{ib \to jb}(M^2, t) \underset{M^2 \to \infty}{\sim} \sum_k \beta_k^{b\bar{b}}(0) \, (M^2)^{\alpha_k(0) - \alpha_i(t) - \alpha_j(t)} f_{kij}(0, t, t) \,. \tag{6.16}$$

This is the so-called triple-Regge behavior [see fig. 6.5(c)] valid for $s \gg M^2 \gg 1$ ($x \approx 1$). The derivation of (6.16) and its relation to (6.15) through finite energy sum rules will be discussed in detail in section 6.3. Combining (6.16) and (6.15) gives

$$d^3\sigma/d^2p_\perp \, dy \sim \frac{1}{s} \sum_{i,j,k} \xi_i \xi_j^* \, \beta_i^{a\bar{c}}(t) \, \beta_j^{a\bar{c}}(t) \, (s/M^2)^{\alpha_i(t)+\alpha_j(t)} f_{kij}(0, t, t) (M^2)^{\alpha_k(0)} \beta_k^{b\bar{b}}(0) \,. \tag{6.17}$$

Moving away from $x = 1$, we enter the fragmentation region (a $\to$ c|b). (Since p_c is finite in the rest frame of a, c may be thought of as a "fragment of a".) From (6.12) we can see that this limit corresponds to the single-Regge limit on A_6 shown in fig. 6.6. Labelling the particles as in (6.5) we have from section 2.2:

$$A_6 \sim \sum_k \beta_k^{b\bar{b}'}(t_{b\bar{b}'}) \, \xi_k \, \Gamma(-\alpha_k) (M^2)^{\alpha_k} R_k(s_{a\bar{c}}, s_{a'\bar{c}'}, t_{a\bar{a}'}, s_{a\bar{a}'c'}, s_{a'\bar{a}c}, t_{b\bar{b}'}; s_{ab}/M^2, s_{a'b'}/M^2) \,. \tag{6.18}$$

One easily sees that all the arguments of R_k are fixed in the fragmentation limit as required. In order to obtain the inclusive cross section using the optical theorem (6.6) we must take the M^2 discontinuity of (6.18). This cannot be done without a detailed knowledge of the singularity structure of R_k in s_{ab}/M^2 and $s_{a'b'}/M^2$. We shall assume that the analogous analysis for A_5 (see section 3) can be generalized and the discontinuity taken, although this has not yet been carried out by anyone. Furthermore we assume the discontinuity factorizes; the analysis of section 5 makes it clear that this is not a trivial result although at the same time it is very plausible.

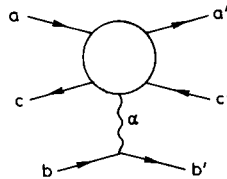Therefore in the fragmentation region (a $\to$ c|b), we can write (see fig. 6.7)

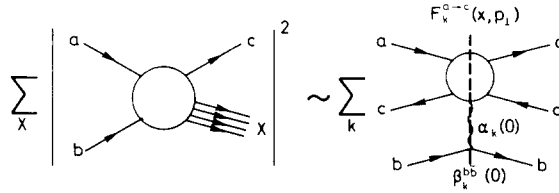Fig. 6.6. Single-Regge limit of the six-particle amplitude A_6.

Fig. 6.7. Single-Regge limit (a → c|b) for the inclusive process a + b → c + X in the fragmentation region of a.

$$\frac{d^3\sigma}{d^2p_\perp\,dy} \sim x\frac{d^3\sigma}{d^2p_\perp\,dy} \sim \frac{1}{s}\sum_k \beta_k^{b\bar b}(0)\,s^{\alpha_k(0)}\,F_k^{a\to c}(x,p_\perp)\,.$$ (6.19)

The function $F_k^{a\to c}$ is the fragmentation vertex coupling the reggeon α_k to the four particles $a\bar c \to a\bar c$.

The fragmentation region for $F_k^{b\to c}(x,p_\perp)$ is handled in exactly the same way except a ↔ b and $-1 \leqslant x < 0$, or $y - y_b$ fixed. The two regions $x < 0$ and $x > 0$ are separated by an infinite rapidity gap as $Y \to \infty$, so $F^{a\to c}(x)$ does not analytically continue into $F^{b\to c}$ as x is continued through $x = 0$.

The central region, which lies between the two fragmentation regions at $x = 0$, has two large rapidity gaps $y_a - y$ and $y - y_b$. Again we should do a careful double-Regge analysis of A_6 for abc → a'b'c', where there are three clusters of particles (aa', cc' and bb'). The result of this analysis is the double-Regge formula for the central region (fig. 6.8):

$$\frac{d^3\sigma}{d^2p_\perp\,dy} \sim \frac{1}{s}\sum_{kl} \beta_k^{b\bar b}(0)\,s_{bc}^{\alpha_k(0)}\,f_{kl}^c\,\overline{\left(\frac{s_{ac}s_{cb}}{s_{ab}}\right)}\,s_{ac}^{\alpha_l(0)}\,\beta_l^{a\bar a}(0)\,.$$ (6.20)

By the general rules of section 2.2, the only variable in the forward direction ($p_a = p_{a'}$, $p_b = p_{b'}$, $p_c = p_{c'}$) that is held fixed is

$$s_{ac}s_{cb}/s_{ab} \sim p_\perp^2 + m_c^2 = \omega_c^2\,.$$ (6.21)

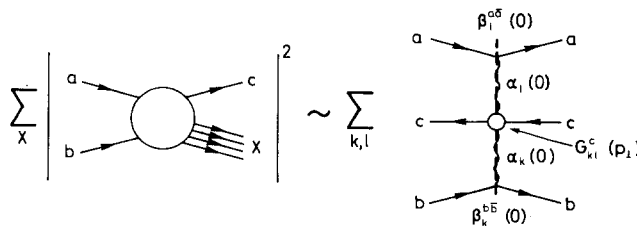We may re-express the formula (6.20) in rapidity variables as

Fig. 6.8. Double-Regge limit (a|c|b) for the inclusive reaction a + b → c + X in the central region.

$$\frac{d^3\sigma}{d^2p_\perp \, dy} \sim \frac{1}{s} \sum_{kl} \tilde{\beta}_k^{\rm b} \exp\{\alpha_k(y - y_{\rm b})\} G_{kl}^{\rm c}(p_\perp^2) \exp\{\alpha_l(y_{\rm a} - y)\} \tilde{\beta}_l^{\rm a} \,, \tag{6.22}$$

where

$$\tilde{\beta}_l^{\rm a} = m_{\rm a}^{\alpha_l(0)} \beta_l^{\rm a\bar{a}}(0) \,, \qquad\qquad G_{kl}^{\rm c}(p_\perp^2) = \omega_{\rm c}^{\alpha_k(0) + \alpha_l(0)} f_{kl}^{\rm c}(p_\perp^2 + m_{\rm c}^2) \,.$$

Consistency with triple-Regge and double-Regge limits puts boundary conditions on $F_k^{\rm a \to c}(x, p_\perp)$ at $x = 1$ and $x = 0$, respectively (fig. 6.4). The triple-Regge condition is

$$F_k^{\rm a \to c}(x, p_\perp) \sim \sum_{i,j} \xi_i \beta_i^{\rm a\bar{c}}(t) \, \xi_j^* \beta_j^{\rm a\bar{c}}(t) \, f_{kij}(0, t, t) \, (1 - x)^{\alpha_k(0) - \alpha_i(t) - \alpha_j(t)} \,, \tag{6.23}$$

as $x \to 1$, where $t = (p_{\rm a} - p_{\rm c})^2 \sim -p_\perp^2$. The triple-Regge behavior (6.17) is therefore the behavior necessary to provide a smooth connection between the fragmentation region (6.19) and the fixed M^2 region (6.15) [40,32,60,124]. The double-Regge boundary condition [24] is

$$F_k^{\rm a \to c}(x, p_\perp) \sim \sum_l \beta_l^{\rm a\bar{a}}(0) \, [m_{\rm a} \exp(y_{\rm a} - y)]^{\alpha_l(0) - \alpha_k(0)} G_{kl}^{\rm c}(p_\perp^2) \,, \tag{6.24}$$

as $x \sim \exp(y - y_{\rm a}) \to 0$. These boundary conditions assume uniformity in the interchange of Regge limits. Often the first term in the boundary conditions

$$F_k \sim (1 - x)^{\alpha_k(0) - 2\alpha_{\rm P}(t)} \,, \qquad\qquad F_k \sim \left(\frac{1}{x}\right)^{\alpha_{\rm P}(0) - \alpha_k(0)} \,, \tag{6.25}$$

accounts for the qualitative structure of the fragmentation vertex function $F_k(x, p_\perp^2)$.

6.2.2. General Regge limits of inclusive reactions*

For $a + b \to c_1 + \ldots + c_n + X$ there are as many Regge limits as we can group a, b, c_1, ..., c_n into clusters in the rapidity space**. With the bar denoting a large rapidity gap, the single inclusive Regge limits are designated $(a \to c|b)$, $(a|c|b)$ and $(a|c \leftarrow b)$. For $n = 2$, there are three limits replacing c by $c_1 c_2$, which are analyzed as in the $n = 1$ example, as well as the limits $(a \to c_1|c_2 \leftarrow b)$ and $(a|c_1|c_2|b)$.

The Regge formulae are easily "guessed". For example, for $Y \to \infty$, $(a \to c_1 c_2|b)$ is

$$E_1 E_2 \frac{d^6\sigma}{d^3p_1 \, d^3p_2} \sim \frac{1}{s} \sum_k \beta_k^{\rm b\bar{b}}(0) \, s^{\alpha_k(0)} F^{\rm a \to c_1 c_2}(x_1, p_{\perp 1}, x_2, p_{\perp 2}) \,, \tag{6.26}$$

the two-particle fragmentation formula. This involves a new vertex $F^{\rm a \to c_1 c_2}$ for a reggeon and six particles (see fig. 6.9(a)). We have

---

* See, for example, Abarbanel [1].

** The exclusive channel $a + b \to c_1 + \ldots + c_n$ has the same number of multi-peripheral Regge limits (section 2.4).

$$x_i \sim \exp(-\delta y_i) , \qquad\qquad i = 1, 2, \tag{6.27}$$

where $\delta y_i = y_{\max} - y_i$.

The limits $(a \to c_1|c_2 \leftarrow b)$ and $(a|c_1|c_2|b)$ involve only vertices defined for $n = 1$. Therefore we must make certain that our formulae are consistent with the assumed factorization of the Regge residues. The correct expression for double fragmentation $(a \to c_1|c_2 \leftarrow b)$ is (see fig. 6.9(b))

$$E_1 E_2 \frac{d^6\sigma}{d^3 p_1 d^3 p_2} \sim \frac{1}{s} \sum_k F_k^{a \to c_1}(x_1, p_{\perp 1}) s^{\alpha_k(0)} F_k^{b \to c_2}(x_2, p_{\perp 2}) . \tag{6.28}$$

Factorization has important consequences for the correlation function C defined as

$$C^{ab \to c_1 c_2} = \frac{E_1 E_2}{(\sigma_{\mathrm{Tot}}^{ab})^2} \frac{d^3\sigma}{d^3 p_1} \frac{d^3\sigma}{d^3 p_2} - \frac{E_1 E_2}{\sigma_{\mathrm{Tot}}^{ab}} \frac{d^6\sigma}{d^3 p_1 d^3 p_2} . \tag{6.29}$$

For a leading *factorized* pole (usually taken to be the pomeron at $J = \alpha_P(0) = 1$), correlations vanish

$$C^{ab \to c_1 c_2} \to 0, \qquad\qquad \text{as } s^{-\Delta\alpha}, \tag{6.30}$$

where $\Delta\alpha$ is the spacing between the leading pole and the next singularity. For a leading pole at $J = \alpha_P(0)$ and a secondary set (ρ, ω, A_2, f^0) at $\alpha(0) \approx \frac{1}{2}$, the correlations to leading order are

$$. \ (\sigma_{\mathrm{Tot}}^{ab})^2 C^{ab \to c_1 c_2} \sim \frac{1}{\sqrt{s}} \sum_{k=\rho,\omega,A_2,f} (\beta_P^{a\bar{a}} F_k^{a \to c_1} - \beta_k^{a\bar{a}} F_P^{a \to c_1})(\beta_P^{b\bar{b}} F_k^{b \to c_2} - \beta_k^{b\bar{b}} F_P^{b \to c_2}) , \tag{6.31}$$

and factorize. Some crude efforts have been made to check this factorization [22].

The Regge limit $(a|c_1|c_2|b)$ in fig. 6.9(c) becomes

$$E_1 E_2 \frac{d^6\sigma}{d^3 p_1 d^3 p_2} \sim \frac{1}{s} \sum_{k,l,m} \tilde{\beta}_k^a \exp\{\alpha_k(y_a - y_1)\} \, G_{kl}^{c_1}(p_{\perp 1}^2) \, \exp\{\alpha_l(y_1 - y_2)\} \, G_{lm}^{c_2}(p_{\perp 2}^2) \exp\{\alpha_m(y_2 - y_b)\} \, \tilde{\beta}_m^b \tag{6.32}$$
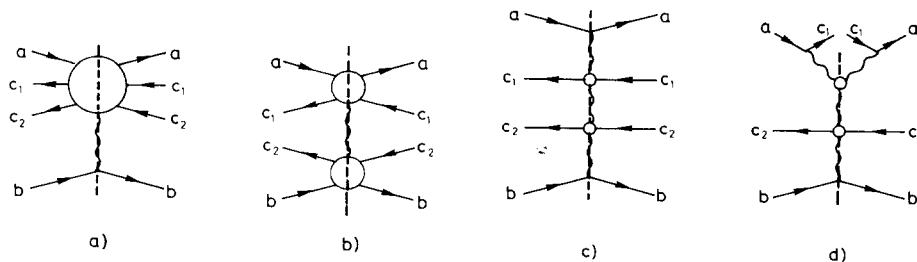

Fig. 6.9. Examples of Regge limits for the inclusive reaction $a + b \to c_1 + c_2 + X$: (a) diparticle fragmentation of a, $(a \to c_1 c_2|b)$; (b) single fragmentation of a and b, $(a \to c_1|c_2 \leftarrow b)$; (c) all large rapidity gaps $(a|c_1|c_2|b)$; (d) c_1 in triple-Regge region and c_2 in central region.

Again factorization has simple consequences for C. For pomerons on the ends (or $y_a - y_1 \to \infty$, $y_2 - y_b \to \infty$), we have

$$C^{ab \to c_1 c_2} \sim \sum_l G_{\mathrm{p}l}^{c_1} \exp\{-(\alpha_p(0) - \alpha_l(0)) \Delta y\} G_{l\mathrm{p}}^{c_2}, \tag{6.33}$$

where $\Delta y = |y_1 - y_2|$. This gives a correlation length $\sim 1/\Delta\alpha \sim 2$.

The rules for writing a general Regge limit of $a + b \to c_1 + ... + c_n + X$ are quite simple:

(1) Pick a clustering of the particles [e.g. $(a \to c_1|c_2 c_3|c_4|b)$] and for each cluster introduce a vertex $G_{k_1}^{c\cdots}$ as a function of each particle c_i, each transverse momenta $p_{\perp c_i}$ and all the rapidity differences in the cluster.

(2) For each reggeon introduce the Regge power $\exp\{\alpha_i(y_r - y_l)\}$ where $y_l(y_r)$ is a standard choice in the left (right) hand cluster.

(3) The clusters at the ends are given special symbols

$$\tilde{\beta}_i^a = (m_a)^{\alpha_i} \beta_i^{a\bar{a}}, \qquad \tilde{F}_i^{a \to c_1, ..., c_m} = (m_a)^{\alpha_i} F_i^{a \to c_1, ..., c_m}$$

because the factors of masses are needed to convert $\exp\{(y_a - y_b)\alpha_i\}$ into s in the simple cases.

For example $(a \to c_1|c_2 c_3|c_4|b)$ is

$$\prod_{i=1}^{4} E_i \frac{d^3}{d^3 p_i} \ \sigma^{ab} \sim \frac{1}{s} \sum_{i,j,k} \tilde{F}_i^{a \to c_1}(y_a - y_1, p_{\perp 1}) \exp\{\alpha_i(y_a - y_2)\}$$

$$\times \ G_{ij}^{c_2 c_3}(p_{\perp 2}, y_2 - y_3, p_{\perp 3}) \exp\{\alpha_j(y_2 - y_4)\} G_{jk}^{c_4}(p_{\perp 4}) \exp\{\alpha_k(y_4 - y_b)\} \tilde{\beta}_k^b . \tag{6.34}$$

These rules exhaust the multi-Regge formulae for the inclusive reaction $a + b \to c_1 + ... + c_n + X$ *except* for the triple-Regge limits (see, e.g., fig. 6.9(d)), the simplest of which is to be discussed in the next subsection. The rules incorporate the assumed factorization properties of Regge poles.

6.3. Triple-Regge behavior

Here we wish to derive the "triple-Regge" contribution (6.17) for the inclusive reaction,

$$\frac{d^2\sigma}{dt\, d(M^2/s)} \sim \frac{\pi}{s} \xi_1 \xi_2^* \beta_1(t)\beta_2(t) \left(\frac{s}{M^2}\right)^{\alpha_1(t)+\alpha_2(t)} f_{312}(0, t, t)(M^2)^{\alpha_3(0)}\beta_3(0), \tag{6.35}$$

from the triple-Regge and helicity limits of the six-particle amplitude of section 4 [49,91,51]*. If we return to the labelling of the energies of fig. 4.1 (note the labelling of the external lines is different), we have

$$s_3 = M^2, \qquad s_{31} = s, \qquad s_{23} = s^*,$$

$$s_1 = s_2 = m_a^2, \qquad s_{12} = 0, \qquad t_3 = 0, \qquad t_1 = t_2 = t, \tag{6.36}$$

---

* Here we follow the discussion of the last authors.

and thus

$$s_3, \eta_{23}, \eta_{31} \to \infty .$$

Since s_1 and s_2 remain finite this is certainly not a triple-Regge limit, but instead the mixed Regge-helicity limit discussed in section 4.3. From (4.24) we see that the signatured amplitude has the form

$$A_6^{\tau_1 \tau_2 \tau_3} \sim (-M^2)^{\alpha_3(0) - \alpha_1(t) - \alpha_2(t)} (-s)^{\alpha_1(t)} (-s^*)^{\alpha_2(t)} \Gamma(-\alpha_3(0) + \alpha_1(t) + \alpha_2(t)) \Gamma(-\alpha_1(t)) \Gamma(-\alpha_2(t))$$

$$\times \ \beta_3(0) \beta_1(t) \beta_2(t) \beta(0, \alpha_2(t), \alpha_1(t); t, t, 0) + (-s)^{\alpha_3(0)} U(t) . \tag{6.37}$$

Only the first term in (6.37) has a discontinuity in M^2 and thus contributes to the inclusive cross section,

$$E \frac{d^3\sigma}{d^3p} \sim \frac{1}{2is} \text{disc}_{M^2} A_6 \sim \beta_3(0) \, (M^2)^{\alpha_3(0)} \left(\frac{s}{M^2} \right)^{\alpha_1(t) + \alpha_2(t)} \beta_1(t) \beta_2(t) [\xi_1(t) \Gamma(-\alpha_1(t))] [\xi_2^*(t) \Gamma(-\alpha_2(t))]$$

$$\times \ \{\sin \pi(-\alpha_3(0) + \alpha_1(t) + \alpha_2(t)) \ \Gamma(-\alpha_3(0) + \alpha_1(t) + \alpha_2(t)) \ \beta(0, \alpha_2(t), \alpha_1(t); t, t, 0)\} , \tag{6.38}$$

where the signature factors arise from forming the full amplitude.

Although the limit under consideration is not a triple-Regge limit, the contribution to the discontinuity is precisely the same as the triple-Regge contribution. The triple-Regge form for the amplitude is given in (4.7). Only the first term contributes to the $M^2 = s_3$ discontinuity. The vertex part V_{12} is given by (4.21), from which we see that, for η_{31}, η_{23}, $1/\eta_{12} \to \infty$, only the leading term contributes, yielding precisely (6.38). Thus one can legitimately speak of the (6.35) as "triple-Regge behavior" of the inclusive cross section.

Comparing (6.35) and (6.38), we find

$$f_{312}(0, t, t) = \frac{\pi \Gamma(-\alpha_1(t)) \ \Gamma(-\alpha_2(t))}{\Gamma(\alpha_3(0) + 1 - \alpha_1(t) - \alpha_2(t))} \beta(0, \alpha_2(t), \alpha_1(t); t, t, 0) . \tag{6.39}$$

The denominator is a generalized nonsense wrong-signature zero and will cause f to vanish at nonsense angular momenta in the absence of multiplicative fixed poles. The nonsense points are

$$\alpha_3(0) = \alpha_1(t) + \alpha_2(t) + N_3 , \qquad N_3 = -1, -2, -3, \ldots \qquad \text{and} \qquad \tau_1 \tau_2 \tau_3 = (-1)^{N_3} . \tag{6.40}$$

These are shifted from the negative integers since the trajectories in the $t_1 = t_2 = t$ channels have helicities $\alpha_1(t)$ and $\alpha_2(t)$ of opposite sign* yielding a total t_3-channel helicity $\alpha_1(t) + \alpha_2(t)$. The multiplicative fixed poles which remove these zeros are those of (4.22) which give singularities

$$\frac{1}{\alpha_3(0) - \alpha_1(t) - \alpha_2(t) - N_3} \tag{6.41}$$

---

* These are helicities in a frame where t_1, t_2 and t_3 are collinear. Thus pomeron trajectories at $t = 0$ carry helicity one. This is perfectly consistent with their having helicity zero in the s-channel center-of-mass as is appropriate for a Toller $M = 0$ trajectory.
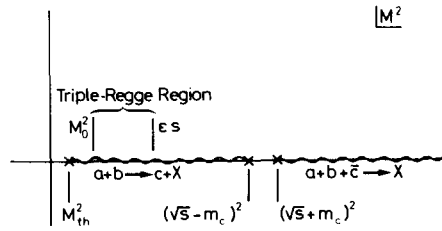
Fig. 6.10. Kinematic regions in M^2.

in β. As usual the fixed powers in the full amplitude which would arise from such fixed poles cancel due to the restriction $\tau_1\tau_2\tau_3 = (-1)^{N_3}$. However in the signatured amplitude the fixed pole (4.22) leads to a contribution

$$A_6^{\tau_1\tau_2\tau_3} \sim (-M^2)^{N_3} (-s)^{\alpha_1(t)+\alpha_2(t)} R_{N_3}(t) , \tag{6.42}$$

where

$$R_{N_3} \propto (\alpha_3(0) - \alpha_1(t) - \alpha_2(t) - N_3)^{-1} .$$

Due to the singularities (6.41), the first term in (6.37) can in general have spurious singularities at $\alpha_3(0) - \alpha_1(t) - \alpha_2(t) = I$ (I any positive or negative integer). The singularities for $I \geqslant 0$ are cancelled by the second term in (6.37) and the singularities for $I < 0$ by contributions of the form (6.42). These contributions which compensate the spurious singularities can be seen to arise in a very natural manner along the lines of Low (private communication)* and Iwasaki and Yazaki [85]. In fig. 6.10 we show some of the cuts in M^2 in the signatured amplitude. In the triple-Regge region we know the discontinuity so we can compute the contribution $\tilde{A}$ of this region to the full amplitude using a dispersion relation

$$\tilde{A}_6^{\tau_1\tau_2\tau_3} = \frac{1}{\pi} \int\limits_{M_0^2}^{\epsilon s} \frac{dM'^2}{M'^2 - M^2} (M'^2)^{\alpha_3(0) - \alpha_1(t) - \alpha_2(t)} s^{\alpha_1(t)+\alpha_2(t)} \tilde{f}(t) \tag{6.43}$$

where

$$\tilde{f}(t) = \beta_3(0) \, \beta_1(t) \, \beta_2(t) f_{312}(0, t, t) .$$

The full amplitude has contributions from integrals on the remaining cuts, but (6.43) alone already reveals the compensation mechanism for the spurious singularities since it is not singular for $\alpha_3(0) - \alpha_1(t) - \alpha_2(t) = I$. The integral can be rewritten as

$$\int\limits_{M_0^2}^{\epsilon s} = \int\limits_{0}^{\infty} - \int\limits_{\epsilon s}^{\infty} - \int\limits_{0}^{M_0^2}$$

and the three pieces separately evaluated,

* See also Chang, Gordon, Low and Treiman [35].

$$\tilde{A}_6^{\tau_1\tau_2\tau_3} = (-M^2)^{\alpha_3 - \alpha_1 - \alpha_2}\, s^{\alpha_1 + \alpha_2}\, \tilde{f}(t)/\sin\pi(-\alpha_3 + \alpha_1 + \alpha_2)$$

$$+ \frac{1}{\pi}\sum_{I=0}^{\infty} \frac{\epsilon^{\alpha_3 - \alpha_1 - \alpha_2 - I}}{\alpha_3 - \alpha_1 - \alpha_2 - I}\, \tilde{f}(t)\left(\frac{M^2}{s}\right)^{I} s^{\alpha_3} - \frac{1}{\pi}\sum_{I=-1}^{-\infty} \frac{(M_0^2)^{\alpha_3 - \alpha_1 - \alpha_2 - I}}{\alpha_3 - \alpha_1 - \alpha_2 - I}\, \tilde{f}(t)\,(-M^2)^I s^{\alpha_1 + \alpha_2}. \quad (6.44)$$

Thus the second term in (6.37) and the cancellation of spurious singularities for $I \geqslant 0$ is associated with contributions for $M^2 > \epsilon s$, while the fixed poles (6.40) and the cancellation of spurious singularities for $I < 0$ is associated with contributions for $M^2 < M_0^2$. When the dispersion contributions for the remaining cuts are added to (6.44) to obtain $A_6^{\tau_1\tau_2\tau_3}$, the precise form of the second two terms is modified but the general mechanism for cancellation of spurious singularities is expected to be preserved.

Finally we remark that finite energy sum rules (FESR) can presumably be written for the reggeon-particle scattering amplitude of fig. 6.5(b) which connect the low M^2 behavior to the triple-Regge behavior. The prototypal FESR obtained by integrating along the right-hand cut in M^2 and around a circle of radius $M^2 = N$ in fig. 6.10 is

$$\int_{M_{\text{th}}^2}^{N} \mathrm{d}M^2\, f^{ib \to jb}(M^2, t) = \sum_k \beta_k^{b\bar{b}}(0)\, f_{kij}(0, t, t)\, \frac{\sin\pi(\alpha_k - \alpha_i - \alpha_j)}{\alpha_k + 1 - \alpha_i - \alpha_j}\, N^{\alpha_k + 1 - \alpha_i - \alpha_j}$$

$$+ \pi R_{-1}(t)[\beta_i^{a\bar{c}}(t)\,\beta_j^{a\bar{c}}(t)]^{-1}, \qquad (6.45)$$

where R_{N_1} is the fixed pole residue (6.42). We refer the reader to Einhorn, Ellis and Finkelstein [59], Kwiecinski [95], and Sanda [121] for further details. We note that in this case we do not expect the complications discussed in section 3.6 for the reggeon and three-particle amplitude. This is because the relevant $\eta_{ij} \to \infty$ (see (6.36) and (4.21)), so that only the leading term in $1/\eta_{ij}$ in the amplitude contributes.

6.4. Inclusive sum rules

Here we consider some consequences of direct channel unitarity for the discontinuities that enter into the above expressions for inclusive reactions. Although we present the results in preparation for applications to Regge theory of the pomeron (section 7), they are entirely *general* and *exact* consequences of unitarity.

Unitarity for the 2–2 matrix element (see (6.1) to (6.3)) of $A_4^{ab \to a'b'} = \langle p_a p_b | T | p_{a'} p_{b'}\rangle$ is

$$\frac{1}{2i}\,\text{disc}\,\langle p_a p_b | T | p_{a'} p_{b'}\rangle =$$

$$\frac{1}{2}\sum_{n=2}^{\infty}\frac{1}{n!}\int \mathrm{d}p_1 \dots \mathrm{d}p_n (2\pi)^4 \delta^4(p_a + p_b - \Sigma p_i)\langle p_a p_b | T^+ | p_1 \dots p_n\rangle \langle p_1 \dots p_n | T | p_{a'} p_{b'}\rangle, \quad (6.46)$$

where we have assumed all identical particles. This is a complicated nonlinear relation between the $2 \to n$ amplitude for $n \geq 2$. However, suppose we consider the Mueller discontinuity (see (6.4) to (6.6))

$$\frac{1}{2i} \mathrm{disc}_{M^2} \langle p_a p_b p_c' | T | p_{a'} p_{b'} p_c \rangle = \frac{1}{2} \sum_{n=2}^{\infty} \frac{1}{(n-1)!} \int dp_2 \dots dp_n (2\pi)^4 \delta^4 (p_a + p_b - p_c - \Sigma p_i)$$

$$\times \langle p_a p_b | T^+ | p_c p_2 \dots p_n \rangle \langle p_{c'} p_2 \dots p_n | T | p_{a'} p_{b'} \rangle . \tag{6.47}$$

If we set $p_c = p_{c'}$ and integrate over dp_c, we *almost* get the 2–2 discontinuity. Only the statistical factor $1/(n-1)!$ is incorrect. Instead we multiply by p_c^μ and then integrate. Since the amplitudes are symmetric in $1, 2, \dots, n \ (c=1)$, this can be replaced by

$$p_c^\mu \to \frac{1}{n} \sum_{i=1}^{n} p_i^\mu = \frac{1}{n} (p_a + p_b)^\mu \tag{6.48}$$

using energy-momentum conservation. We thus obtain the exact unitarity sum rule [48;137]

$$(p_a + p_b)^\mu \mathrm{disc}_s \langle p_a p_b | T | p_{a'} p_{b'} \rangle = \sum_c \int dp_c \, p_c^\mu \, \mathrm{disc}_{M^2} \langle p_a p_b p_c | T | p_{a'} p_{b'} p_c \rangle , \tag{6.49}$$

where for generality a sum over (nonidentical) particle types c is included. This is a remarkably simple expression. Instead of a non-linear relation to the $2 \to n$ amplitudes, we relate the $2 \to 2$ amplitude linearly to the $3 \to 3$ amplitude. If, as is the case for Regge theory, one has an ansatz for the two discontinuities this relation is nontrivial to satisfy.

In the forward direction ($p_a = p_{a'}$, $p_b = p_{b'}$), we can rewrite (6.49) using (6.3) and (6.6) to obtain [41],

$$(p_a + p_b)^\mu \sigma_{\mathrm{Tot}}^{ab} = \sum_c \int dp_c \, p_c^\mu \, \frac{d\sigma^{ab}}{dp_c} . \tag{6.50}$$

In terms of cross sections the sum rule is a *trivial* consequence of conservation of energy. Its interpretation is very simple. An event with n_c particles of type c contributes delta functions to the inclusive cross section at n_c points in phase space. If we integrate over dp_c multiplying by p_c^μ we obtain the total momentum times the probability of the event. Summing over events gives the total cross section. Only if we theoretically relate the cross sections by unitarity to discontinuities do they constrain the expressions allowed for the four- and six-body amplitudes.

If we do not insert an energy factor p_i^μ, each event contributes n_c times its probability. We then obtain the particle number sum rule

$$\langle n_c \rangle \sigma_{\mathrm{Tot}}^{ab} = \int dp_c \, \frac{d\sigma^{ab}}{dp_c} , \tag{6.51}$$

for the average number of particles $\langle n_c \rangle$.

The particle number (6.51) and the conservation of energy (6.50) sum rules have been known for some time. However, recently it has been realized that there are an infinite class of sum rules like these. We may look at the discontinuity expression involving amplitudes for
$a + b \to c_1 + \ldots + c_n + X$

$$\frac{1}{2i} \mathrm{disc}_{M^2} \langle p_a p_b p_{c_1'} \cdots p_{c_n'} | T | p_{a'} p_{b'} p_{c_1} \cdots p_{c_n} \rangle$$

$$= \frac{1}{2i} \sum_{l=n+1}^{\infty} \frac{1}{n!} \int dp_{n+1} \cdots dp_l (2\pi)^4 \delta^4 (p_a + p_b - \sum_{i=1}^{n} p_{c_i} - \sum_{l=n+1}^{\infty} p_l)$$

$$\times \langle p_a p_b | T^+ | p_{c_1} \cdots p_{c_n} p_{n+1} \cdots p_l \rangle \langle p_{c_1'} \cdots p_{c_n'} p_{n+1} \cdots p_l | T | p_{a'} p_{b'} \rangle. \tag{6.52}$$

Multiplying by any k momentum factors $p_{c_i}^\mu$ and integrating gives sum rules relating discontinuities of $2(2+n)$ particle amplitudes to discontinuity of $2(2+n-k)$ particle amplitudes. For elegant formulations, see Brown [28] and Predazzi and Veneziano [114]. The constraints implied by the complete set of these linear sum rules are equivalent to the usual unitarity equations [137].

As an example, consider $n = 2$ [48]. One factor of $p_{c_2}^\mu$ gives*

$$(p_a + p_b - p_{c_1})^\mu \mathrm{disc}_{M^2} \langle p_a p_b p_{c_1'} | T | p_{a'} p_{b'} p_{c_1} \rangle$$

$$= 2i\pi (p_a + p_b - p_{c_1})^\mu \sum_{c_2} \delta(M^2 - m_{c_2}^2) \langle p_a p_b | T | p_{c_1} p_{c_2} \rangle \langle p_{c_1'} p_{c_2} | T | p_{a'} p_{b'} \rangle$$

$$+ \sum_{c_2} \int dp_{c_2} p_{c_2}^\mu \mathrm{disc}_{\bar{M}^2} \langle p_a p_b p_{c_1'} p_{c_2} | T | p_{a'} p_{b'} p_{c_1} p_{c_2} \rangle, \tag{6.53}$$

where

$$\bar{M}^2 = (p_a + p_b - p_{c_1} - p_{c_2})^2.$$

For the inclusive cross section ($p_a = p_{a'}$, $p_b = p_{b'}$, $p_{c_1} = p_{c_1'}$), eq. (6.53) becomes

$$(p_a + p_b - p_{c_1})^\mu \frac{d\sigma^{ab}}{dp_{c_1}} = \sum_{c_2} \int dp_{c_2} p_{c_2}^\mu \frac{d\sigma^{ab}}{dp_{c_1} dp_{c_2}}. \tag{6.54}$$

Integrating over p_{c_1} and combining with the earlier sum rules (6.50) and (6.51) we obtain the mixed momentum-conservation number-average sum rule,

$$(p_a + p_b)^\mu \left(\sum_c \langle n_c \rangle - 1 \right) \sigma^{ab} = \sum_{c_1, c_2} \int dp_{c_1} dp_{c_2} p_{c_2}^\mu \frac{d\sigma^{ab}}{dp_{c_1} dp_{c_2}}, \tag{6.55}$$

* The first term on the right is necessary to give the two-particle discontinuity on the left.

or, multiplying by p_c^ν then integrating, we get the second energy-momentum sum rule

$$(p_a+p_b)^\mu (p_a+p_b)^\nu \sigma_{Tot}^{ab} = \sum_c \int dp_c p_c^\mu p_c^\nu \frac{d\sigma^{ab}}{dp_c} + \sum_{c_1,c_2} \int dp_{c_1} dp_{c_2} p_{c_1}^\mu p_{c_2}^\nu \frac{d\sigma^{ab}}{dp_{c_1} dp_{c_2}}. \qquad (6.56)$$

If we contract the μ, ν indices, we get the Lorentz invariant equation

$$s\sigma_{Tot}^{ab} = \sum_c m_c^2 \langle n_c \rangle \sigma^{ab} + \sum_{c_1,c_2} \int dp_{c_1} dp_{c_2} p_{c_1} \cdot p_{c_2} \frac{d\sigma^{ab}}{dp_{c_1} dp_{c_2}}. \qquad (6.57)$$

In addition to energy momentum conservation, we may use any discrete additive quantum number such as charge, baryon number, etc. For example, multiplying (6.47) by the charge of c, Q_c, and integrating, we get

$$Q_a + Q_b = \sum_c \langle n_c \rangle Q_c, \qquad (6.58)$$

or from an expression like (6.53), we get

$$(Q_a + Q_b) \langle n_{c_1} \rangle = \sum_{c_2} Q_{c_2} \langle n_{c_1} n_{c_2} \rangle. \qquad (6.59)$$

Similar equations also hold for the isospin I. Various relations can be obtained by contracting with different fixed isospin vectors. For further discussion, see Di Giacomo [52].

The inclusive sum rules clearly constrain the Regge couplings of fig. 6.2 and section 6.2 which enter in the Regge analysis of inclusive cross sections. They are examples of direct (s) channel unitarity constraints on the crossed (t) channel Regge exchanges. Clearly a complete Regge theory should satisfy these constraints. While Regge exchanges are constructed to satisfy the requirements of t-channel unitarity, for the most part, we can at present only enforce s-channel unitarity by hand in a piecemeal manner. In section 7 we shall investigate some particularly striking consequences of these constraints.

7. Applications to pomeron Regge pole

In this section we apply the general analysis of the preceding sections to the study of the properties of a pomeron Regge pole with unit intercept, $\alpha_P(0) = 1$. This is done to provide a pedagogical example and also to illustrate the importance of the further constraints on Regge pole properties imposed by s-channel unitarity.

7.1. Introduction

The fundamental property of Regge poles (and Regge cuts) is that they are believed to satisfy completely the requirements of t-channel unitarity. So far we have concerned ourselves here with

investigating the constraints imposed on them by *s-channel analyticity*. But we know that the Regge expansion should also satisfy *s-channel unitarity*. Indeed, it is well known that s-channel unitarity gives further constraints. The celebrated Froissart [65] bound for $s \to \infty$

$$\sigma^{ab}_{\text{Tot}} \lesssim \pi/m^2_\pi \ln^2 s \tag{7.1}$$

follows from s-channel unitarity and t-channel analyticity in the neighborhood of $t = 0$. Any Regge pole contribution

$$\sigma^{ab}_{\text{Tot}} \sim \beta^{aa}(0) \, \beta^{bb}(0) \, s^{\alpha(0)-1} \tag{7.2}$$

must therefore have $\alpha(0) \leqslant 1$.

The Regge saturation of (7.1) gives the standard pomeron Regge pole model for diffractive scattering* ($\alpha_P(0) = 1$) and

$$\sigma^{ab}_{\text{Tot}} \sim \text{const.} \tag{7.3}$$

However, there are even further s-channel unitarity constraints on an *isolated* pomeron pole with $\alpha_P(0) = 1$. We shall see that such a pomeron pole must essentially decouple from all processes. This raises the possibility that even a stronger bound than (7.1) or (7.3) exists (Chew, private communication), namely, $\alpha_P(0) < 1$, or, as $s \to \infty$,

$$\sigma^{ab}_{\text{Tot}} \sim 0. \tag{7.4}$$

Since the Froissart bound uses only a small part of the full content of unitarity and analyticity, the existence of such stronger bounds would not be surprising. However, while the full exploitation of t-channel unitarity may indeed require only Regge pole and cut contributions and thus a strengthening of (7.1), we believe that it is likely that Regge cuts play a crucial, and, as yet, not fully understood role which would circumvent (7.4) and allow constant cross sections (7.3). Cuts which accomplish this would have a number of rather unconventional properties in addition to the usual ones of allowing σ^{ab}_{Tot} to increase to its asymptotic value and giving long-range correlations.**

This section will be devoted to a discussion of the constraints on an isolated pomeron pole with $\alpha_P(0) = 1$.** We ignore cuts by invoking the popular "soft" cut ansatz that *all* cuts at $J = 1$ are damped by logarithmic factors relative to the pole. In section 7.2 we apply the unitarity sum rules of section 6.4 to the Regge expansions for inclusive reactions (sections 6.2 and 6.3). We begin by showing that the triple-pomeron coupling vanishes for $t = 0$ (e.g. $f_{PPP}(0, 0, 0) = 0$ as defined in fig. 6.2(b)). From this a large number of further decouplings can be deduced. Then in section 7.3 we show these results can be extended using the analytic properties of reggeon couplings (section 3) to the vanishing of the elastic coupling, e.g. eq. (7.4). Finally, in section 7.4 we give alternative derivations of weaker forms of the decoupling theorems of section 7.2 which involve discontinuities of vertices and do not conflict with (7.3). In view of the poorly understood role of cuts, which may destroy some or all of these decoupling results, this section may only turn

---

  * For a review of diffractive scattering, see Horn and Zachariasen [81].

** For a more detailed discussion we refer the reader to Brower and Weis [27] and White [146].

out to be a pedagogical exercise in applying the results of the preceding sections in a too ideal-ized situation. On the other hand, however, it also illustrates the power of the s-channel unitar-ity constraints which must be reckoned with in any theory of diffractive scattering.

7.2. Inclusive sum rule decoupling theorems

In the inclusive approach to the decoupling theorems all the results follow from the vanishing of the "triple-pomeron" vertex. This condition, which was first discovered by Gribov and Migdal [74] is fundamental to the iterative approach to diffractive cuts in the Gribov calculus and the multiperipheral bootstrap [74,3].

7.2.1. Triple-pomeron zero

We consider the inclusive process a + b → c + X studied in section 6 in the triple-Regge limit $s \gg M^2 \gg 1$, where $s = (p_a + p_b)^2$ and $M^2 = (p_a + p_b - p_c)^2$ (see fig. 6.5 and eq. (6.35)). The leading pomeron term $(\alpha_3(0) = \alpha_P(0))$ gives that portion of diffractive production $(\alpha_1(t) = \alpha_2(t) = \alpha_P(t))$ that contributes to scaling

$$E_c \frac{d^3\sigma}{d^3 p_c} = G_P(t)\, s^{\alpha_P(0)-1} \left(\frac{s}{M^2}\right)^{2\alpha_P(t)-\alpha_P(0)} ,$$ (7.5)

where

$$G_P(t) = |\,\xi_P\, \beta_P^{a\bar{c}}(t)\,|^2\, f_{PPP}(0, t, t)\,\beta_P^{b\bar{b}}(0)\,.$$

We now ask whether the factor

$$(s/M^2)^{2\alpha_P(t)-\alpha_P(0)} = (1/(1-x))^{2\alpha't+\alpha_P(0)},$$ (7.6)

which is singular at the phase-space boundary $x = 1$, is consistent with unitarity and constant cross sections. The conservation of energy sum rule (6.50) is

$$(p_a + p_b)^\mu \sigma_{Tot}^{ab}(s) = \sum_c \int dp_c\, p_c^\mu\, d\sigma^{ab}/dp_c ,$$ (7.7)

where the sum is over all particle types c. Adding the energy and longitudinal momentum compo-nents of eq. (7.7) in the center of mass, we have the exact unitarity sum rule for $s \to \infty$

$$\sigma_{Tot}^{ab}(s) = \pi \sum_c \int_0^\infty dp_\perp^2 \int_0^1 dx \left(E_c \frac{d^3\sigma^{ab}}{d^3 p_c}\right).$$ (7.8)

Restricting ourselves to the channel (c = ā) and the phase-space region dominated by the triple pomeron, we have an inequality

$$\sigma_{\text{Tot}}^{ab}(s) \geqslant \pi \int_0^c dp_\perp^2 \int_\delta^{1-M_0^2/s} \frac{dx}{1-x}(1-x)^{2\alpha't} G_P(t) , \tag{7.9}$$

where $p_\perp^2 = -t + t_{\text{min}}(s, x)$. Let us look at the leading term coming from the singularity at $x = 1$. Since $s \gg M^2$, $t_{\text{min}} \to 0$ and by integrating by parts in $p_\perp^2$ we obtain

$$\frac{\pi G_P(0)}{2\alpha'} \int_\delta^{1-M_0^2/s} \frac{dx}{1-x} \frac{1}{-\ln(1-x)} + \text{const.} \tag{7.10}$$

and after performing the integral over $-d(\ln(1-x))$

$$\sigma_{\text{Tot}}^{ab} \geqslant \frac{\pi G_P(0)}{2\alpha'} \ln \ln(s/M_0^2) . \tag{7.11}$$

Consequently a nonvanishing triple-pomeron coupling at $t = 0$ gives a term in violation of $\sigma_{\text{tot}} \to$ const. Consistency requires

$$f_{PPP}(0, t, t) = 0 \qquad \text{for} \quad t = 0 , \tag{7.12}$$

and analyticity requires it to be a zero at least linear in t.

From eq. (6.39) we see that such a zero can arise from a nonsense wrong-signature zero [51]. However, such a zero is probably not how eq. (7.12) is satisfied in a realistic theory* including Regge cuts [21,68,156–159].

7.2.2. Stronger consequences

By a further application of the unitarity sum rules [88] additional decoupling theorems are obtained. Here we use the sum rule (6.54) relating the double inclusive (a + b → c + d + X) to the single inclusive (a + b → c + X) cross section.

Introducing the Feynman variables $x_c = 2p_{\|c}/\sqrt{s}$, $x_d = 2p_{\|d}/\sqrt{s}$ in the center of mass of $p_a + p_b$, the energy plus longitudinal momentum component gives

$$\frac{d\sigma^{ab}}{dp_c} \geqslant \frac{1}{2(2\pi)^3} \int\int d^2 p_{\perp d} \int_0^1 \frac{dx_d}{1-x_c} \left(\frac{d\sigma^{ab}}{dp_c \, dp_d}\right) . \tag{7.13}$$

In the limit $1 - x_c \ll 1$, this becomes an inequality for the triple-pomeron vertex

$$f_{PPP}(0, t, t) \geqslant \int\int d^2 p_{\perp d} \int dy(1-y)^{\alpha P(0)} B(t, \bar{t}, y, \eta) . \tag{7.14}$$

The quantity B is essentially the Mueller vertex (fig. 6.2 (c)) for the process pomeron(t) + b → d + X. We have $y = 1 - \bar{M}^2/M^2$, where $\bar{M}^2 = (p_a + p_b - p_c - p_d)^2$, $\bar{t} = (p_a - p_c - p_d)^2 = (p_P - p_d)^2$. The dependence on the additional Toller angle-like variable $\eta = s_{ab}/s_{cd}\bar{M}^2$ arises from the helicity of the pomeron (t).

---

* A more serious attempt at studying the triple-pomeron zero in the presence of the infinite number of multi-pomeron cuts has been recently made using renormalization group techniques [156–159].

For $t = 0$, the integral gives a lower bound on $f_{PPP}(0, 0, 0)$ and must therefore vanish from eq. (7.12). The integral is a positive definite phase space integral so that

$$\tag{7.15}$$

identically for p_d in the physical region. This is an extremely strong result with many consequences. In particular, if we consider the limit $y \to 1$ (e.g. $s \gg M^2 \gg \bar{M}^2 \gg 1$), we may pick out the Regge pole in the pomeron + d-channel, which gives

$$B \sim (1 - y)^{-2\alpha_R(t)} f_{PRR}(0, \bar{t}, \bar{t}) | \xi_P \, \Gamma(-\alpha_P) \, R_{PR}^d(0, \bar{t}; \eta) \, \xi_R \, \Gamma(-\alpha_R)|^2 = 0 , \tag{7.16}$$

or representing this diagrammatically we have

$$\tag{7.17}$$

Since the PRR vertex is easily shown to be non-zero because of the elastic poles at $\bar{t} = m^2$, we have

$$R_{PR}^d(0, \bar{t}; \eta = 1/(m^2 - \bar{t})) = 0 \tag{7.18}$$

for all $\bar{t} \leq 0$. From the expression (3.12) we see that $\eta^{-1} \to m^2 - \bar{t}$ as $t \to 0$ for physical (i.e. real) ω. This lack of ω dependence as $t \to 0$ is a consequence of the required analyticity of the amplitude in the channel invariants.*

By considering inclusive processes with more particles, one can obtain an infinte number of similar decoupling theorems with d replaced by a cluster of particles (X')

$$\tag{7.19}$$

---

* This is true for Toller $M = 0$ trajectories. For $M \neq 0$, there is ω dependence arising from a pair of trajectories with opposite parity. The trajectories have compensating singularities in t which are not allowed in the full amplitude.
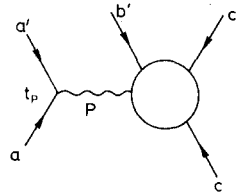
Fig. 7.1. Pomeron three-particle coupling in the five-particle amplitude A_5.

Other regions of phase space for B can also be considered. For example, with p_d in the central region, we get

$$= 0. \tag{7.20}$$

7.3. Elastic decoupling

Here we consider further decoupling theorems that can be obtained by analytically continuing the results of section 7.2 from the physical regions where they were originally obtained. Before discussing these results in detail, we give a simple example which illustrates some of the technical difficulties in such analytic continuation [26,73].

Suppose it has been possible to analytically continue the pomeron—reggeon two-particle vertex (7.19) to the particle pole to obtain the decoupling of the pomeron from three particles (see fig. 7.1). We would like to know whether it is possible to make a further continuation to an internal particle pole to obtain the vanishing of the pomeron-particle—particle coupling (and thus total cross-sections); i.e. a continuation to, say, $s_{cc'} = m_{b'}^2$.

The pomeron three-particle coupling generally has the form (3.6)

$$R(s_{a'b'}/s_{ac}, s_{b'c'}, t_P, s_{cc'}) \tag{7.21}$$

where $s_{cc'} + s_{c'b} + s_{cb'} = m_c^2 + m_{c'}^2 + m_{b'}^2 + t_P$, and $t_P = (p_a + p_{a'})^2$. However, the vanishing of (7.21) is only known in the physical region for $t_P = 0$. In this case there are further constraints among the variables (see e.g. [27])

$$\frac{s_{ac}}{s_{b'c'} - m_c^2} = \frac{s_{ac'}}{s_{b'c} - m_{c'}^2} = \frac{s_{ab'}}{s_{cc'} - m_{b'}^2}. \tag{7.22}$$

It is clear we cannot continue to the pole at $s_{cc'} = m_{b'}^2$ without simultaneously going on top of the poles at $s_{cb'} = m_{c'}^2$ and $s_{b'c'} = m_c^2$. To get a rough idea of what happens, let us consider a simple model for R — just the sum of these three poles

$$A_5 \approx ig_a \left[\frac{s_{ac}g_c}{s_{b'c'} - m_c^2} + \frac{s_{a'c'}g_{\bar{c}'}}{s_{b'c} - m_{c'}^2} + \frac{s_{a'b'}g_{\bar{b}'}}{s_{cc'} - m_b^2} \right] g_{cc'b'} \, , \tag{7.23}$$

where g_i is the coupling of the pomeron to particle i at $t_P = 0$. Using (7.22) and $s_{a'c'} \sim -s_{ac'}$, etc., the vanishing of (7.23) implies only

$$g_c - g_{\bar{c}'} - g_{\bar{b}'} = 0 \tag{7.24a}$$

and not the vanishing of the individual elastic couplings g_i.

We can also consider the reactions obtained by crossing pairs of particles and obtain

$$-g_{\bar{c}} + g_{c'} - g_{\bar{b}'} = 0 \tag{7.24b}$$

and

$$-g_{\bar{c}} - g_{\bar{c}'} + g_{b'} = 0 \, . \tag{7.24c}$$

Since the couplings of the pomeron to particle and antiparticle are equal,

$$g_i = g_{\bar{i}} \, , \tag{7.25}$$

eqs. (7.24) clearly give

$$g_c = g_{c'} = g_{b'} = 0 \, . \tag{7.26}$$

Therefore, in this simple model the vanishing of elastic couplings is obtained but it requires a knowledge of the crossing (or signature) properties of the pomeron (7.25). This input is non-trivial since for exchanges of opposite signature like the photon we do not obtain decoupling. Indeed for the proton

$$e_i = g_i \, , \qquad e_{\bar{i}} = -e_i \, , \tag{7.27}$$

and all three eqs. (7.24) reduce to the same charge-conservation equation

$$e_c + e_{c'} + e_{b'} = 0 \, . \tag{7.28}$$

For a rigorous derivation [26], we consider the implications of the vanishing of the pomeron–reggeon particle vertex (7.18)

$$R_{PR}(t_P = 0, t_R; \eta = 1/(m^2 - t_R)) = 0 \, . \tag{7.29}$$

To get to the pomeron–particle–particle coupling, we need to analytically continue in t_R from $t_R \leqslant 0$ where (7.29) is known to the mass of the particle at $t_R = m^2$. To accomplish this we need to use the detailed analytic properties of the two-reggeon vertex derived in section 3.

Taking $\alpha_1 = \alpha_P$ the pomeron, and $\alpha_2 = \alpha_R$ the reggeon in eq. (3.23), we have

$$\xi_P \xi_R R_{PR} = \xi_P \xi_{RP} \eta^{\alpha_P} V_P(t_P, t_R; \eta) + \xi_R \xi_{PR} \eta^{\alpha_R} V_R(t_P, t_R; \eta) \, , \tag{7.30}$$

where V_P, V_R are polynomials in η^{-1}. Since we are continuing to $t_P \approx 0$, $t_R \approx m^2$ and

$\eta^{-1} = m^2 - t_R \approx 0$, we can approximate V_P and V_R by the first few terms in the expansions of eq. (3.30)

$$\Gamma(-\alpha_P)\,\Gamma(-\alpha_R)\,V_P \approx \frac{v_0^{\tau_{12}}}{\alpha_P - 1} + \frac{v_1^{\tau_{12}}\,\eta^{-1}}{(\alpha_P - 1)(\alpha_R - \alpha_P + 1)}, \tag{7.31}$$

$$\Gamma(-\alpha_P)\,\Gamma(-\alpha_R)\,V_R \approx \frac{v_1^{\tau_{12}}}{\alpha_R(\alpha_R - \alpha_P + 1)}. \tag{7.32}$$

We have exhibited the vertex signature τ_{12} explicitly in (7.31) and (7.32) since in general both signatures can be present. Inserting these expressions in (7.29) we have

$$0 \approx \frac{\exp(i\pi\alpha_R) - 1}{i\pi} \sum_{\tau_{12} = \pm 1} \left\{ \left(\frac{\exp(-i\pi\alpha_R) - 1}{2} \right) \left[\eta\,v_0^{\tau_{12}}(1 + \tau_{12}) + \frac{1}{\alpha_R}\,v_1^{\tau_{12}}(1 - \tau_{12}) \right] \right.$$

$$\left. + \left[\frac{1}{\alpha_R}\,v_1^{\tau_{12}}(1 + \tau_{12}) \right] \right\} \approx 2v_1^{+1}. \tag{7.33}$$

In general the contributions of V_P and V_R occur in V_{PR} with different phases so they must individually vanish. For $\alpha_R = 0$, the contribution of V_P is purely imaginary and vanishes so it gives no constraint on v_0 and v_1, but the contribution of V_R is real and only vanishes if

$$v_1^{+1} = 0. \tag{7.34}$$

However, returning to (7.29) we see that

$$\beta_P(0) = \lim_{t_P \to 0} R_{PR}(t_P, t_R = m^2; \eta) = 2v_1^{+1}. \tag{7.35}$$

Therefore, the vanishing of pomeron—reggeon—particle vertex implies the vanishing of the pomeron—particle—particle elastic coupling (7.35).

We would now like to make a number of comments on this result. As we noted above, the signature of the pomeron plays an essential role. In (7.33) there is a term η which, due to the kinematic constraint, is $1/(m^2 - t_R)$ and looks like the particle pole. However, it is multiplied by the factor ξ_{RP} which is a wrong signature factor for $\alpha_P = 1$ and therefore cannot compensate the particle pole in V_R. The harmlessness of this potentially dangerous kinematic singularity is thus a result of the positive signature for the pomeron. For the photon, on the other hand, only V_P contributes and current conservation requires that the kinematic η singularity exactly cancel the particle pole.

Signature plays a crucial role in another amusing way. Consider a Regge trajectory of negative signature, so $\alpha_R = 0$ is a wrong signature point. Such a trajectory, if it has the same $\alpha_R(t_R)$ as the positive signature trajectory, surprisingly has the same behavior as (7.33) near $\alpha_R = 0$. In this case from (7.30), (7.31) and (7.32), we have

$$R_{PR}\left(0, t_R; \eta = \frac{1}{m^2 = t_R}\right) \approx \frac{2}{i\pi} \sum_{\tau_{12}} \left\{\left[-\eta\, v_0^{\tau_{12}}(1+\tau_{12}) - \frac{1}{\alpha_R} v_1^{\tau_{12}}(1-\tau_{12})\right]\right.$$

$$\left. + \left[\frac{1}{\alpha_R} v_1^{\tau_{12}}(1-\tau_{12})\right]\right\} \approx -\frac{4}{i\pi} \eta v_0^{+1} \approx \frac{4}{i\pi\alpha_R} v_0^{+1} . \tag{7.36}$$

The signature factor ξ_{RP} is now right signature so the η kinematic singularity contributes.

Equation (7.36) immediately suggests a mechanism for avoiding the vanishing of the elastic coupling. If the negative signature trajectory is *exactly* degenerate with the positive signature trajectory for $t_R \le 0$ (exchange degeneracy), then the decoupling theorems will apply only to the sum of both their contributions since they cannot be separated by their asymptotic behavior. If the negative signature trajectory also has $\alpha_R(m^2) = 0$, then its contribution will cancel the particle pole if $v_0^{+1}(\tau_R = -1) = v_1^{+1}(\tau_R = +1)$. The source of this cancellation can be seen to arise directly from the absence of a left-hand cut in the amplitude A_5 in s_R.

Unfortunately this exchange degeneracy mechanism for circumventing the vanishing of total cross sections is not physically reasonable. The pion's exchange degenerate partner would have the quantum numbers of the A_1 meson. Such a trajectory could very well exist. However, there is no evidence for a trajectory with $I^G = 1^+$ and $J^P = 0^+$ approximately exchange degenerate with the ρ. While decoupling of the ρ might be tolerated by some people, the absence of such a trajectory also requires the pion to decouple. This can be shown by considering the pomeron $-\pi-\pi-\rho$ Regge vertex which should vanish by (7.19) (see fig. 7.2).

While the exchange degenerate πA_1 eliminate the left-hand cuts in $s_{\pi\pi}$, this is not sufficient to cause the coefficient of α_π^{-1} to vanish at $t_P = 0$. The reason is basically that, as we discussed in section 5.2, a single Regge trajectory of definite signature gives a factorizable contribution to the amplitude, whereas the contribution of a Regge exchange without definite signature (e.g. an exchange degenerate pair) does not factorize. Thus the P$-\pi-(\pi, A_1)$ "vertex" occurring in the $2 \to 3$ amplitude vanishing is not the same P$-\pi- (\pi, A_1)$ "vertex" occurring in the $2 \to 4$ amplitude, so the vanishing does not propagate to more complicated amplitudes.

In conclusion, we should remark that essentially all the decoupling results discussed in sections 7.2 and 7.3 have been known for a long time in the context of the multiperipheral model as plausible extensions of the Finkelstein–Kajantie [61] decoupling theorem.

7.4. Schwartz inequalities

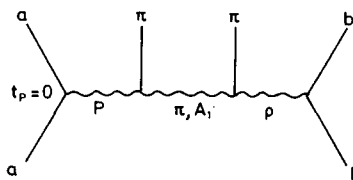Several authors have suggested that cuts enter into the unitarity sum rules of section 7.2

Fig. 7.2. A six-particle amplitude with P, (π, A_1), and ρ exchanges.

[33,78] or into the analytic continuation of section 7.3 [73], just so as to cancel the pole contribution and avoid decoupling the pomeron in σ_{tot}. If this is the case, might any of the decoupling theorems be expected to hold? Yes, without the use of sum rules, Gribov and Migdal [74] argue that the triple-pomeron zero (7.12) may be required to avoid moving the pole from $\alpha_P(0) = 1$ by multi-pomeron interactions.

Therefore, it is interesting to point out that with the use of Schwartz inequalities [4,5,97], the triple-pomeron zero implies a weaker class of decoupling theorems for discontinuities of pomeron vertices that do not lead to decoupling in the total cross section [103]. These zeros could thus still be present in a theory satisfying (7.3). It is also amusing to note that these zeros occur in a dual model as a consequence of an underlying gauge symmetry [27]. The dual model studied in the appendix thus exhibits these zeros.

The Schwartz inequality results start from the ordinary Schwartz inequality

$$|\langle a|b \rangle|^2 \leqslant \langle a|a \rangle \langle b|b \rangle .$$ (7.37)

We choose $|a\rangle$ and $|b\rangle$ to be certain multiparticle states and the inner product to be a sum over a complete set of intermediate states:

(7.38)

As long as these represent multiparticle processes inside the physical region, unitarity can be used to replace the sum over intermediate states by a discontinuity in M^2. Thus again s-channel unitarity plays a central role. Taking M^2 and s/M^2 large, the leading term on the right-hand side is the triple-pomeron:

(7.39)

For $t_3 = 0$ we can compare the coefficient of $(s/M^2)^{2\alpha_P(0)}$ $(M^2)^{\alpha_P(0)}$ on both sides of (7.39) and use $f_{PPP}(0, t, t) = 0$ to obtain

$$= 0$$ (7.40)

for any state X. If pomeron cuts are weak, this can be obtained for arbitrary t_3 of the lower pomeron. It should be carefully noted that one pomeron has a discontinuity taken through it.

Clearly from (7.40) one can obtain an endless variety of decoupling theorems. Two particularly interesting ones are obtained by taking X to be a two-particle state. A further Regge limit can be taken in either of two ways giving:

$$= 0 \tag{7.41}$$

or

$$= 0 . \tag{7.42}$$

Let us discuss the implications of these results. From section 5 we know that (7.41) factorizes into the product of the upper and lower vertices and the cut Regge propagator. The upper vertex is from fig. 5.8 and (7.31)

$$\frac{\sin \pi(\alpha_R - \alpha_P)}{\sin \pi \alpha_R} \eta^{\alpha_P} V_P \approx \sum_{\tau_{12}} \frac{1}{\alpha_R} \left[-(\alpha_R - \alpha_P + 1) v_0^{\tau_{12}}(1 + \tau_{12}) + \alpha_R v_1^{\tau_{12}}(1 - \tau_{12}) \right]. \tag{7.43}$$

Thus (7.41) implies

$$v_0^{+1} \approx v_1^{-1} \tag{7.44}$$

at $\alpha_R \approx 0$ and gives no constraint on the elastic coupling v_1^{+1}. Hence, it is satisfied without elastic decoupling [103].

In (7.42) it is important to realize that the constraint is on the full triple-Regge vertex and not on the amplitude with maximum helicity for the cut pomeron. This is because (7.42) must be obtained by taking the triple-Regge limit and not the helicity limit of inclusive reactions (section 6.3). The basic equation (7.40) is derived only inside the physical region, and as discussed in section 4.1 the helicity limit is inside the physical region for $\lambda(t_1, t_2, t_3) \leq 0$ which is not the case here. Thus all helicities of the cut pomeron contribute. From (4.2) we have (keeping $t_3 \neq 0$ for the moment)

$$\eta_{31} = -\eta_{12} = \frac{1}{t_2 - t_3}, \qquad \eta_{23} = \frac{2\sqrt{t_2 t_3} \cos \omega_{23} - t_2 - t_3}{(t_2 - t_3)^2}, \tag{7.45}$$

so the dependence on η_{23} gives the dependence on the helicity of the cut pomeron.

From fig. 5.8 we have that (7.42) is

$$\frac{\sin\pi(\alpha_3 - \alpha_1 - \alpha_2)}{\sin\pi\alpha_3} V_{12}(t_1, t_2, t_3; \eta_{12}, \eta_{23}, \eta_{31}) \,, \tag{7.46}$$

where V_{12} is given by (5.27). Using (7.45), we see that for arbitrary t_3 eq. (7.42) gives a relationship between the functions β,

$$\frac{\Gamma(\alpha_3+1)\, \Gamma(-\alpha_2+n)}{\Gamma(\alpha_3-\alpha_2+n+1)\, \Gamma(-\alpha_2)} \eta_{31}^1 \eta_{23}^{\alpha_2-n} \left[(\alpha_2 - \alpha_3 - n)\beta_{0,n,0} - (t_2 - t_3)\beta_{1,n,0} + \beta_{0,n-1,1} \right] = 0 \tag{7.47}$$

by equating powers of η_{23}, where

$$\beta_{m,n,p} = \beta(p, \alpha_2 - n - p, \alpha_1 - m - p; t_1, t_2, t_3) \,.$$

This condition cannot be satisfied by a nonsense zero as (7.12) can be. It, as well as (7.44), can be interpreted as the condition that the pomeron couples like a conserved vector current at $t = 0$ [27].

8. Regge cuts

8.1. General discussion

Just as poles in the energy plane generate cuts through unitarity, Regge poles give rise to Regge cuts. One might ask, how would Regge cuts modify the multi-Regge asymptotic behavior we have found so far? One way to approach this problem would be to apply directly the analysis outlined here for poles, reconciling the expected Regge-cut asymptotic behavior with the desired analytic structure. This is the approach one would be forced to take, if he thought that his Regge cuts had an origin independent of Regge poles (e.g. the eikonal cut for the pomeron in the Cheng and Wu model [36] or the self-consistent cut of the Finkelstein, Zachariasen model [62] or the model of Auerbach, Aviv, Blankenbecler and Sugar [11]). However, for those Regge cuts generated from Regge poles through unitarity, the analytic structure of Regge-cut dominated amplitudes is connected through unitarity to the structure of Regge-pole dominated amplitudes. In order to understand this connection, let us first see how cuts are generated from poles. For a more comprehensive review of Regge cuts, see Collins [44].

Regge cuts were first found in a calculation of the absorptive part of an elastic amplitude from a production model which involved the exchange of Regge poles [16,8]. We can easily see that cuts should appear by considering in the s channel at large s the contribution to the imaginary part of the elastic amplitude due to the elastic intermediate state (fig. 8.1). At large s the contribution from the elastic channel is

$$\text{Im}\, A(s, t) \propto \frac{1}{s} \iint_{\lambda < 0} \frac{\mathrm{d}t_1 \mathrm{d}t_2}{[-\lambda(t, t_1, t_2)]^{\frac{1}{2}}} A(s, t_1)\, A^*(s, t_2) \,. \tag{8.1}$$

The region of integration over t_1 and t_2 is the interior of a hyperbola given by the zeros of λ, as
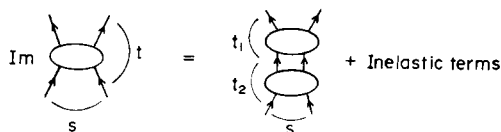
Fig. 8.1. Unitarity for the s-channel.

shown in fig. 8.2. If we assume that the elastic amplitude is dominated by a single Regge pole, so that

$$A(s, t) \sim s^{\alpha(t_1)} \gamma(t_1) ,$$ (8.2)

then

$$\mathrm{Im}\, A(s, t) \sim \iint\limits_{\lambda < 0} \frac{\mathrm{d}t_1 \mathrm{d}t_2}{[-\lambda(t, t_1, t_2)]^{\frac{1}{2}}} \gamma(t_1)\, \gamma^*(t_2)\, s^{\alpha(t_1) + \alpha(t_2) - 1} .$$ (8.3)

We see that the asymptotic behavior of this contribution to $\mathrm{Im}\,A(s, t)$ is bounded by a power, but it is not a pure power behavior (unless the Regge pole is fixed, i.e. $\alpha(t) = \mathrm{const.}$). The behavior (8.3) is in fact characteristic of a cut and can be written

$$\mathrm{Im}\, A(s, t) \sim \int\limits_{-\infty}^{\alpha_c(t)} \mathrm{d}\alpha\, s^{\alpha}\, \gamma_{\alpha}(t) ,$$ (8.4)

where $\alpha_c(t)$ is the maximum power of s in the integral over t_1 and t_2. It is therefore the trajectory of a branch point in the complex angular momentum of the t-channel. If the trajectory is monotonically increasing, it is not hard to show (see fig. 8.2) that the maximum occurs when $t_1 = t_2 = t/4$, so that

$$\alpha_c(t) = 2\alpha(t/4) - 1 .$$ (8.5)

Whether the Regge cut is actually present in the full elastic amplitude cannot be determined until we add up the contributions from the inelastic channels as well. This has been done in various models, e.g. the multi-Regge model [39,97] where a J-plane cut was found with the same trajectory (8.5).
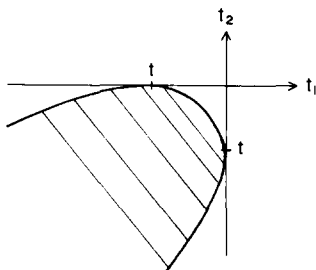

Fig. 8.2. Region of integration over t_1 and t_2.

Fig. 8.3. Archetypical multi-Regge model generating a Regge cut.

A striking property of the cuts obtained in these models is that when $t = 0$, they necessarily contribute a positive definite piece to the total cross section. This property can be seen most directly by considering a model for particle production sketched in fig. 8.3 due to Abarbanel [2], where the clusters are assumed not to have a Regge-cut behavior at large cluster masses (i.e. they are two-reggeon irreducible). In these models the exchange of a leading Regge trajectory is associated with the presence of a phase space (rapidity) separation of the particles into clusters somewhat like fireballs. Each term is thus a phenomenologically distinct contribution to the cross section hence positive. The positivity of the cut contribution can then be shown to follow essentially from the positivity of each term.

By contrast, calculations in perturbation theory have always yielded a sign for the cut contribution that depended on the trajectories. In the case of the pomeron—pomeron (PP) cut this sign is exactly opposite the one calculated from the multi-Regge model.

An example of such a calculation is the familiar one due to Mandelstam [99]. The ladders in fig. 8.4 add up to give Regge trajectories $\alpha_1(t_1)$ and $\alpha_2(t_2)$. The diagram produces a cut at the same position as the elastic unitarity calculation (8.5), but with opposite sign for the PP cut. The opposite sign here comes from the fact that the signature factor for the pomeron on the bottom multiplies the factor on the top to produce $i \times i = -1$, whereas in the multi-Regge calculation, the factor on the bottom is multiplied by the complex conjugate of the one on top to produce $i \times (-i) = +1$.

So where did the multiperipheral argument go wrong? The answer can be found by taking the s-channel discontinuity of the Mandelstam graph. The total discontinuity is the sum of the discontinuities corresponding to the various Cutkosky slicings of the graph and are enumerated by Abromovskii, Gribov and Kancheli [7], the important classes of which are indicated in fig. 8.4.
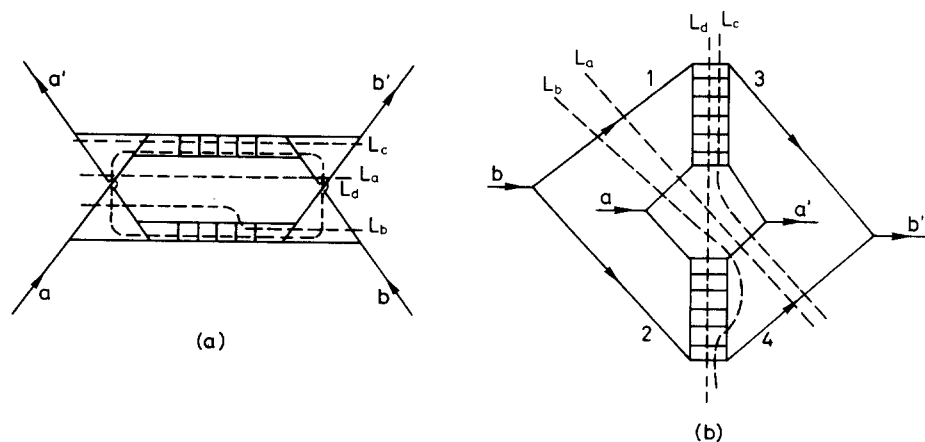
Fig. 8.4. Two equivalent orientations of the Mandelstam graph showing slicings associated with s-channel discontinuities.
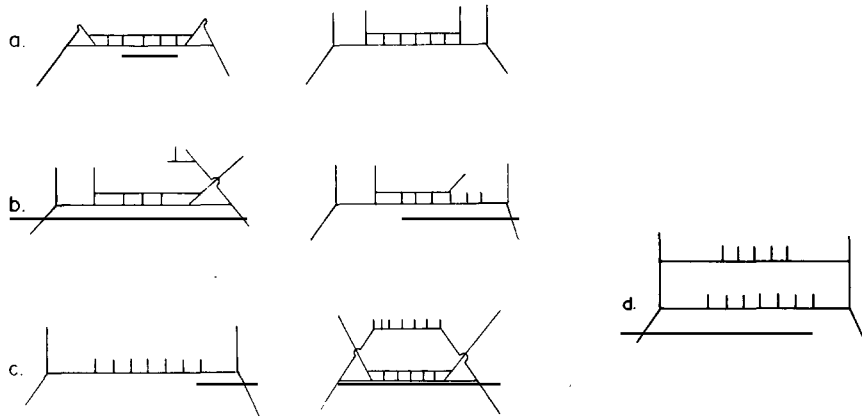
Fig. 8.5. Fragments of the Mandelstam graph generated by cuts L_a, L_b, L_c and L_d, respectively.

Also shown in fig. 8.4 is the planar form of the Mandelstam graph, which makes it easier to visualize the topology of the slicings. There are three classes of slicings: those which avoid the ladders or cut only a few rungs as in L_a and L_b, those which cut one of the ladders completely as in L_c and those which cut both as in L_d. The resulting fragments of the respective slicings are shown in fig. 8.5. These fragments represent multiple production amplitudes which, inserted into the unitarity formula for the discontinuity of the four-particle amplitude, reproduce the integrals implied by the Cutkosky slicings (plus some extra integrals corresponding to orders in perturbation theory different from the graph of fig. 8.4 and not apparently associated with the two-reggeon cut).

Comparing the terms in fig. 8.5 with terms in fig. 8.3 we see that those of fig. 8.5, a and b, may be grouped naturally into the single-pomeron-exchange amplitudes in the second term of fig. 8.3, whereas those of fig. 8.5, c and d, must be grouped into the first term of fig. 8.3, since they have small rapidity gaps. But when the amplitudes are summed and squared to form the total cross section, the interference between the graphs of fig. 8.5c produces a PP cut behavior contrary to the irreducibility assumption that the clusters are free of such behavior. The interference term is in fact negative [7,78] and overwhelms the contributions from the other slicings.

Therefore, it could be argued that too much was assumed in the construction of the blobs in fig. 8.3 — that separating the pomerons in the manner shown was incompatible with the notion of "two-pomeron irreducibility" of the clusters.

The weighting of the various discontinuities of the Mandelstam two-reggeon graph is a subject of recent controversy and provides an interesting application of the principles outlined in this review. At first sight it would appear that all Cutkosky slicings of fig. 8.4 produce contributions to the total discontinuity with an asymptotic behavior characteristic of the two-reggeon cut [7, 78]. However, on second thought, should the graph conform to the assumptions of section 1.4,
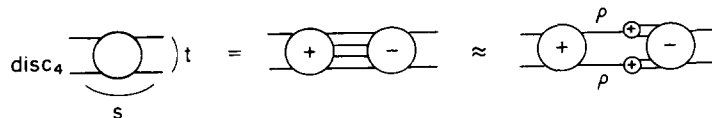

Fig. 8.6. Unitarity for the four-body t-channel cut, showing the $\rho\rho$ cut in the t-channel.
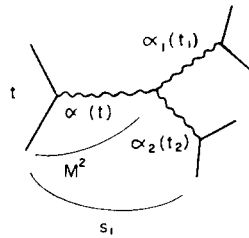
Fig. 8.7. Definition of variables and Regge trajectories that control the helicity asymptotic limit.

one would expect that it would not [152]. The argument follows the same line of reasoning as the proof that the AFS diagram does not have the two-reggeon-cut asymptotic behavior [154]. The essential point is that in order for a particular graph to have two-reggeon asymptotic behavior, both of the two-reggeon—two-particle amplitudes contained in it should have third double spectral functions. That is why there it a twist in the boxes on the right and left of the Mandelstam graph (see fig. 8.4a). However, the slicing L_d changes the analytic structure of the graph. This can be seen by considering the internal six-point function of fig. 8.4b corresponding to the process $1 + a + 2 \rightarrow 3 + a' + 4$. The channels in which the desired third double spectral singularity is required are the channels (a 1 3̄) and (a 2 4̄). However, they both overlap the channel (1 a 2) whose discontinuity is taken in the slicing L_d. According to the assumptions listed in section 1.4, there should therefore be no discontinuities at all in the channels (a 1 3̄) and (a 2 4̄), let alone any associated with a third double spectral singularity. Thus one would expect the only contributions to the two-reggeon cut come from the slicings of the type L_a, L_b and L_c. A detailed analysis of the graph [152,153], however, shows that it does not conform to the assumptions of section 1.4 to the extent that anomalous singularities are present which allow the slicings L_d to have a bonafide two-reggeon cut, although not with the same strength as proposed by less detailed analyses [7,78]. This result is interesting in itself because the slicing L_d corresponds to a physical double-scattering cross section and its presence or absence at high energies would be a direct physical consequence of the validity of a particular application of the assumptions of section 1.4.

One's preference for the sign of the cut need not be based on which model, multi-Regge, or Feynman graphs, one is more comfortable with. It turns out that the sign of the cut is determined by methods that are essentially model independent. This was first suggested in the pioneering work of Gribov, Pomeranchuk and Ter-Martirosyan [75] and demonstrated more recently with more rigour by White [145]. In fact cuts can be shown to come about as a consequence of Regge poles and unitarity. To deduce the presence of cuts, one begins with the discontinuity formula in the t-channel for the four-particle cut, as shown in fig. 8.6. Now this may sound like a very unlikely place to begin, but it is precisely the same starting point for demonstrating, for example,

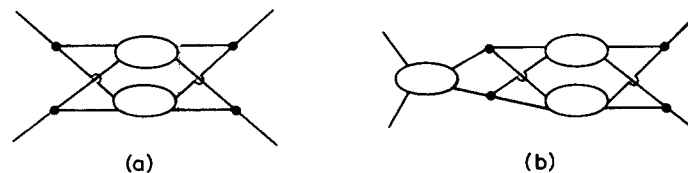(a)   (b)

Fig. 8.8. Examples of Feynman graphs used by Gribov [72] to obtain the two-reggeon cut. The bubbles represent elementary scattering amplitudes with Regge-pole asymptotic behavior. The graph (b) contains a Regge pole in addition to the cut.

the existence of a complex branch point in t due to the production of a pair of ρ mesons in the t-channel. In that case we would look at the four-particle-discontinuity equation and then perform a continuation of the equation in t. The integration over the subenergies of the pairs of particles, say t_1 and t_2 is constrained by conservation of energy so that $\sqrt{t} \geqslant \sqrt{t_1} + \sqrt{t_2}$. As t is varied into the complex plane the t_1 and t_2 contours are pinched at the upper end point against the complex poles at $t_1 = m_\rho^2$, $t_2 = m_\rho^2$. This produces a branch point at $t = 4m_\rho^2$ in the integration. One can even derive a discontinuity formula for the $\rho\rho$ cut that looks exactly like an ordinary two-body discontinuity, except that the intermediate moments are on a complex mass shell. (See Eden, Landshoff, Olive and Polkinghorne [58].)

By the same token, to get to the Regge cuts from unitarity, it is necessary to consider a channel which couples to the cut; the four-body channel is the simplest. The actual proof that Regge cuts are generated from Regge poles in the t_1 and t_2 channels is too involved to present here (see White [145]). It is amusing, however, that in the proof it is necessary to take into account all of the features of Regge asymptotic behavior which we have discussed the foregoing sections. In particular it is necessary to know that the six-point amplitude which enters into the integration in the middle term of fig. 8.6 has the asymptotic helicity behavior which we discussed in section 6, eq. (6.37), namely, that

$$A_6^{\tau \tau_1 \tau_2} \sim F(M^2, t, t_1, t_2)(-s_1)^{\alpha_1(t_1) + \alpha_2(t_2)} + (-s_1)^{\alpha(t)} U(t, t_1, t_2),$$ (8.6)

where the variables are defined in fig. 8.7. The first term, it turns out, is the only one that contributes to the Regge cut, as suggested by the power of s_1.

It is possible to derive a discontinuity formula in the J plane for the discontinuity across the two-reggeon cut:

$$\text{disc}\, a(J, t) \propto \int \frac{dt_1 \, dt_2}{\sqrt{-\lambda(t, t_1, t_2)}} N(t, t_1, t_2) N^*(t, t_1, t_2)\, \xi_1(t_1)\, \xi_2(t_2)\, \delta[J - \alpha_1(t_1) - \alpha_2(t_2) + 1],$$ (8.7)

where $N(t, t_1, t_2)$ is the coefficient of $(M^2)^{-1}$ in the asymptotic behavior of F in the case that $\tau = +1$; and ξ_1 and ξ_2 are signature factors. In the forward direction $N(0, t_1, t_2 = t_1)$ can be calculated directly from the inclusive cross section described by $\text{disc}_{M^2} A_6$ with some assumptions, thus providing a phenomenological determination of the strength of the cut [106].

The result (8.7) is the statement of a sort of J-plane unitarity condition. Its importance in understanding the singularity structure of the J-plane is as profound as the importance of conventional unitarity in understanding the singularity structure of the energy plane.

The negative sign of the contribution of the PP cut to the total cross section is then found by inserting the expression for the discontinuity (8.7) into the Sommerfeld–Watson transform. It is completely determined by the dynamical quantities in eq. (8.7).

We have seen that there are basically three ways of generating Regge cuts from Regge poles. The first is through s-channel unitarity which, as we have seen, is not sufficient in and of itself to describe such crucial features as the contributions of the cuts to total cross sections. The second is through Feynman graphs such as that of fig. 8.4, which describe the Regge cuts adequately, but which by themselves fail to provide a unitary S matrix theory. The third is through t-channel unitarity, which is capable of a rigorous treatment of the discontinuity of the two-reggeon cut, but which is technically so cumbersome that it has not been applied to the rigorous study of higher

cuts or to multi-particle amplitudes. There is yet a fourth approach, called the reggeon calculus, developed by Gribov and others [72,156–159], which combines features of the second and third methods. As originally formulated, the calculus was simply a systematic procedure for calculating the asymptotic behavior of certain Feynman graphs, constructed from elementary amplitudes possessing Regge behavior. Thus the two-reggeon cut was obtained from graphs of which two examples are given in fig. 8.8. In subsequent work the calculus developed into a sort of perturbation theory for reggeons. A Lagrangian field theory for reggeons was developed [74], which provided an explicit perturbative solution to the J-plane discontinuity formulae described above. Its relationship to J-plane unitarity can be compared to the relationship of Feynman perturbation theory to ordinary energy-plane unitarity. And so it can be used as a laboratory for investigating the way J-plane unitarity requires J-plane singularities to proliferate in much the same way that one uses Feynman perturbation theory to learn about singularities required by conventional unitarity [156–159].

The reggeon calculus can be thought of as the ultimate statement of the consequences of t-channel unitarity for the proliferation of J-plane singularities which arise from Regge poles. It would be desirable, of course to have a theory which incorporates s-channel unitarity as well. To the extent that Feynman perturbation theory satisfies both s- and t-channel unitarity, one would think that if the reggeon calculus could be reformulated as a systematic procedure for summing Feynman graphs in a particular order at asymptotic values of s, one would then be in the possession of a theory capable of incorporating constraints of both s- and t-channel unitarity at once. Some work in this direction has been attempted by DeTar [154].

8.2. Regge cuts in multiparticle amplitudes

Through the work of Gribov, Pomeranchuk and Ter-Martirosyan [75] and White [145] we now understand Regge cuts in four-particle amplitudes fairly well. However, as soon as we start combining cuts with multi-Regge asymptotic limits, we reach an area where much less is understood. No one has yet attempted a thoroughgoing analysis of the energy-plane singularity structure of amplitudes with multiple Regge cuts, at least at the level of rigor that we have outlined here for the single-Regge limit.

As an example, let us consider the contribution of Regge cuts to the five-particle amplitude in the double-Regge limit. These can be studied from the s-channel point of view [76,111,112]. However, we expect that, as with the four-particle amplitude, to study the full J-plane singularity, it is necessary to approach the problem from the t-channel point of view. In that case we would have to begin by considering the simultaneous discontinuity across the four-particle cuts in both t_1 and t_2 as shown in fig. 8.9. By analogy with the discussion of the four-particle ampli-
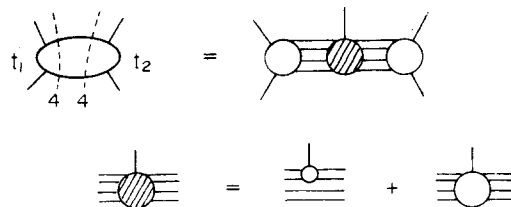

Fig. 8.9 Discontinuity across four-particle cuts in t_1 and t_2 from unitarity.
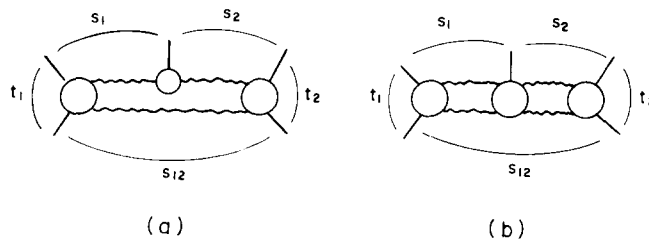
Fig. 8.10. Two-types of multi-Regge cuts in the five-particle amplitude.

tude, we might expect two types of cuts to be generated by the unitarity equation (see fig. 8.10). The second contribution, fig. 8.10b, would appear to have a structure very much like that of the double-Regge limit of Regge poles. However, the first contribution, fig. 8.10a, which arises from the disconnected piece of the central blob in fig. 8.9, has a rather different structure. As yet no one has derived a general formula for the simultaneous discontinuity across the cuts in the J planes of the t_1 and t_2 channels.

The "reggeon-triangle" graph of fig. 8.10a has been studied by Drummond [55] using the reggeon calculus. The behavior for large s_{12} was found to be

$$A_5 \sim s_{12}^{\gamma(t_1, t_2, \eta_{12})}/\ln s_{12} , \qquad (8.8)$$

which is indeed quite different from the behavior of double-Regge exchange and has no analog in the four-particle amplitude. Evidently there is a hierachy of J-plane "Landau singularities" just as in the energy plane. For further applications to production amplitudes, we refer the reader to Campbell [31] and for applications to inclusive cross sections to Abramovskii, Gribov and Kancheli [7], Botke [19] and Cardy and White [33].

One of the intriguing questions about Regge cuts in multiparticle amplitudes is the question of what singularities they represent asymptotically. In our analysis of Regge poles, we assumed they asymptotically represented thresholds in energy channels; and this allowed us to analyze the structure of multi-Regge exchange amplitudes in some detail. Before a similar analysis can be performed for multi-Regge cut amplitudes, we need to know what energy-plane Landau singularities they represent asymptotically. It is quite possible that a knowledge of the energy-plane singularities of Regge-pole dominated amplitudes alone is sufficient to deduce via unitarity the energy-plane singularity structure of Regge-cut dominated amplitudes. Present approaches to this problem, however, have relied instead on analysis of various Feynman graphs or specific s-channel discontinuities containing Regge cuts in order to investigate the nature of the asymptotic singularities. For example, it has been remarked that the reggeon-triangle graph appears to reflect a Landau singularity in s_{12}, s_1 and s_2 of an order higher than normal thresholds [71]. Some discussion of these very fundamental questions has also been given by Patrascioiu [111,112].

We have stressed above that a knowledge of the structure of multi-Regge amplitudes is necessary for understanding Regge cuts. Conversely, the structure of Regge cut amplitudes is not without influence on the behavior of Regge pole contributions. For example, in general one expects collisions between Regge poles and Regge cuts in the same channel, since their trajectories have

Fig. 8.11. Contribution to the five-particle amplitude with a collision between Regge poles and the reggeon triangle singularity.

different slopes. In the four-particle amplitude Regge poles and cuts might occur multiplicatively as*

$$a(J, t) = \frac{1}{J - \alpha(t)} \int_{-\infty}^{\alpha_c(t)} d\alpha \, \frac{\beta(\alpha, t)}{J - \alpha} . \tag{8.9}$$

The residue of the pole is then given by

$$a(J, t) \approx \frac{1}{J - \alpha(t)} \int_{-\infty}^{\alpha_c(t)} \frac{\beta(\alpha, t)}{\alpha(t) - \alpha} \approx - \frac{1}{J - \alpha(t)} \ln \left[\alpha(t) - \alpha_c(t) \right] , \tag{8.10}$$

which gives a singularity in the Regge-pole contribution at $\alpha(t) = \alpha_c(t)$, which is not present in the full amplitude and thus was excluded in our analysis of Regge-pole contributions. The sum of all contributions to the asymptotic behavior must have the correct analytic structure, but when two contributions have the same asymptotic behavior, the individual contributions need not respect the analytic structure that the sum must.

Similar phenomena are to be expected in multiparticle amplitudes. As an example, the reggeon-triangle graph can occur multiplicatively with Regge poles in the t_1 and t_2 channels (fig. 8.11). The behavior of this amplitude has been studied by Green [71]. He found that the double-Regge vertex has an extra singularity $[\eta_{12} - \eta_{12}^{(s)}]^{-\frac{1}{2}}$, where $\eta_{12}^{(s)}$ is a particular value of η_{12} actually inside the physical region, multiplying the form discussed in section 3.

9. Conclusion and discussion

We could summarize our approach to the Regge behavior of multiparticle amplitudes in the following way: It is necessary to take account of the interplay between analyticity and unitarity in the t and s channels. We began by assuming a simple property of unitarity in the t channel, namely the presence of a family of factorizable poles linked by a Regge-pole trajectory. We proceeded to investigate the compatibility of this ansatz with simple "s-channel" analyticity, in particular assuming asymptotic singularities behaved like normal thresholds. This was the basis of the major part of this review. We found that it was indeed possible to construct amplitudes compatible with these properties. Further application of unitarity led to the consideration of Regge cuts generated by Regge poles. These in turn could be associated with more complicated s-channel

---

* An example of such a structure arises from the triple-Regge contribution to the inclusive sum rule in the non-forward case, discussed in section 7.2. At $\alpha(0) = \alpha_c(0) = 1$ it is more singular than a simple pole, giving $\sigma \sim \ln \ln s$.

singularities. Of course, we are at the moment only beginning to understand how the various s-channel Landau singularities are represented asymptotically.

We speculated in section 1.1 on a parallel between the generation of higher order Landau singularities in the energy plane and in the J plane, and suggested a maximal analyticity of the J-plane analogous to first-degree analyticity of the energy plane in which all singularities are built up from poles through unitarity. In the energy plane this iterative picture of the generation of higher order Landau singularities made perturbation theory a relevant "laboratory" for investigating the nature and locations of singularities [58]. By the same token an iterative approach to J-plane singularities makes the reggeon calculus a useful tool. As it is presently formulated however, the reggeon calculus does not attempt a careful treatment of asymptotic singularities in the energy plane [154]. We emphasize that an understanding of the generation of these energy-plane singularities in parallel with J-plane singularities is necessary for a rigorous approach to the reggeon calculus. In view of the complexities of a completely unitary theory, one may in the end have to resort to a perturbative approach along the lines of the reggeon calculus for approximating actual amplitudes.

A simple analytic structure for the Regge pole dominated amplitudes would greatly facilitate such an iterative approach to the generation of higher order singularities. We have treated the restriction to normal threshold singularities as a working hypothesis. It entered into our arguments in two ways:

(i) Interpretation of asymptotic expressions. A term of the form $(-s_A)^{\alpha A}(-s_B)^{\alpha B}$ corresponds to a product of two functions, one cut for $\arg s_A = 0$, the other, for $\arg s_B = 0$. If the cuts were not due to normal threshold singularities, it is quite possible that cuts in s_A could move as s_B varied, or even that the asymptotic expression would be valid only on top of the cuts and that entirely different expressions were needed on other sides of the cuts.

(ii) Independence of overlapping channel singularities. We ruled out terms of the form $(-s_A)^{\alpha A}(-s_B)^{\alpha B}$, when s_A and s_B were overlapping channels. As a corollary we required that left- and right-hand cuts be additively separable, thereby permitting us to construct signatured amplitudes.

In support of this point of view, we noted in section 1.4 the lack of models generating simple Regge poles which violate these properties — models which nevertheless appear to have higher order Landau singularities at least nonasymptotically. In further support we mentioned that the Steinmann relations provide that (ii) is true in the physical region. Unfortunately, we require property (i) in order to implement (ii) and we often require (ii) outside the physical region.

Nevertheless, even if our assumptions prove to be illfounded, we hope that our approach to the subject will serve as a guide to future work. In particular we would emphasize the following subjects for further research:

(i) The Sommerfeld–Watson representation for multiparticle amplitudes.

(ii) Properties of scattering amplitudes involving reggeons (unitarity and analyticity).

(iii) An understanding of the role of energy plane singularities in the derivation of the reggeon calculus.

(iv) Rigorous J-plane unitarity expressions for singularities of higher order than two-reggeon branch points.

(v) The asymptotic structure of amplitudes containing higher order Landau singularities and their relationship to Regge cuts.

Acknowledgement

Appendix. Multi-Regge behavior in the dual resonance model

We illustrate the general discussion in the main body of the text by computing the Regge and helicity asymptotic limits in the dual resonance model*. This is the simplest known model for multi-Regge behavior. The reader may find it useful to compare the general discussion with the specific forms in the dual model at each stage. Dual resonance amplitudes have right-hand singularities in a planar set of channels. They are therefore analogous to signatured amplitudes.

A.1. The five-particle amplitude

The channels are defined as usual (see fig. 3.1). The Bardakci—Ruegg representation for the dual amplitude is

$$B_5 = \int_0^1 dx_1 \int_0^1 dx_2 \, x_1^{-\alpha_1-1} (1-x_1)^{-\alpha(s_1)-1} x_2^{-\alpha_2-1} (1-x_2)^{-\alpha(s_2)-1} (1-x_1 x_2)^{-\alpha(s_{12})+\alpha(s_1)+\alpha(s_2)} \quad (A.1)$$

where $\alpha(s) = s + \alpha_0$, $\alpha_1 = \alpha(t_1) = t_1 + \alpha_0$, etc. Starting from (A.1) we compute the various asymptotic limits studied in section 3.

A.1.1. Single-Regge limit

Since (A.1) is only defined for negative α, we first take $s_1, s_{12} \to -\infty$ (s_1/s_{12} fixed) and then continue in s_1 and s_{12}. In this limit the region $x_1 \approx 0$ dominates in the integral. We make the usual change of variables

$$x_1 = y_1/(-s_1)$$

and use

$$(1+z/s)^{-s} \underset{s \to \infty}{\sim} e^{-z} \quad (A.2)$$

to obtain

$$B_5 \sim (-s_1)^{\alpha_1} \int_0^\infty dy_1 \int_0^1 dx_2 \, y_1^{-\alpha_1-1} x_2^{-\alpha_2-1} (1-x_2)^{-\alpha(s_2)-1} \exp\left[-y_1(1-x_2)-y_1 x_2 \frac{s_{12}}{s_1}\right].$$

A simple change of variables gives

---

* For recent reviews of the dual resonance model, see for example, Schwarz [122] and Veneziano [151].

$$B_5 \sim (-s_1)^{\alpha_1} \int\limits_0^\infty dy_1 \int\limits_0^1 dx_2 \; y_1^{-\alpha_1-1} x_2^{-\alpha_2-1} (1-x_2)^{-\alpha(s_2)+\alpha_1-1} \exp\left[-y_1 - y_1 \left(\frac{x_2}{1-x_2}\right)\frac{s_{12}}{s_1}\right]. \quad (A.3)$$

The integral in (A.3) converges only for $s_1/s_{12} \geq 0$. It is therefore not an entire function of s_1/s_{12}. We wish to find the nature of its singularity and obtain the analytic continuation of (A.3). We use the identity

$$e^x = \frac{1}{2\pi i} \int\limits_{-i\infty}^{i\infty} d\lambda \; \Gamma(-\lambda) \, (-x)^\lambda , \quad (A.4)$$

which is simply verified by closing the contour to the right, on the second term of the exponenial in (A.3). The y_1 and x_2 integrals can then be done yielding

$$B_5 \sim (-s_1)^{\alpha_1} \frac{1}{2\pi i} \int\limits_{-i\infty}^{i\infty} d\lambda \; \frac{\Gamma(-\alpha_1+\lambda) \, \Gamma(-\alpha_2+\lambda) \, \Gamma(-\alpha(s_2)+\alpha_1-\lambda) \, \Gamma(-\lambda)}{\Gamma(-\alpha(s_2)+\alpha_1-\alpha_2)} \left(\frac{s_{12}}{s_1}\right)^\lambda , \quad (A.5)$$

where the contour separates the poles in the first two gamma functions from those in the second two. Eq. (A.5) is recognized as the integral representation of the hypergeometric function,

$$\frac{1}{2\pi i} \int\limits_{-i\infty}^{i\infty} d\lambda \; \Gamma(a+\lambda) \, \Gamma(b+\lambda) \, \Gamma(c-a-b-\lambda) \, \Gamma(-\lambda) z^\lambda$$

$$= \frac{\Gamma(a) \, \Gamma(b) \, \Gamma(c-a) \, \Gamma(c-b)}{\Gamma(c)} \; {}_2F_1(a, b; c; 1-z) . \quad (A.6)$$

The singularity in s_1/s_{12} can be easily found from (A.5). For $s_1/s_{12} < 1$, the contour can be closed to the left, picking up the poles at $\lambda = \alpha_1, \alpha_1 - 1, ...,$ and $\lambda = \alpha_2, \alpha_2 - 1, ...$ (see, for example, Białas and Pokorski [17]),

$$B_5 \sim (-s_1)^{\alpha_1} \left\{ \left(\frac{s_{12}}{s_1}\right)^{\alpha_1} \sum_{n=0}^\infty \frac{\Gamma(-\alpha_1+n) \, \Gamma(-\alpha_2+\alpha_1-n) \, \Gamma(-\alpha(s_2)+n)}{\Gamma(-\alpha(s_2)+\alpha_1-\alpha_2)n!} \left(-\frac{s_1}{s_{12}}\right)^n \right.$$

$$\left. + \left(\frac{s_{12}}{s_1}\right)^{\alpha_2} \sum_{n=0}^\infty \frac{\Gamma(-\alpha_2+n) \, \Gamma(-\alpha_1+\alpha_2-n) \, \Gamma(-\alpha(s_2)+\alpha_1-\alpha_2+n)}{\Gamma(-\alpha(s_2)+\alpha_1-\alpha_2)n!} \left(-\frac{s_1}{s_{12}}\right)^n \right\} . \quad (A.7)$$

Equation (A.7) exhibits explicitly the singularities in s_{12}/s_1 of the reggeon coupling to three particles discussed in sections 3.1 and 3.6. The first term has the behavior $(-s_{12})^{\alpha_1}$ times a function with poles in $\alpha(s_2)$, and the second term has the behavior $(-s_1)^{\alpha_1-\alpha_2}(-s_{12})^{\alpha_2}$ times a function with no singularities in $\alpha(s_2)$. Thus, there are no simultaneous discontinuities in overlapping energy invariants. To obtain an expression valid for $s_1/s_{12} > 1$, the roles of s_1 and s_{12} and t_2 and s_2 must be exchanged in (A.5) and (A.7).

A.1.2. Double-Regge limit

The double-Regge limit can be obtained by taking the further limit $s_2 \to \infty$ ($s_{12}/s_1 s_2$ fixed) on (A.3), (A.5) and (A.7). Thus making the usual change of variables

$$x_2 = y_2/(-s_2)$$

on (A.3) gives (see for example, Bardakci and Ruegg [14])

$$B_5 \sim (-s_1)^{\alpha_1} (-s_2)^{\alpha_2} \int_0^\infty dy_1 \int_0^\infty dy_2 \, y_1^{-\alpha_1 - 1} y_2^{-\alpha_2 - 1} \exp[-y_1 - y_2 + \eta_{12} y_1 y_2] \, . \tag{A.8}$$

Similarly (A.5) becomes (see, for example, Drummond, Landshoff and Zakrewski [56])

$$B_5 \sim (-s_1)^{\alpha_1} (-s_2)^{\alpha_2} \frac{1}{2\pi i} \int_{-i\infty}^{i\infty} d\lambda \, \Gamma(-\alpha_1 + \lambda) \, \Gamma(-\alpha_2 + \lambda) \, \Gamma(-\lambda) \, (-\eta_{12})^\lambda . \tag{A.9}$$

This is of the general form (3.28) with $\beta(\lambda, t_1, t_2) = 1$. Eq. (A.7) yields the expansions (3.29) and (3.30) of the double-Regge vertex, with

$$V_1(t_1, t_2; \eta_{12}) = \frac{1}{\Gamma(-\alpha_1) \Gamma(-\alpha_2)} \sum_{n=0}^\infty \Gamma(-\alpha_1 + n) \, \Gamma(-\alpha_2 + \alpha_1 - n) \frac{\eta_{12}^{-n}}{n!} \, , \tag{A.10}$$

and similarly for V_2.

When the λ contour in (A.9) is closed to the left, an exact expression for $V(t_1, t_2; \eta_{12})$ is obtained. This expression also clearly exhibits the behavior as $\eta_{12} \to \infty$. Eq. (A.9) can also be used to obtain the behavior as $\eta_{12} \to 0$. In this case the expression is only asymptotic since the integrand behaves like $(\eta_{12} \lambda)^\lambda$ and hence the contour at infinity does not vanish. We pick up the poles in $\Gamma(-\lambda)$

$$V(t_1, t_2; \eta_{12}) \underset{\eta_{12} \to 0}{\sim} 1 + \alpha_1 \alpha_2 \eta_{12} + \dots \, . \tag{A.11}$$

It is amusing to note that taking the discontinuity of V in η_{12} (equivalently, the discontinuity of B_5 in s_{12}) introduces a factor $\sin \pi \lambda$ in (A.9). Since there are then no singularities to the right of the contour, the discontinuity vanishes faster than any power of η_{12}. A detailed calculation gives

$$\text{disc}_{\eta_{12}} V(t_1, t_2; \eta_{12}) \underset{\eta_{12} \to 0}{\sim} \frac{2\pi i \, \eta_{12}^{\alpha_1 + \alpha_2 + 1}}{\Gamma(-\alpha_1) \Gamma(-\alpha_2)} \exp(-1/\eta_{12}) \, . \tag{A.12}$$

In section 3.4 we argued that, in general, there can be fixed pole singularities (3.40) to the right of the λ contour (see fig. 3.7). Only multiplicative fixed poles give such singularities in the Regge residue. The dual model has no such fixed poles and hence the behavior (A.12). Therefore there appears to be an amusing connection between the behavior as $\eta_{12} \to 0$ and the presence or absence of multiplicative fixed poles.

A.1.3. Helicity asymptotic limits

Examining (A.1), we see that $s_{12} \to -\infty$ causes $x_1 \approx 0$ or $x_2 \approx 0$ to dominate in the integral*. There are therefore two contributions. Taking first

$$x_1 = y_1 /(-s_{12})$$

we have

$$B_5 \sim (-s_{12})^{\alpha_1} \int\limits_0^\infty dy_1 \int\limits_0^1 dx_2 \; y_1^{-\alpha_1-1} x_2^{-\alpha_2-1}(1-x_2)^{-\alpha(s_2)-1} \exp(-y_1 x_2) \, . \tag{A.13}$$

A simple change of variables allows the integrals to be done. Including the contribution from $x_2 \approx 0$, we have [141]

$$B_5 \sim \Gamma(-\alpha_1)\,(-s_{12})^{\alpha_1} \frac{\Gamma(-\alpha(s_2)))\,\Gamma(-\alpha_2+\alpha_1)}{\Gamma(-\alpha(s_2)-\alpha_2+\alpha_1)} + \Gamma(-\alpha_2)\,(-s_{12})^{\alpha_2} \frac{\Gamma(-\alpha(s_1)))\,\Gamma(-\alpha_1+\alpha_2)}{\Gamma(-\alpha(s_1)-\alpha_1+\alpha_2)} \, . \tag{A.14}$$

This is in agreement with the general form (3.59).

The helicity limit behavior is important in the theory of the DRM. It means for negative α_1 and α_2 we can write an unsubtracted dispersion relation in s_{12} with the other α's in (A.1) fixed. Therefore, B_5 can be written exactly as a sum over the poles in s_{12}.

Finally, the combined Regge and helicity limit $s_1 \to \infty$ and $s_{12}/s_1 \to \infty$ is from (A.7) or (A.14),

$$B_5 \sim \Gamma(-\alpha_1)\,(-s_{12})^{\alpha_1} \frac{\Gamma(-\alpha(s_2))\,\Gamma(-\alpha_2+\alpha_1)}{\Gamma(-\alpha(s_2)-\alpha_2+\alpha_1)} + \Gamma(-\alpha_2)\,(-s_{12})^{\alpha_2}\,\Gamma(-\alpha_1+\alpha_2)\,(-s_1)^{\alpha_1-\alpha_2} \, . \tag{A.15}$$

A.2. The six-particle amplitude

We first study the triple-Regge vertex of section 4, and then the linear triple-Regge limit considered in our discussion of factorization in section 5.

A.2.1. Triple-Regge limit

The channels are defined as in fig. 4.1. We start with the integral representation

$$B_6 = \int\limits_0^1 \int\limits_0^1 \int\limits_0^1 dx_1\,dx_2\,dx_3\, x_1^{-\alpha_1-1}(1-x_1)^{-\alpha(s_{12})-1} x_2^{-\alpha(s_1)-1}(1-x_2)^{-\alpha_2-1} x_3^{-\alpha_3-1}(1-x_3)^{-\alpha(s_{23})-1}$$

$$\times (1-x_1 x_2)^{-\alpha(s_2)+\alpha(s_{12})+\alpha_2}(1-x_2 x_3)^{-\alpha(s_3)+\alpha(s_{23})+\alpha_2}(1-x_1 x_2 x_3)^{-\alpha(s_{31})+\alpha(s_2)+\alpha(s_3)-\alpha_2} \, . \tag{A.16}$$

As $s_1, s_2, s_3 \to -\infty$, $x_1 \approx 0$, $x_2 \approx 1$ and $x_3 \approx 0$ dominate the integrand. We thus substitute

---

* The integral does not converge if both x_1 and $x_2 \approx 0$.

$$x_1 = y_1/(-s_1), \qquad x_2 = 1 + y_2/s_2, \qquad x_3 = y_3/(-s_3)$$

and find [96,101]

$$B_6 \sim (-s_1)^{\alpha_1} (-s_2)^{\alpha_2} (-s_3)^{\alpha_3} \int_0^\infty \int_0^\infty \int_0^\infty dy_1 dy_2 dy_3 \; y_1^{-\alpha_1-1} y_2^{-\alpha_2-1} y_3^{-\alpha_3-1}$$

$$\times \exp[-y_1 - y_2 - y_3 + \eta_{12} y_1 y_2 + \eta_{23} y_2 y_3 + \eta_{31} y_3 y_1].$$ (A.17)

Using the identity (A.4) on the last three terms in the exponential, we have [51]

$$B_6 \sim (-s_1)^{\alpha_1} (-s_2)^{\alpha_2} (-s_3)^{\alpha_3} \left(\frac{1}{2\pi i}\right)^3 \int_{-i\infty}^{i\infty} \int_{-i\infty}^{i\infty} \int_{-i\infty}^{i\infty} d\lambda_{12} d\lambda_{23} d\lambda_{31}$$

$$\times \Gamma(-\alpha_1 + \lambda_{12} + \lambda_{31}) \Gamma(-\alpha_2 + \lambda_{23} + \lambda_{12}) \Gamma(-\alpha_3 + \lambda_{31} + \lambda_{23}) \Gamma(-\lambda_{12}) \Gamma(-\lambda_{23}) \Gamma(-\lambda_{31})$$

$$\times (-\eta_{12})^{\lambda_{12}} (-\eta_{23})^{\lambda_{23}} (-\eta_{31})^{\lambda_{31}}.$$ (A.18)

The advantage of (A.18) is that it allows continuation to positive η_{ij}. It has the standard form (4.20) with

$$\beta(\lambda_{12}, \lambda_{23}, \lambda_{31}; t_1, t_2, t_3) = 1.$$

We shall not discuss the helicity asymptotic limits of B_6 here (see DeTar and Weis [51] for further details).

A.2.2. Linear triple-Regge limit

The channels are defined as in fig. 5.3. We use again the representation (A.16), but with the channels appropriately redefined,

$$B_6 = \int_0^1 \int_0^1 \int_0^1 dx_1 dx_2 dx_3 \; x_1^{-\alpha_1-1} (1-x_1)^{-\alpha(s_1)-1} x_2^{-\alpha_2-1} (1-x_2)^{-\alpha(s_2)-1} x_3^{-\alpha_3-1} (1-x_3)^{-\alpha(s_3)-1}$$

$$\times (1-x_1 x_2)^{-\alpha(s_{12})+\alpha(s_1)+\alpha(s_2)} (1-x_2 x_3)^{-\alpha(s_{23})+\alpha(s_2)+\alpha(s_3)}$$

$$\times (1-x_1 x_2 x_3)^{-\alpha(s_{123})+\alpha(s_{12})+\alpha(s_{23})-\alpha(s_2)}.$$ (A.19)

For $s_1, s_2, s_3 \to -\infty$, $x_1, x_2, x_3 \approx 0$ dominate the integrand. We thus substitute

$$x_1 = y_1/(-s_1), \qquad x_2 = y_2/(-s_2), \qquad x_3 = y_3/(-s_3)$$

and find

$$B_6 \sim (-s_1)^{\alpha_1} (-s_2)^{\alpha_2} (-s_3)^{\alpha_3} \int\limits_0^\infty \int\limits_0^\infty \int\limits_0^\infty dy_1 dy_2 dy_3 \ y_1^{-\alpha_1-1} y_2^{-\alpha_2-1} y_3^{-\alpha_3-1}$$

$$\times \exp\left[-y_1-y_2-y_3+\eta_{12}y_1y_2+\eta_{23}y_2y_3-\eta_{12}\eta_{23}\left(\frac{s_{123}s_2}{s_{12}s_{23}}\right)y_1y_2y_3\right] . \tag{A.20}$$

Again we use the identity (A.4) on the last three exponentials. After some redefinition of variables we have [140]

$$B_6 \sim (-s_1)^{\alpha_1} (-s_2)^{\alpha_2} (-s_3)^{\alpha_3} \left(\frac{1}{2\pi i}\right)^3 \int\limits_{-i\infty}^{i\infty} \int\limits_{-i\infty}^{i\infty} \int\limits_{-i\infty}^{i\infty} d\lambda_{12} \ d\lambda_{23} \ dp \ \Gamma(-\alpha_1+\lambda_{12}) \ \Gamma(-\alpha_2+\lambda_{12}+\lambda_{23}-p)$$

$$\times \Gamma(-\alpha_3+\lambda_{23}) \ \Gamma(-\lambda_{12}+p) \ \Gamma(-\lambda_{23}+p) \ \Gamma(-p) \ (-\eta_{12})^{\lambda_{12}} (-\eta_{23})^{\lambda_{23}} \left(\frac{s_{123}s_2}{s_{12}s_{23}}\right)^p . \tag{A.21}$$

As usual the integration contours separate the infinite sequences of poles which run to the left from those which run to the right.

As usual we wish to extract the singularities in the energy invariants. Using the integral representation of the hypergeometric function (A.6), we have

$$B_6 \sim (-s_1)^{\alpha_1} (-s_2)^{\alpha_2} (-s_3)^{\alpha_3} \left(\frac{1}{2\pi i}\right)^2 \frac{1}{\Gamma(-\alpha_2)} \int\limits_{-i\infty}^{i\infty} \int\limits_{-i\infty}^{i\infty} d\lambda_{12} \ d\lambda_{23} \ \Gamma(-\alpha_1+\lambda_{12}) \ \Gamma(-\alpha_2+\lambda_{12}) \ \Gamma(-\lambda_{12})$$

$$\times (-\eta_{12})^{\lambda_{12}} \Gamma(-\alpha_2+\lambda_{23}) \ \Gamma(-\alpha_3+\lambda_{23}) \ \Gamma(-\lambda_{23})$$

$$\times (-\eta_{23})^{\lambda_{23}} \ {}_2F_1\left(-\lambda_{12}, -\lambda_{23}; -\alpha_2; 1 - \frac{s_{123}s_2}{s_{12}s_{23}}\right) . \tag{A.22}$$

Due to the cut in $_2F_1(z)$ for $1 \leqslant z \leqslant \infty$, this expression only allows us to evaluate the amplitude for $-\pi < \arg(s_{123}s_2/s_{12}s_{23}) < \pi$. In order to extract the singularity in this variable, we use the formula for analytic continuation of the hypergeometric function

$$_2F_1(a, b; c; 1-z) = \frac{\Gamma(c) \ \Gamma(b-a)}{\Gamma(b) \ \Gamma(c-a)} z^{-a} \ {}_2F_1(a, c-b; a-b+1; 1/z) + (a \leftrightarrow b) . \tag{A.23}$$

We can set $s_{123}s_2/s_{12}s_{23} = 1$ inside the hypergeometric functions on the right-hand side of (A.23) and still have an expression valid for all $s_{123}s_2/s_{12}s_{23} = e^{\pm 2n\pi i}$ ($n = 0, 1, 2, ...$). Using

$$_2F_1(a, c-b; a-b+1; 1) = \Gamma(a-b+1) \ \Gamma(-c+1)/\Gamma(-b+1) \ \Gamma(-c+a+1)$$

we have

$$B_6 \sim (-s_1)^{\alpha_1} (-s_2)^{\alpha_2} (-s_3)^{\alpha_3} \frac{1}{\Gamma(-\alpha_2)} \left(\frac{1}{2\pi i}\right)^2 \int_{-i\infty}^{i\infty} \int_{-i\infty}^{i\infty} d\lambda_{12} \, d\lambda_{23} \, \Gamma(-\alpha_1+\lambda_{12}) \, \Gamma(-\alpha_2+\lambda_{12})$$

$$\times \Gamma(-\lambda_{12}) \, (-\eta_{12})^{\lambda_{12}} \, \Gamma(-\alpha_2+\lambda_{23}) \, \Gamma(-\alpha_3+\lambda_{23}) \, \Gamma(-\lambda_{23}) \, (-\eta_{23})^{\lambda_{23}}$$

$$\times \left[\frac{\sin\pi(\lambda_{12}-\alpha_2) \sin\pi\lambda_{23}}{\sin\pi\alpha_2 \, \sin\pi(\lambda_{12}-\lambda_{23})} \left(\frac{s_{123}s_2}{s_{12}s_{23}}\right)^{\lambda_{12}} + \frac{\sin\pi(\lambda_{23}-\alpha_2) \sin\pi\lambda_{12}}{\sin\pi\alpha_2 \, \sin\pi(\lambda_{23}-\lambda_{12})} \left(\frac{s_{123}s_2}{s_{12}s_{23}}\right)^{\lambda_{23}} \right]. \tag{A.24}$$

The λ_{12} and λ_{23} contours can be closed in their left-half planes analogously to the case for the double-Regge vertex. Of the eight possible terms, only five are non-vanishing, since one of the two factors in the final bracket vanishes if $\lambda_{12} = \alpha_2$ or $\lambda_{23} = \alpha_2$. We then have, using (A.10)

$$B_6 \sim \Gamma(-\alpha_1) \, \Gamma(-\alpha_2) \, \Gamma(-\alpha_3) \left\{ (-s_1)^{\alpha_1-\alpha_2} (-s_{12})^{\alpha_2-\alpha_3} (-s_{123})^{\alpha_3} V_2(\eta_{12}) V_3(\eta_{23}) \right.$$

$$+ (-s_2)^{\alpha_2-\alpha_1} (-s_{12})^{\alpha_1-\alpha_3} (-s_{123})^{\alpha_3} \frac{\sin\pi(\alpha_2-\alpha_3) \sin\pi\alpha_1}{\sin\pi\alpha_2 \, \sin\pi(\alpha_1-\alpha_3)} V_1(\eta_{12}) V_3(\eta_{23})$$

$$+ (-s_1)^{\alpha_1-\alpha_2} (-s_3)^{\alpha_3-\alpha_2} (-s_{123})^{\alpha_2} V_2(\eta_{12}) V_2(\eta_{23})$$

$$+ (-s_2)^{\alpha_2-\alpha_3} (-s_{23})^{\alpha_3-\alpha_1} (-s_{123})^{\alpha_1} \frac{\sin\pi(\alpha_2-\alpha_1) \sin\pi\alpha_3}{\sin\pi\alpha_2 \, \sin\pi(\alpha_3-\alpha_1)} V_1(\eta_{12}) V_3(\eta_{23})$$

$$\left. + (-s_3)^{\alpha_3-\alpha_2} (-s_{23})^{\alpha_2-\alpha_1} (-s_{123})^{\alpha_1} V_1(\eta_{12}) V_2(\eta_{23}) \right\}, \tag{A.25}$$

in agreement with (5.13).

A.3. Inclusive cross sections

We discuss in some detail the dual model results for the single-partical inclusive cross section for a + b → $\bar{c}$ + anything [18, 25, 50, 70, 138]. Many particle inclusive cross sections have also been studied in the dual model, and in particular it has been found that they factorize as expected. We refer the reader to the papers of Jen, Kang, Shen and Tan [87] and Hoyer and Lam [83] for further details. For phenomenological studies see Thomas [131]; Bebel, Biebel, Ebert and Otto [15], and references therein.
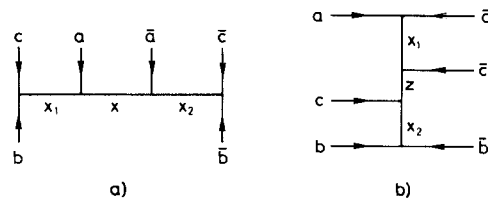

Fig. A.1. Tree diagrams used for calculating dual amplitudes for (a) fragmentation region, (b) central region.

A.3.1. Fragmentation region

We study the term with the ordering of particles shown in fig. A.1a. Using the variables appropriate for this tree diagram, we have

$$B_6 = \int\limits_0^1 dx_1 \int\limits_0^1 dx \int\limits_0^1 dx_2 \; x_1^{-\alpha_{bc}-1}(1-x_1)^{-\alpha_{ac}-1} x^{-\alpha-1}(1-x)^{-\alpha_{a\bar{a}}-1} x_2^{-\alpha_{\bar{b}\bar{c}}-1}(1-x_2)^{-\alpha_{\bar{a}\bar{c}}-1}$$

$$\times \; (1-x_1 x)^{-\alpha_{\bar{a}ac}+\alpha_{ac}+\alpha_{a\bar{a}}}(1-xx_2)^{-\alpha_{a\bar{a}\bar{c}}+\alpha_{\bar{a}\bar{c}}+\alpha_{a\bar{a}}}(1-x_1 xx_2)^{-\alpha_{b\bar{b}}+\alpha_{\bar{a}ac}+\alpha_{a\bar{a}\bar{c}}-\alpha_{a\bar{a}}} , \qquad (A.26)$$

where $\alpha_{bc} = \alpha(s_{bc})$, $\alpha_{ac} = \alpha(s_{ac})$, etc., and $\alpha = \alpha(M^2) = \alpha(s_{acb})$. We study the limit corresponding to the fragmentation of b:

$$\alpha, \; \alpha_{ac}, \; \alpha_{\bar{a}\bar{c}} \to -\infty .$$

The dominant contribution comes from $x \approx 1$, so we make the change of variables

$$x = 1 + y/\alpha .$$

The y integral can then be done, and changing variables to $z_i = x_i/(1-x_i)$ we have

$$B_6 \sim \Gamma(-\alpha_{a\bar{a}}) \int\limits_0^\infty \int\limits_0^\infty dz_1 \, dz_2 \; z_1^{-\alpha_{bc}-1}(1+z_1)^{\alpha_{bc}+\alpha_{b\bar{b}}-\alpha_{\bar{a}ac}} z_2^{-\alpha_{\bar{b}\bar{c}}-1}(1+z_2)^{\alpha_{\bar{b}\bar{c}}+\alpha_{b\bar{b}}-\alpha_{\bar{a}ac}}$$

$$\times \; (1+z_1+z_2)^{-\alpha_{a\bar{a}}-\alpha_{b\bar{b}}+\alpha_{\bar{a}ac}+\alpha_{\bar{a}ac}} \, (-\alpha-\alpha_{ac}z_1-\alpha_{\bar{a}\bar{c}}z_2)^{\alpha_{a\bar{a}}} . \qquad (A.27)$$

For the inclusive cross section we need the discontinuity in $M^2(\alpha)$ for $M^2 \geq 0$. This discontinuity comes from the last term in (A.27) which develops a phase for positive M^2. An easy calculation gives

$$\mathrm{disc}_{M^2} B_6 \sim \frac{2\pi i}{\Gamma(\alpha_{a\bar{a}}+1)} \alpha^{\alpha_{a\bar{a}}} \left(-\frac{\alpha_{ac}}{\alpha}\right)^{\alpha_{b\bar{b}}} \left(-\frac{\alpha_{\bar{a}\bar{c}}}{\alpha}\right)^{\alpha_{\bar{b}\bar{c}}} \int\limits_0^\infty \int\limits_0^\infty dy_1 \, dy_2 \, \theta(1-y_1-y_2) y_1^{-\alpha_{bc}-1} y_2^{-\alpha_{\bar{b}\bar{c}}-1}$$

$$\times \left(1-\frac{\alpha}{\alpha_{ac}} y_1\right)^{\alpha_{bc}-\alpha_{b\bar{b}}-\alpha_{\bar{a}\bar{c}}} \left(1-\frac{\alpha}{\alpha_{\bar{a}\bar{c}}} y_2\right)^{\alpha_{\bar{b}\bar{c}}+\alpha_{b\bar{b}}-\alpha_{\bar{a}ac}}$$

$$\times \left(1-\frac{\alpha}{\alpha_{ac}} y_1 - \frac{\alpha}{\alpha_{\bar{a}\bar{c}}} y_2\right)^{-\alpha_{a\bar{a}}-\alpha_{b\bar{b}}+\alpha_{\bar{a}ac}+\alpha_{\bar{a}ac}} (1-y_1-y_2)^{\alpha_{a\bar{a}}} , \qquad (A.28)$$

where

$$y_1 = -\frac{\alpha_{ac}}{\alpha} z_1 , \qquad y_2 = -\frac{\alpha_{\bar{a}\bar{c}}}{\alpha} z_2 .$$

We note two features of (A.28). In the triple-Regge region, $s/M^2 \to \infty$, and hence $\alpha_{ac} = \alpha_{\bar{a}\bar{c}} \approx -s$, we have the usual behavior

$$\mathrm{disc}_{M^2} B_6 \sim \frac{2\pi i}{\Gamma(\alpha_{a\bar{a}}+1-\alpha_{bc}-\alpha_{\bar{b}\bar{c}})} M^{2\alpha_{a\bar{a}}} \Gamma(-\alpha_{bc}) (s/M^2)^{\alpha_{bc}} \Gamma(-\alpha_{\bar{b}\bar{c}}) (s/M^2)^{\alpha_{\bar{b}\bar{c}}} . \qquad (A.29)$$

There is an exponential cut-off for large transverse momentum at fixed

$x = 1 - M^2/s \approx (M^2/s_{ac} - 1)^{-1}$. Since

$$s_{bc} = m_b^2 + m_c^2 - (p_\perp^2 + m_c^2 + m_b^2 x^2)/x \approx -p_\perp^2/x,$$

large $p_\perp^2$ is large $\alpha_{bc} = \alpha_{\bar{b}\bar{c}}$. The dependence on α_{bc} and $\alpha_{\bar{b}\bar{c}}$ in (A.28) is

$$\left(1 - \frac{1}{(1-1/x)y_1}\right)^{\alpha_{bc}} \left(1 - \frac{1}{(1-1/x)y_2}\right)^{\alpha_{\bar{b}\bar{c}}} \tag{A.30}$$

so the dominant contribution will be for the largest y_1 and y_2, i.e. $y_1 \approx y_2 \approx \frac{1}{2}$. Then (A.30) gives the behavior [138]

$$\exp\left[-\frac{2p_\perp^2}{x} \ln \frac{1+x}{1-x}\right]. \tag{A.31}$$

Three other dual model terms contribute to the b fragmentation region – those corresponding to interchanging b and c, and/or $\bar{b}$ and $\bar{c}$. We refer the reader to DeTar, Kang, Tan and Weis [50] for a detailed discussion of these terms.

A.3.2. Central region

It is convenient to begin with the choice of variables corresponding to the tree diagram of fig. A.1b. The same result could, of course, be obtained by taking the limit $\alpha_{bc}, \alpha_{\bar{b}\bar{c}} \to \infty$ on (A.28). We have

$$B_6 = \int_0^1 \int_0^1 \int_0^1 dx_1 \, dz \, dx_2 \, x_1^{-\alpha_{a\bar{a}}-1} z^{-\alpha_{a\bar{a}c}-1} x_2^{-\alpha_{b\bar{b}}-1}(1-x_1)^{-\alpha_{ac}-1}(1-z)^{-\alpha_{\bar{a}ac}-1}(1-x_2)^{-\alpha_{bc}-1}$$

$$\times (1-x_1 z - x_2 z + x_1 x_2 z)^{\alpha_{a\bar{a}c}} \left[\frac{(1-x_1 z - x_2 z + x_1 x_2 z)}{(1-x_1 z)(1-x_2 z)}\right]^{\alpha-\alpha_{ac}-\alpha_{bc}}. \tag{A.32}$$

For $\alpha, \alpha_{ac}, \alpha_{bc} \to -\infty$ ($\alpha/\alpha_{ac}\alpha_{bc}$ fixed), the important region of integration is x_1 and $x_2 \approx 0$. The usual exponentiation procedure gives

$$B_6 \sim \Gamma(-\alpha_{a\bar{a}}) (-s_{ac})^{\alpha_{a\bar{a}}} \Gamma(-\alpha_{b\bar{b}}) (-s_{bc})^{\alpha_{b\bar{b}}} \int_0^1 dz \, z^{-\alpha_{a\bar{a}c}-1} (1-z)^{-\alpha_{\bar{a}ac}-1} V(\alpha_{a\bar{a}}, \alpha_{b\bar{b}}; z(1-z)\eta). \tag{A.33}$$

where $\eta = M^2/s_{ac}s_{bc} \sim s/s_{ac}s_{bc}$ and V is the double-Regge vertex of subsection A.2 above. Thus the structure of the two-reggeon and two-particle amplitude resembles both that of the four-particle amplitude and the double-Regge vertex*. The discontinuity in M^2 is equivalent to the discontinuity in η of the vertex function. The behavior for small $p_\perp^2$ ($\eta \to \infty$) is of course controlled by the usual helicity poles [151]. The behavior (A.31) for $p_\perp^2 \to \infty$ ($\eta \to 0$) goes over into $\exp(-4p_\perp^2)$. This can also be obtained from (A.12) and (A.33). The exponential decrease for $p_\perp^2 \to \infty$ thus appears to be connected with the absence of multiplicative fixed poles. Therefore, the helicity and angular momentum plane structure seems to control the asymptotic behavior in a rather unexpected kinematic region.

---

* One should note that the rather simple form (A.33) holds only for the forward configuration where $\alpha_{ac} = \alpha_{\bar{a}\bar{c}}$, etc.

References

[1] H.D.I. Abarbanel, Phys. Rev. D3 (1971) 2227.
[2] H.D.I. Abarbanel, Phys. Rev. D6 (1972) 2788.
[3] H.D.I. Abarbanel, G.F. Chew, M.L. Goldberger and L.M. Saunders, Phys. Rev. Letters 26 (1971) 937.
[4] H.D.I. Abarbanel, S.D. Ellis, M.B. Green and A. Zee, 1972 (unpublished).
[5] H.D.I. Abarbanel, V.N. Gribov and O.V. Kanchelli, 1972 (unpublished).
[6] H.D.I. Abarbanel and A. Schwimmer, Phys. Rev. D6 (1972) 3018.
[7] V.A. Abramovskii, V.N. Gribov and O.V. Kancheli, in: Proc. XVI Intern. Conf. on High-Energy Physics, Vol. I (1973) p. 389.
[8] D. Amati, S. Fubini and A. Stanghellini, Nuovo Cimento 26 (1962) 896.
[9] H. Araki, J. Math. Phys. 2 (1960) 163.
[10] Ya.I. Asimov, A.A. Anselm, V.N. Gribov, G.S. Danilov and I.T. Dyatlov, Zh. Eksperim. i. Teor. Fiz. 49 (1965) 549[Soviet Phys. JETP 22 (1966) 383].
[11] S. Auerbach, R. Aviv, R. Blankenbecler and R. Sugar, Phys. Rev. D6 (1972) 2216; Phys. Rev. Letters 29 (1972) 522.
[12] M. Baker and D. Coon, Phys. Rev. D4 (1971) 1234.
[13] N. Bali, G.F. Chew and A. Pignotti, Phys. Rev. Letters 19 (1967) 614; Phys. Rev. 163 (1967) 1572.
[14] K. Bardakci and H. Ruegg, Phys. Letters 28B (1969) 342.
[15] D. Bebel, K.J. Biebl, D. Ebert and H.J. Otto, Fortschr. Phys. 20 (1972) 555.
[16] L. Bertocchi, S. Fubini and M. Tonin, Nuovo Cimento 25 (1962) 626.
[17] A. Białas and S. Pokorski, Nucl. Phys. B10 (1969) 399.
[18] K.J. Biebl, D. Bebel and D. Ebert, Fortschr. Phys. 20 (1972) 541.
[19] J.D. Botke, Nucl. Phys. B42 (1972) 589.
[20] J.F. Boyce, J. Math. Phys. 8 (1967) 675.
[21] J.B. Bronzan, Phys. Rev. D7 (1972) 480.
[22] R.C. Brower, R.N. Cahn and J. Ellis, Phys. Rev. D7 (1973) 2080.
[23] R.C. Brower, M. Einhorn, M. Green, A. Patrascioiu and J. Weis, Phys. Rev. D8 (1973) 2524.
[24] R.C. Brower and J. Ellis, Phys. Rev. D5 (1972) 2253.
[25] R.C. Brower and R.E. Waltz, Nuovo Cimento 10A (1972) 833.
[26] R.C. Brower and J.H. Weis, Phys. Letters 41B (1972) 631.
[27] R.C. Brower and J.H. Weis, Pomeron Decoupling Theorems, report No. UCSC 74/102 (1974).
[28] L.S. Brown, Phys. Rev. D6 (1972) 748.
[29] K.E. Cahill and H.P. Stapp, Phys. Rev. D6 (1972) 1007.
[30] K.E. Cahill and H.P. Stapp, Phys. Rev. D8 (1973) 2714.
[31] D.K. Campbell, Phys. Rev. 188 (1969) 2471.
[32] L. Caneschi and A. Pignotti, Phys. Rev. Letters 22 (1969) 1219.
[33] J. Cardy and A. White, Phys. Letters 47B (1973) 445; CERN TH-1740.
[34] Chan Hong-Mo, K. Kajantie and G. Ranft, Nuovo Cimento 49A (1967) 157.
[35] S.-J. Chang, D. Gordon, F.E. Low and S.B. Treiman, Phys. Rev. D4 (1971) 3055.
[36] H. Cheng and T.T. Wu, Phys. Rev. Letters 24 (1970) 1456.
[37] G.F. Chew, The Analytic S-Matrix (W.A. Benjamin, Inc., New York, 1966).
[38] G.F. Chew and S.C. Frautschi, Phys. Rev. Letters 7 (1961) 394.
[39] G.F. Chew, M. Goldberger and F.E. Low, Phys. Rev. Letters 22 (1969) 208.
[40] G.F. Chew and A. Pignotti, in NAL Summer Study Report No. E-68-53 (1968).
[41] T.T. Chou and C.N. Yang, Phys. Rev. Letters 25 (1970) 1072.
[42] M. Ciafaloni and C.E. DeTar, Phys. Rev. D1 (1970) 2917.
[43] M. Ciafaloni, C.E. DeTar and M.N. Misheloff, Phys. Rev. 188 (1969) 2522.
[44] P.D.B. Collins, Phys. Reports 1C (1971) 103.
[45] P.D.B. Collins and E.J. Squires, Regge Poles in Particle Physics (Springer-Verlag, Berlin, 1968).
[46] J. Dash, Phys. Rev. D3 (1971) 1016.
[47] C.E. DeTar, Phys. Rev. D3 (1971) 128.
[48] C.E. DeTar, D.Z. Freedman and G. Veneziano, Phys. Rev. D4 (1971) 906.
[49] C.E. DeTar, C.E. Jones, F.E. Low, C.-I Tan, J.H. Weis and J.E. Young, Phys. Rev. Letters 26 (1971) 675.
[50] C.E. DeTar, K. Kang, C.-I Tan and J.H. Weis, Phys. Rev. D4 (1971) 425.
[51] C.E. DeTar and J.H. Weis, Phys. Rev. D4 (1971) 3141.
[52] A. DiGiacomo, Phys. Letters 40B (1972) 569.
[53] A. DiGiacomo, S. Fubini, L. Sertorio and G. Veneziano, Phys. Letters 33B (1970) B171.
[54] I.T. Drummond, Phys. Rev. 153 (1967) 1565.

[55] I.T. Drummond, Phys. Rev. 176 (1968) 2003.
[56] I.T. Drummond, P.V. Landshoff and W.J. Zakrewski, Nucl. Phys. B11 (1969) 383.
[57] I.T. Drummond, P.V. Landshoff and W.J. Zakreswki, Phys. Letters 28B (1969) 676.
[58] R.J. Eden, P.V. Landshoff, D.I. Olive and J.C. Polkinghorne, The Analytic S-Matrix (Cambridge, University Press, 1966).
[59] M.B. Einhorn, J. Ellis and J. Finkelstein, Phys. Rev. D5 (1972) 2063.
[60] R.P. Feynman, in: High-Energy Collisions, Third Intern. Conf., Stony Brook, N.Y., 1970.
[61] J. Finkelstein and K. Kajantie, Phys. Letters 26B (1968) 305; Nuovo Cimento 56A (1968) 659.
[62] J. Finkelstein and F. Zachariasen, Phys. Letters 34B (1971) 631.
[63] G.M. Frazer and R.G. Roberts, Nuovo Cimento 47A (1967) 339.
[64] W.R. Frazer, L. Ingber, C.H. Mehta, C.H. Poon, D. Silverman, K. Stowe, P.D. Ting and H.J. Yesian, Rev. Mod. Phys. 44 (1972) 284.
[65] M. Froissart, Phys. Rev. 123 (1961) 1053.
[66] P. Goddard and A.R. White, Nucl. Phys. B17 (1970) 45, 88.
[67] P. Goddard and A.R. White, Nuovo Cimento 1A (1971) 645.
[68] P. Goddard and A.R. White, Phys. Letters 38B (1972) 93.
[69] D. Gordan, Phys. Rev. D5 (1972) 2102.
[70] D. Gordon and G. Veneziano, Phys. Rev. D3 (1971) 2116.
[71] M.B. Green, Nucl. Phys. B71 (1974) 93.
[72] V.N. Gribov, Zh. Eksperim. i Teor. Fiz. 53 (1967) 654 [Soviet. Phys. JETP 26 (1968) 414].
[73] V.N. Gribov, in: Proc. XVI Intern. Conf. on High-Energy Physics, Vol. 2 (1973) p. 491.
[74] V.N. Gribov and A.A. Migdal, Yadern. Fiz. 8 (1968) 1002 [Soviet J. Nucl. Phys. 8 (1968) 583].
[75] V.N. Gribov, I.Ya. Pomeranchuk and K.A. Ter-Martirosyan, Yadern. Fiz. 2 (1965) 361 [Soviet J. Nucl. Phys. 2 (1965) 258] Phys. Rev. 139B (1965).
[76] I.G. Halliday, Nucl. Phys. B33 (1971) 285.
[77] I.G. Halliday and G.W. Parry, Nucl. Phys. B36 (1972) 162.
[78] I.G. Halliday and C.T. Sachrajda, Phys. Rev. D8 (1973) 3598.
[79] I.G. Halliday and L.M. Saunders, Nuovo Cimento 60A (1969) 177.
[80] B. Hasslacher, C.S. Hsue and D.K. Sinclair, Phys. Rev. D4 (1971) 3089.
[81] D. Horn and F. Zachariasen, Hadron Physics at Very High Energies (Addison-Wesley, 1973).
[82] P. Hoyer and J. Kwiecinski, Nucl. Phys. B60 (1973) 26.
[83] P. Hoyer and C.S. Lam, Nucl. Phys. B46 (1972) 253.
[84] C.S. Hsue, Phys. Rev. D4 (1971) 2336.
[85] Y. Iwasaki and S. Yazaki, Nucl. Phys. B51 (1973) 628.
[86] M. Jacob and G.C. Wick, Ann. Phys. 7 (1959) 404.
[87] C. Jen, K. Kang, P. Shen and C.-I Tan, Phys. Rev. Letters 27 (1971) 458; Ann. Phys. (N.Y.) 72 (1971) 548.
[88] C.E. Jones, F.E. Low, S.-H. Tye, G. Veneziano and J.E. Young, Phys. Rev. D6 (1972) 1033.
[89] C.E. Jones, F.E. Low and J.E. Young, Ann. Phys. (N.Y.) 63 (1971) 476.
[90] C.E. Jones, F.E. Low and J.E. Young, Phys. Rev. D4 (1971) 2358.
[91] C.E. Jones, F.E. Low and J.E. Young, Ann. Phys. (N.Y.) 70 (1972) 286.
[92] C.E. Jones, F.E. Low and J.E. Young, Phys. Rev. D6 (1972) 640.
[93] N.N. Khuri, Phys. Rev. Letters 10 (1963) 420; Phys. Rev. 132 (1963) 914.
[94] T.W.B. Kibble, Phys. Rev. 131 (1963) 2282.
[95] J. Kwiecinski, Nuovo Cimento Letters 3 (1972) 619.
[96] P.V. Landshoff and W.J. Zakrzewski, Nucl. Phys. B12 (1969) 216.
[97] H. Lee, Phys. Letters 46B (1973) 117.
[98] S.-Y. Mak, Nucl. Phys. B58 (1973) 598.
[99] S. Mandelstam, Nuovo Cimento 30 (1963) 113, 1127, 1148.
[100] S. Mandelstam, Phys. Rev. D1 (1970) 1720.
[101] M.N. Misheloff, Phys. Rev. 184 (1969) 1732; LBL Report No. UCRL-19795 (1969) unpublished.
[102] I.D. Moen, C. Montonen and W.J. Zakrzewski, Phys. Rev. D9 (1974) 1717.
[103] I.O. Moen and A.R. White, Phys. Letters 42B (1972) 75.
[104] A.H. Mueller, Phys. Rev. D2 (1970) 2963.
[105] A.H. Mueller and I.J. Muzinich, Ann. Phys. (N.Y.) (1970) 500.
[106] I.J. Muzinich, F.E. Paige, T.L. Trueman and L.-L. Wang, Phys. Rev. Letters 28 (1972) 850.
[107] D. Olive, Phys. Rev. 135B (1964) 745.
[108] D. Olive, Nucl. Phys. B15 (1970) 617.
[109] R.L. Omnes and V.A. Alessandrini, Phys. Rev. 136 (1964) 1137.

[110] A. Patrascioiu, Phys. Rev. D6 (1972) 3516.
[111] A. Patrascioiu, Phys. Rev. D7 (1973) 3010.
[112] A. Patrascioiu, Phys. Rev. D7 (1973) 3658.
[113] J. Polkinghorne, Nuovo Cimento 7A (1972) 555.
[114] E. Predazzi and G. Veneziano, Nuovo Cimento Letters 2 (1971) 749.
[115] M.S.K. Razmi, Nuovo Cimento 31 (1964) 615.
[116] T. Regge, Nuovo Cimento 14 (1959) 951.
[117] T. Regge, Nuovo Cimento 18 (1960) 947.
[118] R.G. Roberts, in: 14th Scottish Universities Summer School, Aug. 1973, eds. R.L. Crawford and R. Jennings (London Academic Press, 1974).
[119] R. Roth, Phys. Rev. D6 (1972) 2274.
[120] S. Sakai, Progr. Theoret. Phys. 47 (1972) 260.
[121] A.I. Sanda, Phys. Rev. D6 (1972) 280.
[122] J.H. Schwartz, Phys. Reports 8C (1973) 269.
[123] L. Sertorio and M. Toller, Nuovo Cimento 33 (1964) 413.
[124] D. Silverman and C.-I Tan, Phys. Rev. D2 (1970) 233.
[125] R. Slansky, Phys. Reports 11C (1974) 99.
[126] H.P. Stapp, Phys. Rev. D3 (1971) 3177.
[127] O. Steinmann, Helv. Phys. Acta 33 (1960) 275, 347.
[128] U.P. Sukhatme, Phys. Rev. D6 (1972) 2765.
[129] C.-I Tan, Phys. Rev. D4 (1971) 2412.
[130] K.A. Ter-Martirosyan, Nucl. Phys. 68 (1964) 591.
[131] G.H. Thomas, Phys. Rev. D5 (1972) 2212.
[132] M. Toller, Nuovo Cimento 37 (1965) 631.
[133] M. Toller, Proc. 8th Nobel Symp. on Elementary Particle Theory, Stockholm (1968).
[134] M. Toller, Nuovo Cimento 54A (1968) 295.
[135] M. Toller, Nuovo Cimento 62A (1969) 341.
[136] M. Toller, Riv. Nuovo Cimento 1 (1969) 403.
[137] G. Veneziano, Phys. Letters 36B (1971) 397.
[138] M. Virasoro, Phys. Rev. D3 (1971) 2834.
[139] J.H. Weis, Phys. Rev. D4 (1971) 1777.
[140] J.H. Weis, Phys. Rev. D5 (1972) 1043.
[141] J.H. Weis, Phys. Rev. D6 (1972) 2823.
[142] J.H. Weis, Phys. Letters 43B (1973) 487.
[143] J.H. Weis, Nucl. Phys. B71 (1974) 342.
[144] A.R. White, Nucl. Phys. B39 (1971) 432, 461.
[145] A.R. White, Nucl. Phys. B50 (1972) 93, 130.
[146] A.R. White, in: VIII Rencontre de Moriond, Méribel-les-Allues, Vol. II (1973) p. 105.
[147] A.R. White, Nucl. Phys., B67 (1973) 189.
[148] F. Zachariasen and G. Zweig, Phys. Rev. 160 (1967) 1326.
[149] P. Hoyer and L. Trueman, Brookhaven report, BNL 18735 (1974).
[150] J. Polkinghorne, Nuovo Cimento 36 (1965) 857.
[151] G. Veneziano, Phys. Reports 9C (1974) 200.
[152] T. DeGrand, in preparation.
[153] T. DeGrand and C. DeTar, in preparation.
[154] A. Rothe, Phys. Rev. 159 (1967) 1471.
[155] C. DeTar, MIT report, CTP-421 (1974).
[156] A.A. Migdal, A.M. Polyakov and K.A. Ter-Martirosyan, Phys. Letters 48B (1974) 239.
[157] H.D.I. Abarbanel and J.B. Bronzan, Phys. Letters 48B (1974) 345.
[158] R.C. Brower and J. Ellis, Phys. Letters 51B (1974) 242.
[159] R. Jengo, Phys. Letters 51B (1974) 143.